

Targeted nano-carriers to combat neurodegeneration

by

Benjamin William Schlichtmann

A thesis submitted to the graduate faculty
in partial fulfillment of the requirements for the degree of

MASTER OF SCIENCE

Major: Chemical Engineering

Program of Study Committee:
Balaji Narasimhan, Co-major Professor
Surya Mallapragada, Co-major Professor
Anumantha G Kanthasamy
Vellareddy Anantharam

The student author and the program of study committee are solely responsible for the content of this thesis. The Graduate College will ensure this thesis is globally accessible and will not permit alterations after a degree is conferred.

Iowa State University

Ames, Iowa

2017

Copyright © Benjamin William Schlichtmann, 2017. All rights reserved.

TABLE OF CONTENTS

ABSTRACT.....	v
ACKNOWLEDGMENTS	vi
CHAPTER 1: INTRODUCTION.....	1
1.1 Neurodegenerative Diseases and CNS Drug Delivery	1
1.2 Thesis Organization	3
1.3 Acknowledgments.....	3
1.4 References.....	4
CHAPTER 2: CASCADING MULTISCALE NANODELIVERY DEVICES TO	
COMBAT NEURODEGENERATIVE DISEASE	6
2.1 Abstract	6
2.2 Introduction to Neurodegenerative Disease and Chemical Exposure.....	7
2.2.1 Acute symptoms of chemical exposure	8
2.2.2 Chronic disease progression	9
2.2.3 Therapeutics for chemical exposure and downstream pathologies.....	10
2.3 CNS Delivery Platforms	13
2.3.1 Micelles.....	13
2.3.2 Liposomes	14
2.3.3 Dendrimers.....	14
2.3.4 Nanoparticles	15
2.3.4.1 Poly(estere)s	15
2.3.4.2 Polyanhydrides.....	15
2.4 CNS Targeting Strategies	18
2.4.1 Blood-brain barrier.....	18
2.4.1.1 Receptor-mediated strategies	19
2.4.1.2 Adsorptive-mediated strategies.....	21
2.4.1.3 Cell-mediated strategies.....	21
2.4.1.4 Other strategies	22
2.4.1.5 Obstacles for BBB targeting	23
2.4.2 Diseased neuron	24
2.4.3 Intracellular organelles.....	26
2.4.3.1 Endocytic pathway	27
2.4.3.2 Mitochondria.....	28
2.4.3.3 Nucleus	29
2.4.3.4 Obstacles for organelle targeting	31
2.4.4 Delivery route	32
2.5 Conclusions.....	34
2.6 Author Information	34

2.7 Author Contributions	35
2.8 Tables and Figures	35
2.9 References.....	40
CHAPTER 3: BIODEGRADABLE POLYANHYDRIDE NANOPARTICLE-BASED	
DELIVERY SYSTEM FOR ENHANCED BLOOD-BRAIN BARRIER	
TRANSPORT	56
3.1 Abstract.....	56
3.2 Introduction.....	57
3.3 Experimental Methods.....	59
3.3.1 Polyanhydride synthesis.....	59
3.3.2 Folic acid bulk functionalization	59
3.3.3 Mito-apocynin synthesis	60
3.3.4 NP synthesis.....	60
3.3.5 NP surface functionalization.....	61
3.3.6 Human monocyte isolation	61
3.3.7 Brain endothelial cell culture	61
3.3.8 Cytotoxicity assays	62
3.3.9 Endothelial cell-monocyte NP transfers	62
3.3.10 Immunofluorescence and confocal microscopy.....	63
3.3.11 Fluorescence-activated cell sorting (FACS)	63
3.3.12 Ultra Performance Liquid Chromatography tandem mass spectrometry (UPLC – MS/MS)	64
3.4 Results.....	65
3.4.1 Synthesis and characterization of FA-functionalized polyanhydrides... 65	
3.4.2 Polyanhydride NP synthesis and characterization	66
3.4.3 Limited cytotoxicity of polyanhydride NPs in human monocytes and HBMEC	66
3.4.4 Monocyte-endothelial cell co-cultures transfer NF-NPs to HBMEC	67
3.4.5 UPLC-MS/MS quantification of mAPO in human monocytes and HBMEC	68
3.4.6 Internalization of FA-functionalized NPs by HBMEC.....	69
3.5 Discussion.....	70
3.6 Conclusions.....	74
3.7 Author Information	74
3.8 Author Contributions	74
3.9 Acknowledgments.....	75
3.10 Tables and Figures	75
3.11 References.....	83

CHAPTER 4: NEURONAL TARGETING OF TRIPHENYLPHOSPHONIUM-FUNCTIONALIZED POLYANHYDRIDE NANOPARTICLES TO COMBAT OXIDATIVE STRESS	89
4.1 Abstract	89
4.2 Introduction	90
4.3 Experimental Methods	93
4.3.1 Materials	93
4.3.2 Synthesis of CdSe-ZnS core-shell nanoparticles	94
4.3.3 Polyanhydride bulk functionalization	94
4.3.4 Nanoparticle synthesis and characterization	96
4.3.5 N27 cell culture and cytotoxicity testing	97
4.3.6 Fluorescence-activated cell sorting	97
4.3.7 Confocal microscopy	98
4.3.8 Cell viability by MTS assay	99
4.3.9 Cleaved caspase-3 quantification	99
4.3.10 Statistical analysis	100
4.4 Results	100
4.4.1 Characterization of functionalized polymer	100
4.4.2 Characterization of nanoparticles and drug release kinetics	101
4.4.3 Cytotoxicity and internalization in N27 cells	102
4.4.4 Protection against H ₂ O ₂ challenge in N27 cells	102
4.5 Discussion	103
4.6 Conclusions	106
4.7 Acknowledgments	106
4.8 Author Information	107
4.9 Author Contributions	107
4.10 Tables and Figures	108
4.11 References	113
CHAPTER 5: CONCLUSIONS AND ONGOING/FUTURE WORK	120
5.1 Conclusions	120
5.2 Ongoing and Future Work	121
5.2.1 <i>In vitro</i> polyanhydride NP formulation optimization	121
5.2.2 <i>In vivo</i> biodistribution studies	122
5.2.3 <i>In vivo</i> protection studies	122
5.3 References	123

ABSTRACT

Neurodegenerative diseases are a large burden to the society. They are characterized by a loss of neuronal cells that affect the ability to perform daily activities, and are often caused by environmental or genetic factors. Therapeutics can treat clinical symptoms of chronic disease, but there is a need to additionally treat the underlying mechanisms leading to neuronal atrophy, such as mitochondrial dysfunction and inflammation. Efficacious treatment is very difficult due to the existence of several physiological hurdles, including the blood-brain barrier, diseased neuron, and intracellular organelle. Targeted nano-carriers can enhance local bioavailability by targeting each of these hurdles. Polyanhydride nanoparticles (NPs) in particular are attractive nano-carriers for central nervous system delivery of therapeutics, and can easily be functionalized with targeting ligands to further improve delivery.

The goal of the project detailed herein is to rationally design a functionalized polyanhydride NP drug delivery platform addressing all physiological hurdles of the neurovascular unit to combat neurodegeneration. First, functionalized and non-functionalized 20:80 CPH:SA polyanhydride NPs were evaluated for the ability to cross the BBB in vitro. These NPs demonstrated promise in the ability to cross the BBB. Second, bulk-functionalized 20:80 CPH:SA NPs were evaluated for the ability to be internalized by neurons and enhance protective capability of antioxidants against oxidative stress in vitro. It was found that the functionalized NPs demonstrated superior internalization by N27 neurons compared to non-functionalized NPs, and antioxidant-loaded NPs protected against hydrogen peroxide – induced oxidative stress. Collectively, these studies lay the foundation for further investigation of the functionalized NP platform for central nervous system drug delivery.

ACKNOWLEDGMENTS

First and foremost, thank you to my family. Thanks especially to my parents, Mark and Ginger Schlichtmann, for supporting me around every turn. Your love and support is incredibly appreciated. I truly enjoy all of the Skype calls that we have where you can cheer me up if I had a bad day in the lab, or give me pep talks and words of encouragement, or just simply to talk and catch up. Of course, the numerous trips down to Ames are great, especially when you refuse to leave without completely restocking my fridge. Your presence in my life is truly appreciated, and I am so grateful to have you there for me. Thank you also to my brothers, Scott and Jason Ek, and my sister-in-law, Carrie Ek, for all of the love and support that you give me every time I take trips back to Minnesota. Finally, thanks to all of my nieces, for making me smile every time I see you. You are all very important people in my life.

I cannot send enough thanks to my advisors, Drs. Balaji Narasimhan and Surya Mallapragada, for all that they have done to help me. Your guidance and support for every experiment is greatly appreciated, of course, but your mentoring goes beyond that for me. I can tell that you both truly wish for my success in graduate school, and genuinely strive to help me improve in any way I can. I am additionally thankful that I always feel comfortable talking around both of you, it goes a long way in easing the stress off of grad school.

Thank you to the other two members of my committee, Drs. Vellareddy Anantharam and Anumantha Kanthasamy, for their guidance in my research. Thanks additionally to Dr. Reddy for your willingness to help me get the best results that I can with all of the cell culture experiments I've done so far. I'd also like to thank Shivani Ghaisas, for all of her

hard work with the cell culture experiments we've done, and for never refusing to help me when I have questions.

Thanks also to my friends in the department of Chemical and Biological Engineering. Thanks especially to all of my lab mates: Kathleen Ross, Adam Mullis, Sean Kelly, Sujata Senapati, Honghu Zhang, Metin Uz, and Srikanth Nayak, for all of the helpful advice you've given me in the countless number of discussions we've had about research. Thank you also for simply being friendly and enjoyable people to talk to at work, and outside of work as well. Having colleagues that I feel so comfortable around really makes research easier and more enjoyable.

Lastly, I would like to acknowledge funding support from the US Army Medical Research and Materiel Command under contract W81XWH-11-1-0700.

CHAPTER 1: INTRODUCTION

1.1 Neurodegenerative Diseases and CNS Drug Delivery

Neurodegenerative disease comprises a complex set of pathologies affecting a large proportion of the population. The National Institute for Neurological Disorders and Stroke estimates that 50 million Americans each year suffer from one of over 600 neurological disorders [1]. In general, the disorders are associated with debilitation of physiological and cognitive function, and can result in inability to perform daily living activities [2–4]. Caring for these chronically disabled patients significantly burdens the families of the patient and the national healthcare system; the national cost of Parkinson’s disease (PD) care in the US was greater than \$14.4 billion in 2010, and is expected to increase with the aging “Baby Boomer” population [5]. Both PD as well as other neurodegenerative conditions may be linked to a variety of environmental and genetic factors [6]. One of these factors is chemical exposure. Chemical exposure is a burden to the society, with as many as 3 million individuals being exposed each year worldwide, about 10% of which are fatal [7]. Fatality is often caused by what is known as the organophosphate toxicity phase that leads to status epilepticus, or seizures [8]. Even with survival, many other symptoms occur after the acute phase, and must be treated effectively to avoid progression of neuronal atrophy [8].

A common symptom that occurs in neurons soon after organophosphate exposure is oxidative stress, which progresses towards widespread cell death [9]. Rapid treatment of oxidative stress in neurons is therefore essential to prevent disease progression. Many drugs have been used to treat oxidative stress, but several complex physiological hurdles surrounding the brain make delivery of most therapeutics highly challenging [10].

In order to improve drug delivery by improving half-life and providing sustained release, biocompatible platform technologies are typically used to encapsulate or chemically link a drug payload [11]. Additionally, many of these materials offer suitable chemistry for facile linkage of functional groups, or targeting ligands, to facilitate transport across multiple barriers associated with neural delivery [11,12]. Such simple linkages offer a versatile mix-and-match capability, in that a functionalization used on one platform can often be replicated on another to exploit that platform's physical properties. Polyamides are a particularly attractive option for use as a central nervous system (CNS) therapeutic delivery platform, because of their proven sustained release in the brain and dose-sparing properties, and the feasibility of ligand functionalization onto polyamide copolymer chemistries [13–16].

For maximum efficacy, a drug delivery system must achieve a high local concentration of its payload near the organelle of action within the afflicted cell [17]. To do this, the device must (1) enable delivery across the blood-brain barrier (BBB) from the site of administration to the brain, (2) facilitate uptake by the afflicted neuronal cell, and (3) achieve localization at the desired organelle before releasing the payload. The vastly different biological, chemical, and physical conditions required for navigating each of these barriers present a complex, multiscale problem. To effectively target all of these barriers using targeting ligands, this work investigated a novel bulk functionalization method. With this method, the targeting ligand will remain part of the NP throughout degradation for effective multiscale targeting. The versatility of the polyamide NP platform also allows for functionalizing other ligands to the surface of the NPs (in addition to functionalizing in bulk) for significantly improved multiscale targeting. This thesis describes *in vitro* studies that have been accomplished to demonstrate the promise of this platform for CNS delivery.

1.2 Thesis Organization

Chapter 2 provides a literature review of chemical exposure and chronic neurodegeneration pathology, as well as information on targeting strategies used for delivery across the BBB, to the diseased neurons, and to the mitochondria. Platform technologies that can facilitate delivery are also discussed. The mission of this project is to synthesize this information and develop and optimize a CNS polyanhydride delivery platform for treatment of symptoms associated with chemical exposure, chiefly oxidative stress.

Chapter 3 expands upon the polyanhydride NP platform by investigating the ability of NPs based on 1,6-bis(*p*-carboxyphenoxy)hexane and sebacic acid (i.e., 20:80 CPH:SA) to be transported across the BBB *in vitro*. Chapter 4 then evaluates the potential for 20:80 CPH:SA NPs functionalized with the BBB and mitochondrial targeting ligand triphenylphosphonium (TPP) to be internalized by neurons and co-localize to mitochondria. In addition, the hypothesis of enhanced protection of these NPs (encapsulating the antioxidant Mito-apocynin) over a soluble drug dose is tested. Chapter 5 summarizes the conclusions reached and suggests routes for future work using a cascading multiscale targeting NP platform based on the one tested in Chapters 3 and 4.

1.3 Acknowledgments

Information in this chapter was taken and modified from a review paper to be submitted to the *Biomedical Materials* Journal, July 31 2017, titled “Cascading Multiscale Nanodelivery Devices for CNS Delivery of Regenerative Therapeutics”, as detailed in Chapter 2 below.

1.4 References

- [1] National Institute of Neurological Disorders and Stroke, NINDS Overview, (2014). <https://www.ninds.nih.gov/About-NINDS/Who-We-Are>.
- [2] J. van Uem, J. Marinus, C. Canning, R. van Lummel, R. Dodel, I. Liepelt-Scarfone, D. Berg, M.E. Morris, W. Maetzler, Health-related quality of life in patients with Parkinson's disease - a systematic review based on the ICF model., *Neurosci. Biobehav. Rev.* 61 (2015) 26–34. doi:10.1016/j.neubiorev.2015.11.014.
- [3] F. Chekani, V. Bali, R.R. Aparasu, Quality of life of patients with Parkinson's disease and neurodegenerative dementia: A nationally representative study., *Res. Social Adm. Pharm.* (2015). doi:10.1016/j.sapharm.2015.09.007.
- [4] F. Pagnini, Psychological wellbeing and quality of life in amyotrophic lateral sclerosis: a review., *Int. J. Psychol.* 48 (2013) 194–205. doi:10.1080/00207594.2012.691977.
- [5] S.L. Kowal, T.M. Dall, R. Chakrabarti, M. V Storm, A. Jain, The current and projected economic burden of Parkinson's disease in the United States., *Mov. Disord.* 28 (2013) 311–8. doi:10.1002/mds.25292.
- [6] R.C. Brown, A.H. Lockwood, B.R. Sonawane, Neurodegenerative diseases: an overview of environmental risk factors., *Environ. Health Perspect.* 113 (2005) 1250–6.
- [7] S. Bird, S.J. Traub, J. Grayzel, Organophosphate and carbamate poisoning, *UpToDate.* 14 (2014) 339.
- [8] Y. Chen, Organophosphate-induced brain damage: Mechanisms, neuropsychiatric and neurological consequences, and potential therapeutic strategies, *Neurotoxicology.* 33 (2012) 391–400. doi:10.1016/j.neuro.2012.03.011.
- [9] M.T. Lin, M.F. Beal, Mitochondrial dysfunction and oxidative stress in neurodegenerative diseases., *Nature.* 443 (2006) 787–95. doi:10.1038/nature05292.
- [10] K.J. Barnham, C.L. Masters, A.I. Bush, Neurodegenerative diseases and oxidative stress., *Nat. Rev. Drug Discov.* 3 (2004) 205–14. doi:10.1038/nrd1330.
- [11] Y. Chen, L. Liu, Modern methods for delivery of drugs across the blood-brain barrier, *Adv. Drug Deliv. Rev.* 64 (2012) 640–665. doi:10.1016/j.addr.2011.11.010.
- [12] H.L. Wong, N. Chattopadhyay, X.Y. Wu, R. Bendayan, Nanotechnology applications for improved delivery of antiretroviral drugs to the brain, *Adv. Drug Deliv. Rev.* 62 (2010) 503–517. doi:10.1016/j.addr.2009.11.020.

- [13] M. Westphal, Z. Ram, V. Riddle, D. Hilt, E. Bortey, Gliadel (R) wafer in initial surgery for malignant glioma: Long-term follow-up of a multicenter controlled trial, *Acta Neurochir. (Wien)*. 148 (2006) 269–275. doi:10.1007/s00701-005-0707-z.
- [14] A.M. Binnebose, S.L. Haughney, R. Martin, P.M. Imerman, B. Narasimhan, B.H. Bellaire, Polyanhydride Nanoparticle Delivery Platform Dramatically Enhances Killing of Filarial Worms, *PLoS Negl. Trop. Dis.* 9 (2015) 1–18. doi:10.1371/journal.pntd.0004173.
- [15] L. Huntimer, A.E. Ramer-Tait, L.K. Petersen, K.A. Ross, K.A. Walz, C. Wang, J. Hostetter, B. Narasimhan, M.J. Wannemuehler, Evaluation of Biocompatibility and Administration Site Reactogenicity of Polyanhydride-Particle-Based Platform for Vaccine Delivery, *Adv. Healthc. Mater.* 2 (2013) 369–378. doi:10.1002/adhm.201200181.
- [16] T.M. Brenza, S.G. Ms, J.E.V. Ramirez, D. Harischandra, V. Anantharam, B. Kalyanaraman, A.G. Kanthasamy, B. Narasimhan, Neuronal Protection against Oxidative Insult by Polyanhydride Nanoparticle-based Mitochondria-targeted Antioxidant Therapy, *Nanomedicine Nanotechnology, Biol. Med.* 13 (2017) 809–820. doi:10.1016/j.nano.2016.10.004.
- [17] B. Yameen, W. Il Choi, C. Vilos, A. Swami, J. Shi, O.C. Farokhzad, Insight into nanoparticle cellular uptake and intracellular targeting, *J. Control. Release.* 190 (2014) 485–499. doi:10.1016/j.jconrel.2014.06.038.

CHAPTER 2: CASCADING MULTISCALE NANODELIVERY DEVICES TO COMBAT NEURODEGENERATIVE DISEASE

Modified from a review paper to be submitted to the *Biomedical Materials* Journal, July 31 2017, titled “Cascading Multiscale Nanodelivery Devices for CNS Delivery of Regenerative Therapeutics”.

Benjamin Schlichtmann^{1,a}, Adam Mullis^{1,a}, Rebecca Cademartiri¹, Balaji Narasimhan¹, Surya Mallapragada^{1,*}

¹ Department of Chemical and Biological Engineering, Iowa State University, Ames, IA 50010

^a These authors contributed equally to this work

* To whom correspondence should be addressed

2.1 Abstract

Neurodegeneration is a disabling set of conditions and contributes to around 30% of neurological-related deaths each year [1]. Toxicity from chemical exposure to toxic organophosphates such as nerve agents or pesticides contributes to a large portion of neurodegenerative disease, with as many as 3,000,000 exposure cases every year [2]. While a number of therapeutics have been explored for treatment resulting from chemical exposure, clinical translation has been limited. Improvements with the delivery of therapeutics have the potential to enhance the standard of treatment by increasing local drug concentration at the

pathologically-relevant cells and organelles. However, achieving efficient drug delivery requires the ability to target and overcome three physiological hurdles, including the blood-brain barrier (BBB), the diseased neuron, and the intracellular organelle. These barriers significantly reduce drug bioavailability and overall efficacy, presenting a complex, multiscale problem. Multiscale drug delivery systems could address these issues by incorporating targeting mechanisms for each of the three associated barriers at physiologically relevant times. A large body of work has been performed to address individual aspects of this problem, but few studies address the reality that functionalizations intended to overcome one barrier may hinder or be hindered by the local environment elsewhere along the pathway [3–8]. This review first seeks to provide a background on neurodegenerative disease and therapeutics used to treat it. Delivery platforms for treatment of neurodegenerative disease will additionally be evaluated. Finally, recent literature that addresses the properties needed to target the complex hurdles will be discussed. Synthesizing this information will enable the rational design of multiscale delivery systems for neurodegenerative disease.

2.2 Introduction to Neurodegenerative Disease and Chemical Exposure

Neurodegenerative disease is a complex set of disorders that affect a significant proportion of the population [9]. In general, they are associated with debilitation of physiological and cognitive function, and can result in inability to perform daily living activities [10–12]. Caring for these chronically disabled patients significantly burdens the families of the patient and the national healthcare system; the national cost of Parkinson's disease (PD) care in the US was greater than \$14.4 billion in 2010, and is expected to

increase even further [13]. These diseases may be linked to a variety of environmental and genetic factors, however many of the most prevalent diseases have similar pathology [14]. Oxidative stress, in particular from exposure to dangerous toxins, for example, is often a precursor for chronic neurodegeneration if left untreated [15].

2.2.1 Acute symptoms of chemical exposure

Upon exposure to nerve agents, acute nerve agent toxicity leads to disruption of proper neuronal synaptic function and mitochondrial dysfunction [15]. In the acute toxicity period, the toxic chemicals interfere with central nervous system (CNS) synaptic function by binding to acetylcholinesterase, which normally cleaves and deactivates excess acetylcholine [16]. Excess acetylcholine leads to the persistent activation of ionotropic ligand-gated channels that allow an abnormally high concentration of calcium into the cell and can drastically change expression of enzymes, causing cellular dysfunction [17,18]. Status epilepticus (SE), or seizures, is often the first symptom of nerve agent exposure and is due to a constant firing of action potentials resulting from persistent activation of the nicotinic channels.

In addition, neuron-neuron synaptic function in CNS is affected by increased levels of glutamate, the most ubiquitous neurotransmitter in the CNS [18,19]. The resulting high intracellular calcium concentration increases mitochondrial membrane permeability and leads to production of reactive oxygen and nitrogen species (ROS and RNS, respectively) along with overall mitochondrial dysfunction [18]. High levels of superoxide radicals lead to increased expression of the nicotinamide adenine dinucleotide phosphate-oxidase (NOX-2) enzyme which produces extracellular ROS and RNS that spreads throughout the brain

parenchyma [17,20]. Normally, the mitochondria induces production of antioxidants that can combat the build-up of ROS and RNS [15], but abnormally high levels lead to neuronal atrophy [21]. Associated increased levels of glial cell activation and an inflammatory response by microglial cells in the neurovascular unit (NVU) also appear after insult [22]. It is important to treat oxidative stress quickly, because ensuing neuronal atrophy causes irreversible injury to the brain [22].

2.2.2 Chronic disease progression

Nitric oxide (NO) plays a major role in oxidative stress – induced neurodegeneration [22,23]. NO induces N-methyl-D-aspartate (NMDA) receptor overexpression through interference with glutamate, leading to oxidative stress in the affected cells [22].

Overexpression of NO to toxic levels is apparent in both PD and Alzheimer's disease (AD) [22]. In addition, neuroinflammation of the brain past normal levels will lead to overall loss of function. Specifically, increased expression of isoform NO synthase (iNOS) is commonly associated with neurodegeneration, and serves as a marker for evaluating disease state [22,23].

Many cases of nerve agent exposure will eventually lead to chronic symptoms [18]. The aggregation of misfolded or mutated proteins (also called Lewy bodies (LB)) has been causally linked to chronic disease progression [24–26]. These aggregated deposits inhibit proper synaptic function. AD, which affects pyramidal neurons in the hippocampus, can often be characterized by the aggregation of amyloid-beta ($A\beta$) and tau protein [27–31]. Under normal function, $A\beta$ proteins contribute to proper synaptic function in the CNS, but in

AD, overexpression of this protein leads to significantly inhibited synaptic function [32]. The increase in A β expression also leads to lipid membrane peroxidation [22].

In contrast to AD, PD affects dopaminergic neurons, which exist primarily in the substantia nigra and striatal cortex [24,33,34]. One of the hallmarks of PD is the development of LBs, which are an aggregation of proteins resulting from the inability to degrade misfolded proteins through the polyubiquitination process in the cell [24]. The build-up of α -synuclein protein, specifically from *Leucine-rich repeat kinase 2* (LRRK2) mutations, in the extracellular matrix is one of the most common LB proteinopathies for PD, as well as that of ubiquitin [24,33,35,36]. Like A β , the α -synuclein protein is beneficial at normal levels for protecting degeneration of dopaminergic neurons but overexpression of the protein leads to neuronal toxicity [37]. As a result, a prolonged inflammatory response and NO production in glial cells that interferes with normal cellular function leads to cell atrophy [22].

2.2.3 Therapeutics for chemical exposure and downstream pathologies

There are four primary stages associated with chemical exposure from toxic organophosphates, including organophosphate toxicity, cholinergic excitotoxicity, secondary neuronal damage, and chronic disease progression [18]. An excellent review details therapeutics that have been used to protect against each of these stages resulting from exposure [18]. The following section discusses drugs used to treat each of these stages.

Anti-cholinergic drugs for treatment of organophosphate toxicity, occurring just a few minutes after exposure, must be administered rapidly and therefore are commonly administered in a bolus dose [38]. Atropine is an anticholinergic drug commonly used to alleviate symptoms, like SE, occurring in this phase [18,39]. Benactyzine and scopolamine

are also used to prevent the over-activation of acetylcholine that occurs during organophosphate toxicity [18,39]. When designing a platform for treatment of chemical exposure, incorporation of an anticholinergic drug must be considered.

Cholinergic excitotoxicity occurs within hours after exposure, immediately following organophosphate toxicity [18]. Common symptoms of this phase include inflammatory reaction and excessive calcium influx into neurons, severely damaging the cell [18]. Antiglutamatergic drugs like caramiphen have been used to reduce symptoms of excitotoxicity [39]. Benzodiazepines, which increase the activity of GABA (an inhibitory neurotransmitter) in the brain, have also been used as treatment for this stage [18].

Oxidative stress typically occurs shortly after the end of the cholinergic excitotoxicity phase when the secondary neuronal toxicity phase begins. The onset of this stage occurs hours to days after exposure [40]. Protection against oxidative stress is imperative for preventing neuronal atrophy and progression of disease. Vitamin E, *N-tert-butyl- α -phenylnitron* (PBN), MitoQ, and apocynin are all examples of antioxidants that have been investigated [18,41]. Other enzymatic (superoxide dismutase) and non-enzymatic (vitamin C and coenzyme Q₁₀) antioxidants have also been used to treat oxidative stress [42].

Apocynin combats oxidative stress by inhibiting expression of NOX-2, reducing the rate of ROS and RNS production; to be effective, it must localize to the mitochondria [43–46]. The mitochondrial targeting lipophilic and cationic molecule triphenylphosphonium (TPP) has therefore been conjugated to the drug to improve targeting and efficacy [23]. TPP enhances adsorptive-mediated cellular internalization through electrostatic interactions with the negative neuronal membrane and the even more negative mitochondrial membrane [23,43,47–54]. A recent study found that a two carbon chain TPP conjugated to apocynin

Mito-apocynin C2 (Mito-Apo C2) is up to 100 times more effective than apocynin, and has protected against several oxidative stress and inflammatory markers in a soluble dose *in vitro* and *in vivo* [23]. A separate *in vivo* study with Mito-Apo C11 has shown reduction of the oxidative stress-related marker 4-HNE in the substantia nigra after treatment [55].

Alternatively, the mitochondrially-targeted antioxidant MitoQuinone (MitoQ) has also shown the ability to treat oxidative stress *in vivo* [56–58]. MitoQ has even been approved for human use [59]. As elucidated by the above examples, mitochondrial targeting is an attractive strategy to use for antioxidants [42].

To treat chronic symptoms of neurodegeneration, the drug saracatinib has been used. In contrast to antioxidants, this therapeutic acts by inhibiting src family kinases (SFKs) [60]. These SFKs are upregulated by prion protein, the activation of which is initiated by the binding of A β [61]. SFKs modulate very important cell surface receptors in neurons, the over-expression of which can lead to significant neuronal toxicity [62]. Clinical trials of saracatinib have shown that this drug can reach the CNS and protect against neurodegeneration [60].

Memantine is also a neuroprotective drug for combating neurodegenerative disease. It prevents further degeneration by acting as an NMDA receptor antagonist, therefore limiting excessive ion inflow into neurons [41]. In a combination study with the antioxidants vitamin E and PBN, memantine has successfully protected against ROS and RNS through this mechanism [41]. However, it may not be suited for clinical use due to limited efficacy observed in late stages of AD-based neurodegenerative mouse models [63].

Alternatively, some therapeutics act directly on the aggregated protein deposits that often occur in diseases such as AD or PD. One example evaluated the effect of transcription

factor EB (TFEB) to reduce the amount of aggregated α -synuclein [26]. The study found that TFEB effectively reduced the aggregation of α -synuclein by promoting autophagic clearance [26]. Such a treatment may have promising implications for treatment of chronic symptoms associated with neurodegenerative diseases like PD.

In addition to the listed therapeutics, many other drugs have been incorporated at each level of exposure, from acute to chronic [18]. However, an issue existing with delivery of these therapeutics is achieving specificity (leading to low bioavailability) as well as low therapeutic half-life. These issues can be overcome by (1) using a nanoscale platform to deliver the drug and protect it from degradation (section 2.3), and (2) functionalizing this platform with targeting ligands to further enhance local bioavailability (section 2.4).

2.3 CNS Delivery Platforms

Drug delivery platforms can protect the drug from systemic degradation, provide sustained release, targeting and dose-sparing effects, and overall improve drug efficacy [64]. A number of nanoscale delivery platforms address several challenges associated with neural delivery, and will be discussed below. The most well-studied CNS delivery platforms include micelles, liposomes, dendrimers and nanoparticles (NPs) [65].

2.3.1 Micelles

Micelles have been used in CNS delivery applications. Having amphiphilic properties with a hydrophobic core, they can be used to carry hydrophobic drugs to improve localization [65]. In fact, a study found that micelles can improve the therapeutic effect of antioxidants [66]. However, due to long circulation time, micelles are often unstable in vivo

and therefore display lower improvements in drug efficacy, when not conjugated to stability-enhancing molecules like Poly(ethylene glycol) (PEG) [67].

2.3.2 Liposomes

Liposomes also have several favorable characteristics for CNS multiscale delivery. They have great biocompatibility, ability to encapsulate multiple types of therapeutics, and versatility in the ability to functionalize with targeting ligands [65]. Recent work has shown the ability of liposomes coated with PEG to improve treatment for symptoms associated with AD [68,69]. However, like micelles, liposomes are typically unstable in vivo and cannot easily provide sustained release for therapeutics without modification using molecules like PEG [65].

2.3.3 Dendrimers

Dendrimers are a popular nanoscale delivery option for CNS therapeutic delivery. First, the structures of dendrimers contain many functional groups that allow for the ability to conjugate therapeutics and significantly improve bioavailability, which makes them very versatile [49,70]. Additionally, therapeutics conjugated to dendrimers have demonstrated enhanced circulation times [49]. Dendrimers have been conjugated to the mitochondrial targeting ligand TPP to investigate potential improvements in mitochondrial co-localization [49]. Importantly, dendrimers have also demonstrated great biocompatibility [48]. However, the versatility of this platform is sacrificed by the fact that drugs for treatment of CNS disease are conjugated onto the surface functional groups [71]; this limits the predictability of release timescale that can be seen with NPs.

2.3.4 Nanoparticles

2.3.4.1 Poly(estere)s

Poly(estere)s are a very well-studied therapeutic delivery vehicle, with great support by the FDA. Furthermore, poly(lactic-co-glycolic acid) (PLGA)-based NPs are an attractive option for CNS therapeutic delivery studies [32,50,72–84]. However, a disadvantage of this nanoscale delivery platform is its bulk-eroding properties [85]. By allowing water penetration at a rate faster than polymer bond cleavage, PLGA NPs expose the therapeutic to surrounding fluids prior to presentation at the targeted site [85]; this can lead to significant therapeutic degradation. In addition, the complex release profile of these NPs makes it very difficult to control the therapeutic release rate when designing an optimal delivery platform [86]. These issues are further compounded when sustained therapeutic release of drug is required. Nevertheless, the proven safety and relative ease for conjugation of PLGA makes it an attractive option for overcoming the challenging hurdles associated with CNS delivery [87].

2.3.4.2 Polyanhydrides

Polyanhydrides demonstrate many advantages over competing drug delivery devices in the context of CNS delivery [88]. A significant advantage they hold over popular bulk-eroding nanoscale drug delivery platforms like PLGA is their surface-erosion mechanism. This mechanism occurs based on two main structural features. First, diacid monomers that form the backbone of polyanhydrides are relatively hydrophobic, and therefore reject water from penetrating into the bulk of NPs made from this polymer [89]. Second, the anhydride

bonds that link the monomers are hydrolytically labile [89]. These features lead to the cleavage of anhydride bonds faster than water diffusion into the bulk, or surface erosion [89]. Moreover, surface erosion of drug-encapsulated NPs allows for more predictable drug release rates, governed by near zero-order therapeutic release kinetics [88,90].

Additionally, polyanhydride copolymer chemistries are easily tailorable, which has several advantages. The ability to control chemistries with different hydrophobic and degradative properties allows for precise control of the timescale of release, ranging from days to weeks to months [88,91]. This versatility arises due to differences in monomer hydrophobicity used for the NP formulation [92]. Versatility in polyanhydride chemistry is also beneficial when considering therapeutic thermodynamic compatibility requirements. For example, proteins are amphiphilic molecules; by altering polyanhydride chemistry to be more amphiphilic using 1,8,-bis(*p*-carboxyphenoxy)-3,6-dioxaoctane (CPTEG), a novel polyanhydride developed by the Narasimhan lab, the stability of proteins encapsulated in these NPs can be significantly improved [93].

The surface-eroding properties of polyanhydrides are also advantageous over bulk-eroding NPs because they protect the therapeutic from exposure to, and degradation in, surrounding fluid [94]. Reduced drug degradation and premature release from NPs may lead to increased local bioavailability, improving drug pharmacodynamics [95]. In addition to this enhanced therapeutic protection, polyanhydride degradation products (dicarboxylic acids) do not significantly alter physiological pH, which can otherwise lead to significant therapeutic degradation [89,96].

Polyanhydrides have shown great biocompatibility in numerous studies [88,96,97]. This is attributed to the relatively low inflammatory response [88], as well as the ease with

which both aromatic and aliphatic monomers are removed from the body after degradation [89,92,96]. As an FDA-approved example demonstrating the biocompatibility of polyanhydrides, the carmustine-encapsulated wafer for the treatment of brain cancer shows the benefit of sustained release provided by a surface-eroding polyanhydride formulation of 20 mol% carboxyphenoxypropane (CPP) and 80 mol% SA [98].

The 20:80 CPH:SA chemistry has many advantages that suggest its use as a delivery platform for improving treatment of oxidative stress. 20:80 CPH:SA NPs release payload in 7-10 days [99], a faster timescale that can effectively treat oxidative stress from nerve agent exposure [18]. Superior uptake of 20:80 CPH:SA NPs by monocytes [100] and macrophages [101] suggests this formulation could utilize cell-mediated transcytosis mechanisms (discussed below) for crossing the BBB, even without functionalization. The binding of several serum proteins that have affinity for BBB-expressed receptors, including apolipoprotein E, may further enhance localization efficacy [102–106]. Overall, there may be several mechanisms at play with this formulation where improved cellular internalization could be observed, which make it a promising platform for CNS delivery.

It is imperative, when designing a nano-carrier, to consider thermodynamic compatibility between the drug and the polymer. This compatibility may be affected by the copolymer's microstructure [99]. For example, microphase separation occurs in 20:80 or 80:20 CPH:SA copolymers, but not at 50:50, based on resulting block vs. random monomer organization [99]. Encapsulated therapeutics will often prefer to localize to one of the microphases and then be released while that microphase degrades. Release profiles of Mito-Apo C2-encapsulated 20:80 CPH:SA polyanhydride NPs, a promising nanoscale platform for CNS delivery, have shown compatibility with the SA microphase [40], which degrades faster

than the CPH microphase. This rapid timescale of drug release with this specific drug and chemistry combination is favorable for treatment of oxidative stress-induced toxicity following acute toxic exposure. In addition to the other advantages of polyanhydrides listed above, this platform is a lead candidate for CNS delivery strategies.

2.4 CNS Targeting Strategies

Designing a nanoscale delivery platform that can more effectively cross the complex hurdles in CNS drug delivery (Fig. 2.1) using targeting ligands is essential. Numerous studies and reviews have investigated strategies for targeting one of these hurdles. A summary of several of these solutions can be found in Table 2.1. However, few studies have looked at targeting two and even fewer looked at targeting all three with the same platform. The following section discusses targeting strategies that have been used at each scale, with the goal of being able to rationally design a CNS delivery platform by synthesizing these strategies to optimize a delivery platform.

2.4.1 Blood-brain barrier

The use of targeting ligands to improve the targeting capability of the platform at each level of CNS delivery is imperative for good drug pharmacodynamics. The first hurdle for CNS therapeutics is often the BBB. Parenterally, orally or intravenously administered therapeutics intended for CNS delivery must cross the BBB from the circulation, and to do so, cross BBB endothelial cells. These cells reject transport of most small molecules because of strong tight junctions that are influenced by interaction with glial cells in the NVU and leave little space for paracellular transport [64,107–109]. Extracellular proteins on these

endothelial cells, called efflux pumps, reject small molecule transport, further complicating delivery [64,110].

There are three primary ways by which targeting ligands can improve BBB targeting. These include receptor-, adsorptive-, and cell-mediated transcytosis [64,110]. These mechanisms utilize compositional features of the BBB, such as the high concentration of a particular cell-surface receptor, to improve localization. In addition, the diseased state often has characteristics that targeting ligands can exploit. This may include targeting immune cells during the inflammatory response to facilitate passage across the BBB through these cells as they travel to the site of injury; these cells can be targeted and used to deliver therapeutics across the BBB. Weakened BBB tight junctions in the diseased state may also enhance the paracellular transport rate [110]. In the context of nerve agent exposure, however, these symptoms often do not become severe until chronic neurodegeneration, and therefore may be more difficult to utilize for drug delivery [109]. Nevertheless, the following sections detail methods for targeting using each of the three mechanisms.

2.4.1.1 Receptor-mediated strategies

Receptor-mediated transcytosis mechanisms for therapeutic delivery platforms exploit the endocytic mechanisms of cell-surface receptors existing at the BBB using the appropriate receptor-targeted ligands. Targeting in such a way minimizes therapeutic circulation time. The sugars di-mannose, galactose and glycolic acid have been employed to target lectin receptors [111]. Additionally, receptors for folic acid (FA) and des-octanoyl ghrelin exist in large quantities on the surface of BBB endothelial cells and as such have been incorporated in several drug delivery studies [40,107,112–114].

Some receptor-mediated strategies utilize proteins that have an affinity for BBB cell surface receptors. Some protein-incorporated strategies utilize apolipoproteins A, B, and E, α 2-macroglobulin, and angiopep-2 for targeting the low-density lipoprotein receptor [102–104,115,116]. The glycoprotein 330/megalin receptor can be targeted using apolipoprotein J, and scavenger receptor class A by fucoidin [115]. Interleukin 13 (IL-13) protein can be used target the IL-13 receptor on the BBB [117,118]. Additionally, Intracellular adhesion molecule-1 (ICAM-1) is a receptor expressed on the BBB and can be targeted to improve localization [6,8,115].

Targeting the transferrin receptor is a common BBB targeting strategy. One study found specific CNS localization compared to other organs after conjugating an anti-mouse transferrin receptor monoclonal antibody to a chitosan nano-sphere formulation coated with PEG [119]. A review details that both transferrin and insulin receptors have been targeted using a particular monoclonal antibody, 83-14 MAb [120]. The transferrin and lactoferrin glycoproteins, and a transferrin binding antibody OX-26 have all been used in BBB models [64,121,122]. The OX26 monoclonal antibody has also been used to target the transferrin receptor on the BBB *in vitro* [123]. Other targeting strategies incorporated targeting ligands for both the transferrin receptor (for BBB targeting) as well as for aggregated protein deposits (for neuronal targeting) [68,124–127].

Polymeric or surfactant coatings can also increase localization at the BBB level. Many of these methods demonstrate indirect targeting through the adsorption of serum proteins that will then target a receptor on the BBB. Surfactants Tween-20 and Tween-80 have shown the ability to do so by absorbing serum-rich apolipoproteins that target the BBB

[79,102]. Alternatively, polyethylene glycol (PEG) is used in many formulations incorporating targeting mechanisms to prolong circulation half-life [64,128,129].

2.4.1.2 Adsorptive-mediated strategies

Adsorptive mediated strategies target the BBB by affinity with and adsorption to the lipid membrane. Several peptides have demonstrated the ability to improve targeting using this mechanism [130]. The streptavidin-binding peptide (SBP), fibronectin-binding peptide (FBP), multiple antigenic peptides (MAPs), trans-activating transcriptional activator (TAT), transportan, insulin, pAntp, rabies virus glycoprotein, angiopep, penetratin, SynB1, and SynB3 have all been used to improve therapeutic CNS delivery [64,82,83,131,132]. TAT peptide is a well-researched peptide for cerebral delivery for its ability to enhance BBB passage [131]. BBB shuttle peptides increase therapeutic delivery across the BBB by transcytosis through endocytic vesicles, and are discussed in a recent review [109].

The cationic and lipophilic ligand TPP is a promising molecule for promoting adsorptive-mediated transcytosis at the BBB. A recently submitted patent by Dhar et al. shows that a TPP-functionalized NP has brain-specific bioavailability compared to the same NP platform without functionalization [133]. This work evaluated localization using a porcine model [133]. In this model, drug efficacy and localization was evaluated after traumatic brain injury, with similar downstream pathologies to chemical exposure [133].

2.4.1.3 Cell-mediated strategies

After brain injury, immune cells are recruited into the brain as part of the inflammatory response. These immune cells can internalize the nanoscale delivery platform

as a “Trojan horse” strategy where these cells then guide the platform into the CNS and release them after crossing the BBB. A recent review details strategies that have investigated this mechanism [134]. A major example in this field involves targeting the folate receptor on immune cells by conjugating FA to NPs to combat human immunodeficiency virus (HIV) [135–139].

In one study, conjugation of FA to poloxamer 407, in an antiretroviral NP formulation, improved uptake by mononuclear phagocytes *in vitro*, reduced the amount of HIV-1 gag expression (a marker for HIV pathogenesis) in the brain, and demonstrated enhanced brain uptake *in vivo* in mice compared to non-functionalized NPs [135]. A later study by the same group tested lead candidates and found enhanced uptake and prolonged retention *in vitro* and *in vivo*, as well as increased protection *in vitro* [138]. Similar results were obtained with these lead candidates in a primate model [136]. The group further investigated FA for combating HIV-1p24 antigen [137]. Dose-sparing, in addition to increased overall pharmacokinetics and pharmacodynamics, were observed when coating the lead formulation with FA, specifically by increasing uptake by the folate receptor β [137]. Importantly, dose-sparing was observed in this platform in an *in vivo* mouse model [139]. Overall, cell-mediated transcytosis offers a unique and effective strategy for targeting the BBB, when choosing an appropriate targeting ligand.

2.4.1.4 Other strategies

Alternatively, BBB tight junctions can be disrupted to promote paracellular transport. Granulocyte macrophage colony-stimulating factor (GM-CSF) enhanced BBB transport by activation of monocytes that occurred due to the activation of several expression pathways;

this was coupled with a disruption of BBB tight junctions [140]. Ultrasound has also been used to disrupt the BBB and allow therapeutic delivery [141]. However, these methods are risky because they damage the normal protective function of the BBB that then exposes the brain to other potential toxins.

2.4.1.5 Obstacles for BBB targeting

Issues with ligand specificity are important to consider for platform design. For example, receptor-mediated targeting ligands that improve transcytosis at the BBB often have receptors that are ubiquitous throughout the body [6]. Adsorptive-mediated targeting may experience similar issues with specificity. Poor specificity often necessitates higher dosing and often leads to systemic toxicity. Therefore, the choice of the nanoscale delivery platform is important, to reduce the amount and frequency of doses and improve specificity.

For degradable delivery platforms conjugated to a targeting ligand, incomplete purification may result in an excess of the targeting moiety in the surrounding fluid. It is possible that in this case, the targeting ligand may outcompete the platform for entry [138]. Purification of the platform from the free targeting ligand is important to avoid this possibility. In addition, retention of the targeting ligand throughout degradation of the biodegradable platform is important so that hurdles downstream of the BBB can also be effectively targeted. This requires careful design of the way the ligand is conjugated to the platform. For example, ligands conjugated onto the surface of the platform may not retain the ligand long enough to target these downstream hurdles, but ligands conjugated into the bulk may display longer retention and therefore more effectively target these hurdles.

2.4.2 Diseased neuron

Once a delivery platform is inside the CNS after crossing the BBB, it must then localize to the diseased neuron. Several strategies exist for targeting the neuron, and will be discussed below. In some cases, these strategies may be disease-specific.

In PD, mutations of the LRRK2 gene/receptor often lead to LB formation [142]. Studies have therefore targeted LBs to improve efficacy [31]. One example of such a targeting strategy is to target α -synuclein, the aggregation of which into LBs is often a symptom of PD [36]. Antibodies can be engineered to target these deposits, although it is important with these strategies to ensure specified delivery of the therapeutic to only diseased neurons [31].

Likewise, the formation of A β deposits that disrupt synaptic communication is common in AD. Several targeting strategies have therefore used ligands to target these deposits. For example, a study incorporated an anti-A β peptide antibody along with an anti-transferrin receptor monoclonal antibody, on a polyethylene glycol-modified liposomal platform to improve delivery [124]. There was an interplay where the conjugation method for each antibody affected cellular uptake [124]. The same group later tested improvements in efficacy of a drug to treat A β aggregation in an AD model, again using dual functionalization of both anti-transferrin and anti-A β antibodies, but this time with PLGA NPs [78].

Curcumin can also increase targeting of A β deposits in AD. A multifunctional liposomal formulation incorporating curcumin to target neurons, with a transferrin antibody to target the BBB, showed enhanced localization at both levels [68]. Previous work by this group also showed improved targeting of liposomal-curcumin derivative formulations for A β

fibrils [125]. Yet another study focused on A β targeting by conjugating an A β -binding aptamer to curcumin-PLGA NPs and found success with this strategy [32].

Bispecific antibodies are a recent strategy that can potentially provide more efficacious therapeutic delivery. A study on such a platform found that there is an interplay between the dosing and antibody affinity for the targeted receptor, whereby low-affinity antibodies may be more effective in standard therapeutic dosing concentrations [126]. A different study evaluated these antibodies in a primate model, showing enhanced BBB passage and ability to target β -secretase, which is associated with A β deposition in AD, again showing lower affinity antibodies were more effective at localization [127]. While the use of antibodies as targeting ligands offers its own challenges in device design, including their size and complexity, antibody engineering can enable high specificity for the desired target and may be a promising option for CNS delivery [143].

Specific receptors on neurons have also been targeted to improve localization. The toll-like receptor 2 is commonly expressed on neurons in PD and AD, and therefore could be targeted to enhance drug delivery [30,36]. The gamma-aminobutyric acid (GABA) and dopamine receptors are specific to patients with Huntington's disease and PD, respectively, and accordingly offer other targeting strategies for these diseases [144,145]. NMDA receptors may additionally be an effective neuronal receptor targeting strategy due to their ubiquitous nature on neurons [145,146]. A particular study used the NMDA receptor 1 antibody, anti-NR1R, to improve drug pharmacokinetics [147]. An informative review details methods for synthesizing prodrug/antibody delivery platforms to target other neurotransmitter receptors, such as GABA, AMP and non-NMDA glutamate receptors [145].

In addition to BBB targeting, FA has shown enhanced targeting at the neuronal level [40]. After challenging with an oxidative stress-inducing toxin, protection against oxidative stress in an FA-conjugated polyanhydride NP platform was improved compared to the non-functionalized formulation [40]. Due to the ability to target multiple hurdles to CNS delivery, FA may be a promising option for conjugation to a delivery platform.

There are also hurdles with neuronal delivery that must be considered during platform design. As with BBB receptor-mediated strategies, specificity of receptor-mediated targeting ligands can play a role in overall efficacy. In the example of NMDA receptor targeting methods, the diseased neuron may show an up-regulation of this receptor [145,146]. However, the NMDA receptor is a necessary component of all neuronal synapses, and may deliver drug to unintended neuron populations, in addition to the diseased neuron. Depending on the disease condition, protein deposits in the extracellular matrix may hinder efficient neuronal targeting and internalization [24–26].

2.4.3 Intracellular organelles

The final hurdle to therapeutic delivery is targeting the payload to the desired organelle within the neuron. Therapeutic efficacy can be maximized by delivering the therapeutic payload to the organelle of action within the cell [3]. The scale of impact of organelle delivery is significantly smaller than the previous hurdles: whereas neuronal cell bodies can have a surface area on the order of tens to hundreds of square microns, the most relevant organelles for neurodegenerative disease, the mitochondria and nucleus, typically have surface areas of one to tens of square microns. For example, mitochondria are approximately 75-3.0 square microns in size, which limits the functional surface area for

interaction [148]. At this scale, physical and chemical properties play a larger influence on the success of targeting than seen at the other levels. Whereas crossing the BBB and neuron rely on protein-ligand or membrane interactions, size, morphology, and charge are primary determinants of intracellular accumulation. While a fair amount of work has been devoted to organelle-specific delivery in the CNS, the large majority has focused on other tissue types. Recent techniques for organelle-specific delivery are reviewed below, and their implications for treatment of neurodegenerative conditions are extrapolated.

2.4.3.1 Endocytic pathway

The primary concern in designing organelle-specific delivery devices is surviving the endocytic pathway. Nanoscale delivery platforms that exploit receptor-mediated endocytosis to navigate through the cell must be able to protect their payload from acidic hydrolysis and escape from endosomes and lysosomes. Several techniques for endosomal escape of delivery platforms have been developed (Fig. 2.2). Functionalization with certain classes of peptides, like cationic amphiphilic peptides, provide strong association with the endosomal membrane, which disrupts tension forces that stabilize the endosome resulting in pore formation [149]. Other approaches incorporate release of photoreactive molecules that degrade the endosomal membrane via production of ROS [149]. Alternatively, decoration with buffering agents such as quaternary and tertiary amines can cause an immense inflow of ions and water, which can rupture the endosome membrane due to osmotic pressure; this is commonly referred to as the “proton sponge effect” [149]. For more information, Varkouhi et al. have written an excellent review on ligands available for endosomal escape [149]. Once the delivery device has

escaped the endocytic pathway, other functionalizations or core properties of the platform can mediate transport to the therapeutic organelle of action.

2.4.3.2 Mitochondria

Mitochondrial dysfunction due to oxidative stress is a key pathogenetic pathway for many neurodegenerative diseases. Several therapeutics have been developed to halt or reverse this pathogenesis by interfering with production of superoxide groups. Mitochondria are bound by an inner and outer membrane and have a large transmembrane potential of approximately -180-200 mV [150]. Because of this membrane potential, charged molecules can efficiently localize at the surface of the mitochondria. However, the inner membrane is impervious to charged molecules, which precludes transport to the mitochondrial matrix [150]. These competing requirements are a central challenge for mitochondria-targeted delivery.

Many technologies can be utilized to circumvent this mitochondrial trafficking challenge, the pathway for which is shown in Figure 2.2. An informative review details several methods for targeting the mitochondria [151]. The predominant technique is to conjugate a cationic molecule, such as TPP, to lipophilic platform materials [3,152]. This allows the carrier to be localized to the mitochondria through electrostatic attraction and subsequent permeation of the lipid bilayers by the delivery platform while the cation remains anchored outside the inner membrane [3]. Alternate strategies involve functionalization with ligands for mitochondrial receptors, like the translocator protein (TPSO) [153].

The cationic ligand TPP has demonstrated superior mitochondrial targeting capabilities [3,152]. The cationic properties of TPP may make the delivery platform act as a

proton sponge to escape the endosome inside the neuron. Afterwards, the negative mitochondrial membrane potential will attract the TPP-conjugated platform, where the therapeutic can then be released and internalized [3]. Because of the proven ability to also target and cross the BBB [133] as well as show enhanced neuronal internalization for better protection against oxidative stress using Mito-Apo both in vitro and in vivo [23,43,55], TPP is an excellent option for improving CNS delivery of antioxidants.

It is challenging to determine, however, what qualifies as successful mitochondrial delivery. A large body of work in this field depicts accumulation of delivery devices at the mitochondria, but don't conclusively show that the devices can cross the inner membrane for delivery. While some therapeutics may be able to enter the mitochondria passively given sufficient localization near the organelle, others may require a more active role from the delivery device. This must be carefully considered in platform design.

2.4.3.3 Nucleus

The nucleus can also be an important target for anti-neurodegenerative therapeutics. For example, RNA interference-inducing molecules could allow translational repression of problematic proteins, but must be delivered to the nucleus for processing via Drosha [154]. Alternative treatments include delivery of gene therapies to upregulate expression of regenerative neurotrophic factors in afflicted cells, which require nuclear localization for transcription and translation of the encoded proteins [155]. Additionally, nuclear delivery of genome editing technologies like CRISPR/Cas could allow development of new models of neurodegenerative disease, which could assist development of the next generation of neurodegenerative therapeutics [156]. By integrating nuclear delivery with neuronal delivery,

the off-target effects of this technology could potentially be mitigated, strengthening its potency as a transcription repression-based therapeutic [157].

Efficient nuclear delivery must also address trafficking issues downstream of endosomal/lysosomal escape, in this case to cross the nuclear envelope. Nuclear uptake is mediated by the nuclear pore complex (NPC), which can facilitate both passive and active transport of payloads [158]. Passive transport through the NPC has an effective diameter limit of approximately 9 nm, which means that most small molecule payloads can enter the nucleus without assistance from the carrier, given appropriate localization to the vicinity of the nuclear envelope [159]. Indeed, Shi et al. reported high nuclear localization of plasmid DNA in a DNA/ 25 kDa polyethylenimine polyplex despite a significant diversion of polymer into endosomal and lysosomal cell compartments [160]. Active transport, on the other hand, requires conjugation to a nuclear localization sequence (NLS) and can accommodate molecules up to 40-60 nm in diameter [158]. These NLSs are typically peptides of viral origin containing basic residues that bind NPCs for transport [3]. The most frequently used NLSs are SV40 peptide from simian virus 40 and TAT peptide from HIV-1 [161–163].

Transport of larger macromolecules into the nucleus poses a challenge, since many nano-carrier solutions are on the order of 50-200 nm in diameter. This limit can be increased by exploiting mitotic vulnerabilities in the nuclear membrane. However, this effect is modest, which still could exclude certain delivery platforms [164]. The non-proliferative nature of differentiated neurons further limits this technique's applicability for neurodegenerative condition applications [165]. However, recent experiments have found that particle shape may be able to mitigate this size exclusion effect. Experiments by Chaturbedy et al. using

Fe₃O₄ NPs of different morphologies found that biconcave-shaped 220 nm-diameter NPs achieved relatively high levels of nuclear localization efficiency in U87 MG glial cells, especially when compared to cylindrical and spherical particles of similar hydrodynamic diameter [132]. This effect could greatly diversify the palette of delivery tools for nuclear delivery. These mechanisms for nuclear targeting are summarized in Figure 2.2.

2.4.3.4 Obstacles for organelle targeting

There are several challenges to organelle-specific delivery. Firstly, the therapeutic mechanism of action must be understood to identify appropriate organelle targets, which can be a significant challenge for newly discovered drugs or those with complex interactions. Additionally, pathological deficiencies associated with neurodegenerative disease can limit intracellular transport. For example, Zhao et al. identified deficiencies in lysosomal transport in a murine model of AD, which could have implications for delivery device trafficking and escape from the endocytic pathway [166].

A large challenge at this point lies in the relatively small body of work performed in organelle-specific delivery. Most research at this scale relies on *in vitro* characterization, with little validation *in vivo* [167]. To further compound this issue, a vast majority of publications that utilize a functionalized nano-delivery system fail to investigate the efficiency of organelle targeting of their system, and instead rely on qualitative assessments such as disease phenotype reversal [167]. Ultimately, there is a lack of investigation into which components of the delivery system result in organelle targeting, which hinders the ability to rationally design a nano-carrier for specific applications [167].

Despite these shortcomings, the presented research has elucidated numerous mechanisms for improving localization of drug payloads at organelles of interest for neurodegenerative disease therapeutics. These functionalizations could potentially be combined with those highlighted in sections 2.3.1 and 2.3.2 to allow delivery devices to cross the BBB, and also effectively target the neuron and organelle. Regardless, both during and after the design of a platform, the method of administration must also be considered.

2.4.4 Delivery route

The delivery route also plays a significant role in drug efficacy for CNS delivery. The most common methods are intravenous (IV), intranasal (IN), and oral administration. Stereotaxy has even been used for treatment of brain cancer using biodegradable drug delivery materials, but is a very invasive procedure [98].

IN delivery is advantageous over other routes in that therapeutics delivered in this manner will follow a more direct route to the brain [168]. Instead of having to pass the BBB from the circulation, the therapeutic must instead pass through the olfactory and/or trigeminal nerve epithelial layers [130]. In addition, the comparatively slower mucociliary clearance rate of molecules at the nose-brain barrier (NBB) compared to circulatory clearance at the BBB may allow for greater uptake into these nerve epithelial layers [72].

There are, however, challenges with IN delivery. Achieving deposition on the olfactory region for proper administration of the therapeutic is very difficult [72,168]. Previous work has found that administration and plume angles of the nasal spray play a particularly relevant role in achieving optimal olfactory uptake, with 30° administration angles and <30° plume angles being most effective in these studies [169]. Therefore, IN

delivery may be a difficult procedure to replicate reliably when testing the efficacy of the delivery platform, compared to other targeting strategies.

In addition to difficulty in administration, platform efficacy may suffer without effective targeting ligands due to mucociliary clearance [72]. Chitosan [73,130] and solanum tuberosum lectin [72] are examples of NBB targeting ligands to avoid this issue. The TAT peptide is another ligand that can improve delivery across the NBB [76]. If the administration is performed reliably and an appropriate NBB-targeting ligand is incorporated onto the delivery platform, this method could be very effective at achieving great local drug bioavailability in the brain.

Another route that can be used for CNS delivery is oral administration. The biggest advantage of the oral delivery route is that it is minimally invasive and patient compliant [79]. However, therapeutics administered in this fashion will take a very long time to reach the CNS because they will go through the metabolic process. This involves passing through the stomach, which has an extremely acidic pH that could lead to therapeutic degradation [170]. Once reaching the circulatory system (often through the intestinal track), these therapeutics must then find their way to the BBB.

IV administration directly into the circulatory system, therefore bypassing some issue encountered with oral delivery, is another option. Therapeutics administered in this way must localize to and cross the BBB, like with oral delivery [171]. This route is much more reliable than IN delivery because of less specific administration parameters [171]. However, because IV injection requires skin penetration using a needle, it is significantly more invasive and may lead to poorer patient compliance compared to the other methods, particularly where repeat administrations are necessary [171]. Overall, the decision on delivery route is

important and could dictate or be dictated by the choice in targeting ligand and/or delivery platform, based on the hurdles encountered by that route.

2.5 Conclusions

Multiscale design strategies as outlined in this review offer the potential to maximize clinical translatability of nanoscale delivery platform technologies for therapeutic delivery in neurodegenerative disease. Polyanhydride NPs are an excellent platform choice, with tailorable release timescales, sustained therapeutic release, dose-sparing, superior phagocytic uptake, excellent biocompatibility, and versatility in the ability to conjugate targeting ligands. In addition, the targeting ligands FA and TPP are promising for the ability to target multiple of the physiological hurdles and as such are reasonable choices for conjugating to a polyanhydride NP platform. Overall, rational design of a platform incorporating these strategies could have tremendous implications for treatment of neurodegenerative disease, and requires testing at each scale *in vitro*.

2.6 Author Information

Corresponding Author:

S. Mallapragada, Department of Chemical and Biological Engineering, Iowa State University, 2031 Sweeney Hall, Ames, IA 50011, USA. Tel: +1 515 294 7407; e-mail: suryakm@iastate.edu.

2.7 Author Contributions

The authors for the manuscript titled “Cascading Multiscale Nanodelivery Devices for CNS Delivery of Regenerative Therapeutics” have given approval for the current version.

2.8 Tables and Figures

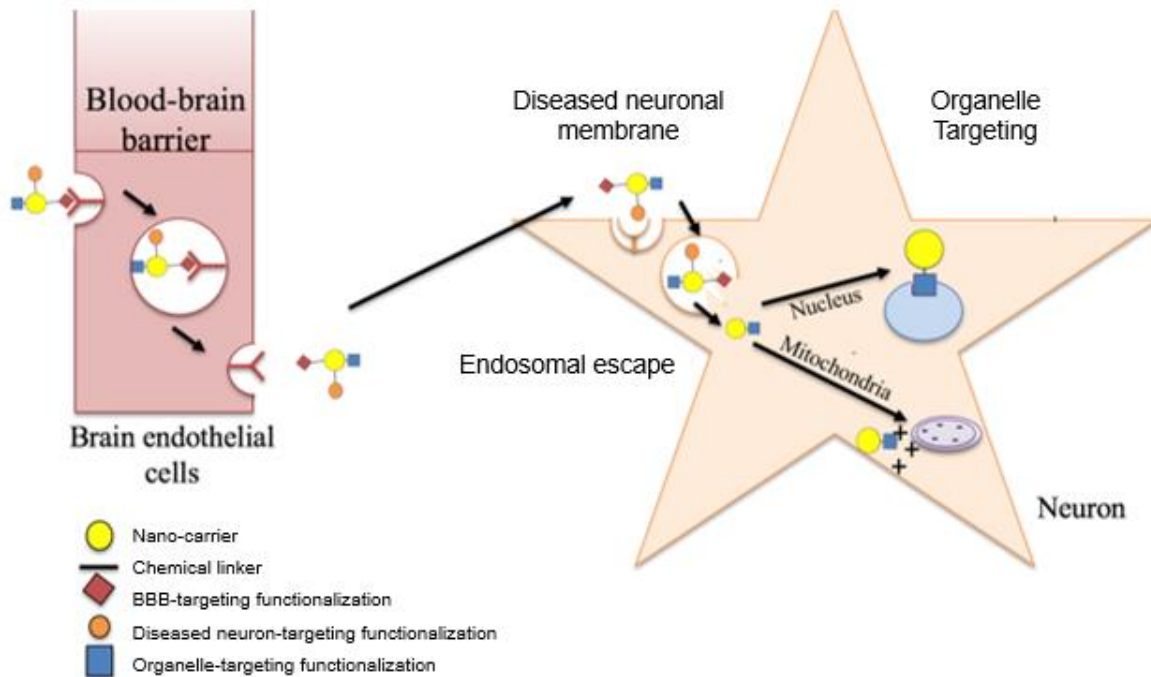


Figure 2.1. Organelle-specific delivery to neurons is a multiscale problem. To cross the BBB, and target the neuron and organelles within the neuron, a multifunctionalized delivery device must be used. Individual functionalizations can potentially cause off-target localization, so a cascading system of functionalizations with sheddable linkers is desired to maximize targeting efficiency. Modified from Chen et al, Li et al. [64,172].

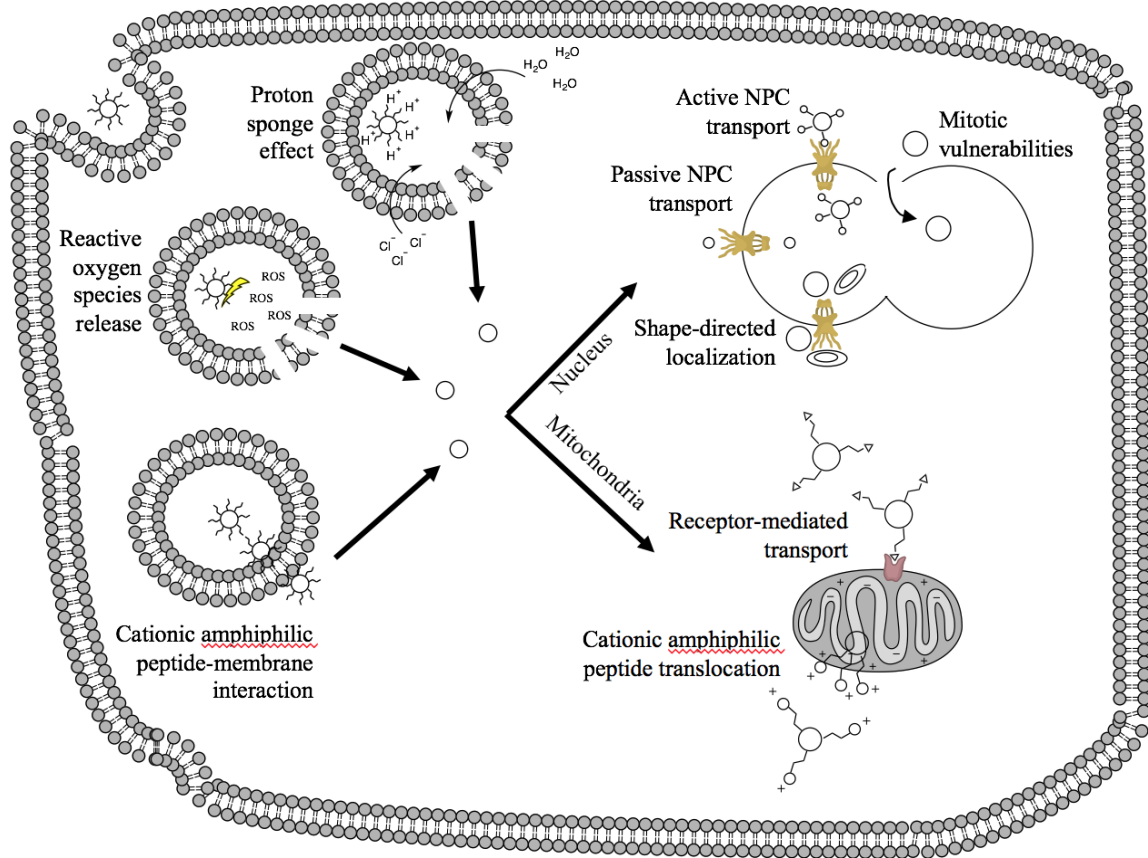


Figure 2.2. Organelle targeting mechanisms for neurodegenerative therapeutic delivery. Endosomal escape downstream of internalization is necessary for cytosolic trafficking to targeted organelles.

Table 2.1. General characteristics of functionalizations for multiscale delivery.

Physiological Hurdle	Mechanism	General characteristics	Examples	Pros	Cons	References
Blood Brain Barrier	Receptor-mediated endocytosis	Carbohydrate	FA, Mannose, Galactose	high expression of receptors, stable	limited selectivity	[40,107,111–114]
		Protein	apolipoprotein, fucoidin, IL-13, angiopep-2, rabies virus glycoprotein	highly specific	limited stability	[7,64,102–104,115–118,121,122]
			Antibodies (OX-26, anti-transferrinR, 83-14 Mab, anti-ICAM-1)	highly specific	limited stability	[6,8,115,119,120,173]
		Peptide	lipoprotein receptor binding sequence, K16ApoE peptide	greater stability		[174]
		Coating	(PEG, SiO ₂ , Tween-20, Tween-80)	outer coating shed ability	limited selectivity	[64,79,102,128,129]
	Adsorptive-mediated endocytosis	Peptide	TAT peptide, transportan, insulin, FBP, MAP, SBP, SynB1, SynB3	greater stability	limited selectivity, systemic toxicity	[64,82,83,131,132]

Table 2.1 continued

Physiological Hurdle	Mechanism	General characteristics	Examples	Pros	Cons	References
Neuron	Receptor-mediated endocytosis	Carbohydrate	FA, Mannose, Galactose	high expression, stable	limited selectivity	[175,176]
		Neurotransmitter	GABA, glutamate, acetylcholine	greater selectivity	interference with signaling	[145]
		Protein	anti-NR1R	highly specific	limited stability	[147]
	Adsorptive-mediated endocytosis	Peptide	TAT peptide, transportan, insulin, FBP, MAP, SBP, SynB1, SynB3	greater stability	limited selectivity, systemic toxicity	
Endosomal Escape	Proton sponge effect	buffering at pH 7.2-5	polyethylenimine, imidazole		[149]	
	Release of ROS	photosensitizer, singlet oxygen production	TPPS ₄ , AlPcS _{2a} , dendrimer phthalocyanine		[149]	
	Pore formation	cationic amphiphilic peptides	penton base, melittin		[149]	

Table 2.1 continued

Physiological Hurdle	Mechanism	General characteristics	Examples	Pros	Cons	References
Organelle	Nucleus					
	passive NPC transport	< 9 nm		fewer chemical modifications	steric limitation	[159]
	active NPC transport	40-60 nm, NLS		greater size capacity	steric limitation	[161–163]
	mitotic vulnerabilities	replicating cells		greater size capacity	exclusive to mitotic cells	[164,165]
	shape-directed localization	biconcave, spherical morphology		fewer chemical modifications, greater size capacity	platform material dependence	[132]
	Mitochondria					
	electrostatic attraction	cationic amphiphilic peptides	TPP, TAT	increased cytoplasmic transport	toxicity, protein aggregation	[3]
receptor-mediated transport	mitochondrial receptor ligand	TPSO ligand	high selectivity		[153]	

2.9 References

- [1] Kondo K 1996 Rising Prevalence of Neurodegenerative Diseases Worldwide *J. Intern. Med.* **35** 238
- [2] Bird S, Traub S J and Grayzel J 2014 Organophosphate and carbamate poisoning *UpToDate* **14** 339
- [3] Biswas S and Torchilin V P 2014 Nanopreparations for organelle-specific delivery in cancer *Adv. Drug Deliv. Rev.* **66** 26–41
- [4] Agarwal R and Roy K 2013 Intracellular delivery of polymeric nanocarriers: a matter of size, shape, charge, elasticity and surface composition. *Ther. Deliv.* **4** 705–23
- [5] Hashida M, Nishikawa M, Fumiyoshi Y and Takakure Y 2001 Cell-specific delivery of genes with glycosylated carriers *Adv. Drug Deliv. Rev.* **52** 187–96
- [6] Jones A R and Shusta E V 2007 Blood-brain barrier transport of therapeutics via receptor-mediation. *Pharm. Res.* **24** 1759–71
- [7] Xin H, Sha X, Jiang X, Zhang W, Chen L and Fang X 2012 Anti-glioblastoma efficacy and safety of paclitaxel-loading Angiopep-conjugated dual targeting PEG-PCL nanoparticles *Biomaterials* **33** 8167–76
- [8] Hsu J, Hoenicka J and Muro S 2015 Targeting, endocytosis, and lysosomal delivery of active enzymes to model human neurons by ICAM-1-targeted nanocarriers. *Pharm. Res.* **32** 1264–78
- [9] National Institute of Neurological Disorders and Stroke, NINDS Overview, (2014). <https://www.ninds.nih.gov/About-NINDS/Who-We-Are>
- [10] van Uem J, Marinus J, Canning C, van Lummel R, Dodel R, Liepelt-Scarfone I, Berg D, Morris M E and Maetzler W 2015 Health-related quality of life in patients with Parkinson's disease - a systematic review based on the ICF model. *Neurosci. Biobehav. Rev.* **61** 26–34
- [11] Chekani F, Bali V and Aparasu R R 2015 Quality of life of patients with Parkinson's disease and neurodegenerative dementia: A nationally representative study *Res. Soc. Adm. Pharm.* **12** 604–13
- [12] Pagnini F 2013 Psychological wellbeing and quality of life in amyotrophic lateral sclerosis: a review. *Int. J. Psychol.* **48** 194–205

- [13] Kowal S L, Dall T M, Chakrabarti R, Storm M V and Jain A 2013 The current and projected economic burden of Parkinson's disease in the United States. *Mov. Disord.* **28** 311–8
- [14] Brown R C, Lockwood A H and Sonawane B R 2005 Neurodegenerative diseases: an overview of environmental risk factors. *Environ. Health Perspect.* **113** 1250–6
- [15] Lin M T and Beal M F 2006 Mitochondrial dysfunction and oxidative stress in neurodegenerative diseases. *Nature* **443** 787–95
- [16] Singh M, Kaur M, Kukreja H, Chugh R, Silakari O and Singh D 2013 Acetylcholinesterase inhibitors as Alzheimer therapy: From nerve toxins to neuroprotection *Eur. J. Med. Chem.* **70** 165–88
- [17] Norenberg M D and Rama Rao K V 2007 The mitochondrial permeability transition in neurologic disease *Neurochem. Int.* **50** 983–97
- [18] Chen Y 2012 Organophosphate-induced brain damage: Mechanisms, neuropsychiatric and neurological consequences, and potential therapeutic strategies *Neurotoxicology* **33** 391–400
- [19] Lewerenz J and Maher P 2015 Chronic Glutamate Toxicity in Neurodegenerative Diseases—What is the Evidence? *Front. Neurosci.* **9** 469
- [20] Reyes R C, Brennan A M, Shen Y, Baldwin Y and Swanson R A 2012 Activation of neuronal NMDA receptors induces superoxide-mediated oxidative stress in neighboring neurons and astrocytes. *J. Neurosci.* **32** 12973–8
- [21] Singhal A, Morris V B, Labhasetwar V and Ghorpade A 2013 Nanoparticle-mediated catalase delivery protects human neurons from oxidative stress *Cell Death Dis.* **4** e903
- [22] Yuste J E, Tarragon E, Campuzano C M and Ros-Bernal F 2015 Implications of glial nitric oxide in neurodegenerative diseases. *Front. Cell. Neurosci.* **9** 322
- [23] Ghosh A, Langley M R, Harischandra D S, Neal M L, Jin H, Anantharam V, Joseph J, Brenza T, Narasimhan B, Kanthasamy A, Kalyanaraman B and Kanthasamy A G 2016 Mitoapocynin Treatment Protects Against Neuroinflammation and Dopaminergic Neurodegeneration in a Preclinical Animal Model of Parkinson's Disease *J. Neuroimmune Pharmacol.* **11** 259–78
- [24] Dauer W and Przedborski S 2003 Parkinson's Disease: Mechanisms and Models *Neuron* **39** 889–909
- [25] Hardy J and Selkoe D J 2002 The amyloid hypothesis of Alzheimer's disease: progress and problems on the road to therapeutics. *Science* **297** 353–6

- [26] Kilpatrick K, Zeng Y, Hancock T and Segatori L 2015 Genetic and chemical activation of TFEB mediates clearance of aggregated alpha-synuclein *PLoS One* **10** 1–21
- [27] Banks W A 2012 Drug delivery to the brain in Alzheimer's disease: Consideration of the blood-brain barrier *Adv. Drug Deliv. Rev.* **64** 629–39
- [28] Jämsä A, Hasslund K, Cowburn R F, Bäckström A and Vasänge M 2004 The retinoic acid and brain-derived neurotrophic factor differentiated SH-SY5Y cell line as a model for Alzheimer's disease-like tau phosphorylation. *Biochem. Biophys. Res. Commun.* **319** 993–1000
- [29] Rahimi J and Kovacs G G 2014 Prevalence of mixed pathologies in the aging brain. *Alzheimers. Res. Ther.* **6** 82
- [30] Limor R, Janice K and Kiran B 2015 The neuropathology and cerebrovascular mechanism of dementia *J. Cereb. Blood Flow Metab.* **1**
- [31] Kovacs G 2016 Molecular Pathological Classification of Neurodegenerative Diseases: Turning towards Precision Medicine *Int. J. Mol. Sci.* **17** 189
- [32] Mathew A, Aravind A, Brahatheeswaran D, Fukuda T, Nagaoka Y, Hasumura T, Iwai S, Morimoto H, Yoshida Y, Maekawa T, Venugopal K and Sakthi Kumar D 2012 Amyloid-binding aptamer conjugated curcumin-PLGA nanoparticle for potential use in Alzheimer's disease *Bionanoscience* **2** 83–93
- [33] Perrett R M, Alexopoulou Z and Tofaris G K 2015 The endosomal pathway in Parkinson's disease *Mol. Cell. Neurosci.* **66** 21–8
- [34] Ghosh A, Saminathan H, Kanthasamy A, Anantharam V, Jin H, Sondarva G, Harischandra D S, Qian Z, Rana A and Kanthasamy A G 2013 The peptidyl-prolyl isomerase pin1 up-regulation and proapoptotic function in dopaminergic neurons: Relevance to the pathogenesis of parkinson disease *J. Biol. Chem.* **288** 21955–71
- [35] Ganesan P, Ko H M, Kim I S and Choi D K 2015 Recent trends in the development of nanophytobioactive compounds and delivery systems for their possible role in reducing oxidative stress in Parkinson's disease models *Int. J. Nanomedicine* **10** 6757–72
- [36] Béraud D and Maguire-Zeiss K A 2012 Misfolded α -synuclein and toll-like receptors: therapeutic targets for Parkinson's disease *Parkinsonism Relat. Disord.* **18** S17–20
- [37] Harischandra D S, Jin H, Anantharam V, Kanthasamy A and Kanthasamy A G 2015 Alpha-Synuclein protects against manganese neurotoxic insult during the early stages

- of exposure in a dopaminergic cell model of Parkinson's disease *Toxicol. Sci.* **143** 454–68
- [38] Loescher W 2015 Single versus combinatorial therapies in status epilepticus: Novel data from preclinical models *Epilepsy Behav.* **49** 20–5
- [39] Weissman B A and Raveh L 2008 Therapy against organophosphate poisoning: The importance of anticholinergic drugs with antiglutamatergic properties *Toxicol. Appl. Pharmacol.* **232** 351–8
- [40] Brenza T M, Ms S G, Ramirez J E V, Harischandra D, Anantharam V, Kalyanaraman B, Kanthasamy A G and Narasimhan B 2017 Neuronal Protection against Oxidative Insult by Polyanhydride Nanoparticle-based Mitochondria-targeted Antioxidant Therapy *Nanomedicine Nanotechnology, Biol. Med.* **13** 809–20
- [41] Zaja-Milatovic S, Gupta R C, Aschner M and Milatovic D 2009 Protection of DFP-induced oxidative damage and neurodegeneration by antioxidants and NMDA receptor antagonist *Toxicol. Appl. Pharmacol.* **240** 124–31
- [42] Jin H, Kanthasamy A, Ghosh A, Anantharam V, Kalyanaraman B and Kanthasamy A G 2014 Mitochondria-targeted antioxidants for treatment of Parkinson's disease: preclinical and clinical outcomes. *Biochim. Biophys. Acta* **1842** 1282–94
- [43] Dranka B P, Gifford A, McAllister D, Zielonka J, Joseph J, O'Hara C L, Stucky C L, Kanthasamy A G and Kalyanaraman B 2014 A novel mitochondrially-targeted apocynin derivative prevents hyposmia and loss of motor function in the leucine-rich repeat kinase 2 (LRRK2(R1441G)) transgenic mouse model of Parkinson's disease *Neurosci. Lett.* **583** 159–64
- [44] Anantharam V, Kaul S, Song C, Kanthasamy A and Kanthasamy A G 2007 Pharmacological inhibition of neuronal NADPH oxidase protects against 1-methyl-4-phenylpyridinium (MPP⁺)-induced oxidative stress and apoptosis in mesencephalic dopaminergic neuronal cells *Neurotoxicology* **28** 988–97
- [45] Cristovao A C, Choi D-H, Baltazar G, Beal M F and Kim Y-S 2009 The Role of NADPH Oxidase 1-Derived Reactive Oxygen Species in Paraquat-Mediated Dopaminergic Cell Death *Antioxid. Redox Signal.* **11** 2105–18
- [46] Gao H, Liu B, Zhang W and Hong J 2003 Critical role of microglial NADPH oxidase-derived free radicals in the in vitro MPTP model of Parkinson's disease *FASEB J.* **17** 1954–6
- [47] Wang X-H, Peng H-S, Yang L, You F-T, Teng F, Tang A-W, Zhang F-J and Li X-H 2013 Poly-L-lysine assisted synthesis of core-shell nanoparticles and conjugation with triphenylphosphonium to target mitochondria *J. Mater. Chem. B* **1** 5143–52

- [48] Biswas S, Dodwadkar N S, Piroyan A and Torchilin V P 2012 Surface conjugation of triphenylphosphonium to target poly(amidoamine) dendrimers to mitochondria *Biomaterials* **33** 4773–82
- [49] Bielski E R, Zhong Q, Brown M and Da Rocha S R P 2015 Effect of the Conjugation Density of Triphenylphosphonium Cation on the Mitochondrial Targeting of Poly(amidoamine) Dendrimers *Mol. Pharm.* **12** 3043–53
- [50] Marrache S and Dhar S 2012 Engineering of blended nanoparticle platform for delivery of mitochondria-acting therapeutics *Proc. Natl. Acad. Sci. U. S. A.* **109** 16288–93
- [51] Powell R D, Swet J H, Kennedy K L, Huynh T T, Murphy M P, Mckillop I H and Evans S L 2015 MitoQ modulates oxidative stress and decreases inflammation following hemorrhage *J Trauma Acute Care Surg* **78** 573–9
- [52] Theodossiou T A, Sideratou Z, Tsiourvas D and Paleos C M 2011 A novel mitotropic oligolysine nanocarrier: Targeted delivery of covalently bound D-Luciferin to cell mitochondria *Mitochondrion* **11** 982–6
- [53] Kelso G F, Porteous C M, Hughes G, Ledgerwood E C, Gane A M, Smith R A J and Murphy M P 2002 Prevention of Mitochondrial Oxidative Damage Using Targeted Antioxidants *New York Academy Sci.* **959** 263–74
- [54] Wladyka C L and Kunze D L 2006 KCNQ/M-currents contribute to the resting membrane potential in rat visceral sensory neurons *J. Physiol.* **575** 175–89
- [55] Langley M, Ghosh A, Charli A, Sarkar S, Ay M, Luo J, Zielonka J, Brenza T, Bennett B, Jin H, Ghaisas S, Schlichtmann B, Kim D, Anantharam V, Kanthasamy A, Narasimhan B, Kalyanaraman B and Kanthasamy A 2017 Mito-apocynin Prevents Mitochondrial Dysfunction, Microglial Activation, Oxidative Damage and Progressive Neurodegeneration in MitoPark Transgenic Mice *Antioxid. Redox Signal.* **7**, accepted
- [56] Miquel E, Cassina A, Martínez-Palma L, Souza J M, Bolatto C, Rodríguez-Bottero S, Logan A, Smith R A J, Murphy M P, Barbeito L, Radi R and Cassina P 2014 Neuroprotective effects of the mitochondria-targeted antioxidant MitoQ in a model of inherited amyotrophic lateral sclerosis *Free Radic. Biol. Med.* **70** 204–13
- [57] McManus M J, Murphy M P and Franklin J L 2011 The Mitochondria-Targeted Antioxidant MitoQ Prevents Loss of Spatial Memory Retention and Early Neuropathology in a Transgenic Mouse Model of Alzheimer's Disease *J. Neurosci.* **31** 15703–15

- [58] Ghosh A, Chandran K, Kalivendi S V., Joseph J, Antholine W E, Hillard C J, Kanthasamy A, Kanthasamy A and Kalyanaraman B 2010 Neuroprotection by a mitochondria-targeted drug in a Parkinson's disease model *Free Radic. Biol. Med.* **49** 1674–84
- [59] Smith R A J and Murphy M P 2010 Animal and human studies with the mitochondria-targeted antioxidant MitoQ. *New York Academy Sci.* **1201** 96–103
- [60] Nygaard H B, Wagner A F, Bowen G S, Good S P, MacAvoy M G, Strittmatter K A, Kaufman A C, Rosenberg B J, Sekine-Konno T, Varma P, Chen K, Koleske A J, Reiman E M, Strittmatter S M and van Dyck C H 2015 A phase Ib multiple ascending dose study of the safety, tolerability, and central nervous system availability of AZD0530 (saracatinib) in Alzheimer's disease. *Alzheimers. Res. Ther.* **7** 35
- [61] Elezgarai S R and Biasini E 2016 Common therapeutic strategies for prion and Alzheimer's diseases *Biol Chem* **397** 1115–24
- [62] Málaga-Trillo E and Ochs K 2016 Uncontrolled SFK-mediated protein trafficking in prion and Alzheimer's disease. *Prion* **6896** 0
- [63] Devi L and Ohno M 2016 Cognitive benefits of memantine in Alzheimer's 5XFAD model mice decline during advanced disease stages. *Pharmacol. Biochem. Behav.* **144** 60–6
- [64] Chen Y and Liu L 2012 Modern methods for delivery of drugs across the blood-brain barrier *Adv. Drug Deliv. Rev.* **64** 640–65
- [65] Wong H L, Yu X and Bendayan R 2012 Nanotechnological advances for the delivery of CNS therapeutics *Adv. Drug Deliv. Rev.* **64** 686–700
- [66] Marushima A, Suzuki K, Nagasaki Y, Yoshitomi T, Toh K, Tsurushima H, Hirayama A and Matsumura A 2011 Newly synthesized radical-containing nanoparticles enhance neuroprotection after cerebral ischemia–reperfusion injury *Neuro-surgery* **68** 1418–26
- [67] Xiong J, Meng F, Wang C, Cheng R, Liu Z and Zhong Z 2011 Folate-conjugated crosslinked biodegradable micelles for receptor-mediated delivery of paclitaxel *J. Mater. Chem.* **21** 5786
- [68] Mourtas S, Lazar A N, Markoutsas E, Duyckaerts C and Antimisiaris S G 2014 Multifunctional nanoliposomes with curcumin-lipid derivative and brain targeting functionality with potential applications for Alzheimer disease *Eur. J. Med. Chem.* **80** 175–83

- [69] Rotman M, Welling M M, Bunschoten A, de Backer M E, Rip J, Nabuurs R J a, Gaillard P J, van Buchem M a, van der Maarel S M and van der Weerd L 2015 Enhanced glutathione PEGylated liposomal brain delivery of an anti-amyloid single domain antibody fragment in a mouse model for Alzheimer's disease. *J. Control. Release* **203** 40–50
- [70] Pathak R K, Kolishetti N and Dhar S 2015 Targeted nanoparticles in mitochondrial medicine. *Wiley Interdiscip. Rev. Nanomed. Nanobiotechnol.* **7** 315–29
- [71] Li T, Smet M, Dehaen W and Xu H 2016 Selenium–Platinum Coordination Dendrimers with Controlled Anti-Cancer Activity *ACS Appl. Mater. Interfaces* **8** 3609–14
- [72] Chen J, Zhang C, Liu Q, Shao X, Feng C, Shen Y, Zhang Q and Jiang X 2012 Solanum tuberosum lectin-conjugated PLGA nanoparticles for nose-to-brain delivery: in vivo and in vitro evaluations *J. Drug Target.* **20** 174–84
- [73] Durán-Lobato M, Martín-Banderas L, Gonçalves L D, Fernández-Arévalo M and Almeida A 2015 Comparative study of chitosan- and PEG-coated lipid and PLGA nanoparticles as oral delivery systems for cannabinoids *J. Nanoparticle Res.* **17** 1–17
- [74] Wohlfart S, Khalansky A S, Gelperina S, Maksimenko O, Bernreuther C, Glatzel M and Kreuter J 2011 Efficient chemotherapy of rat glioblastoma using doxorubicin-loaded PLGA nanoparticles with different stabilizers. *PLoS One* **6** e19121
- [75] Mathew A, Fukuda T, Nagaoka Y, Hasumura T, Morimoto H, Yoshida Y, Maekawa T, Venugopal K and Kumar D S 2012 Curcumin loaded-PLGA nanoparticles conjugated with Tet-1 peptide for potential use in Alzheimer's disease *PLoS One* **7**
- [76] Yan L, Wang H, Jiang Y, Liu J, Wang Z, Yang Y, Huang S and Huang Y 2013 Cell-penetrating peptide-modified PLGA nanoparticles for enhanced nose-to-brain macromolecular delivery *Macromol. Res.* **21** 435–41
- [77] Chigumira W, Maposa P, Gadaga L L, Dube A, Tagwireyi D and Maponga C C 2015 WASHINGTON (MANUSCRIPT) Preparation and evaluation of pralidoxime-loaded PLGA nanoparticles as potential carriers of the drug across the blood brain barrier **2015**
- [78] Loureiro J A, Gomes B, Fricker G, Coelho M A N, Rocha S and Pereira M C 2016 Cellular uptake of PLGA nanoparticles targeted with anti-amyloid and anti-transferrin receptor antibodies for Alzheimer's disease treatment *Colloids Surfaces B Biointerfaces* **145** 8–13

- [79] Mittal G, Carswell H, Brett R, Currie S and Kumar M N V R 2011 Development and evaluation of polymer nanoparticles for oral delivery of estradiol to rat brain in a model of Alzheimer's pathology *J. Control. Release* **150** 220–8
- [80] Sheng J, He H, Han L, Qin J, Chen S, Ru G, Li R, Yang P, Wang J and Yang V C 2016 Enhancing insulin oral absorption by using mucoadhesive nanoparticles loaded with LMWP-linked insulin conjugates. *J. Control. Release* **233** 181–90
- [81] Zhang C, Chen J, Feng C, Shao X, Liu Q, Zhang Q, Pang Z and Jiang X 2014 Intranasal nanoparticles of basic fibroblast growth factor for brain delivery to treat Alzheimer's disease *Int. J. Pharm.* **461** 192–202
- [82] Patel T, Zhou J, Piepmeier J M and Saltzman W M 2012 Polymeric nanoparticles for drug delivery to the central nervous system *Adv. Drug Deliv. Rev.* **64** 701–5
- [83] Rao K S, Reddy M K, Horning J L and Labhasetwar V 2008 TAT-conjugated nanoparticles for the CNS delivery of anti-HIV drugs *Biomaterials* **29** 4429–38
- [84] Wohlfart S, Gelperina S and Kreuter J 2012 Transport of drugs across the blood-brain barrier by nanoparticles *J. Control. Release* **161** 264–73
- [85] Hamdy S, Haddadi A, Hung R and Lavasanifar A 2011 Targeting dendritic cells with nano-particulate PLGA cancer vaccine formulations *Adv. Drug Deliv. Rev.* **63** 943–55
- [86] Sneh-Edri H, Likhtenshtein D and Stepensky D 2011 Intracellular Targeting of PLGA nanoparticles encapsulating antigenic peptide to the endoplasmic reticulum of dendritic cells and its effect on antigen cross presentation in vitro *Mol. Pharm.* **8** 1266–75
- [87] Panyam J and Labhasetwar V 2003 Biodegradable nanoparticles for drug and gene delivery to cells and tissue *Adv. Drug Deliv. Rev.* **55** 329–47
- [88] Kumar N, Langer R S and Domb A J 2002 Polyanhydrides: An overview *Adv. Drug Deliv. Rev.* **54** 889–910
- [89] Jain J, Modi S, Domb A and Kumar N 2005 Role of polyanhydrides as localized drug carriers *J. Control. Release* **103** 541–63
- [90] Göpferich A and Tessmar J 2002 Polyanhydride degradation and erosion *Adv. Drug Deliv. Rev.* **54** 911–31
- [91] Larobina D, Mensitieri G, Kipper M J and Narasimhan B 2002 Mechanistic understanding of degradation in bioerodible polymers for drug delivery *AIChE J.* **48** 2960–70

- [92] Manoharan C and Singh J 2009 Evaluation of polyanhydride microspheres for basal insulin delivery: effect of copolymer composition and zinc salt on encapsulation, in vitro release, stability, in vivo adsorption and bioactivity in diabetic rats. *J. Pharm. Sci.* **98** 4237–50
- [93] Torres M P, Determan A S, Anderson G L, Mallapragada S K and Narasimhan B 2007 Amphiphilic polyanhydrides for protein stabilization and release *Biomaterials* **28** 108–16
- [94] Berklund C, Kipper M J, Narasimhan B, Kim K and Pack D W 2004 Microsphere size, precipitation kinetics and drug distribution control drug release from biodegradable polyanhydride microspheres *J. Control. Release* **94** 129–41
- [95] Binnebose A M, Haughney S L, Martin R, Imerman P M, Narasimhan B and Bellaire B H 2015 Polyanhydride Nanoparticle Delivery Platform Dramatically Enhances Killing of Filarial Worms *PLoS Negl. Trop. Dis.* **9** 1–18
- [96] Katti D S, Lakshmi S, Langer R and Laurencin C T 2002 Toxicity, biodegradation and elimination of polyanhydrides *Adv. Drug Deliv. Rev.* **54** 933–61
- [97] Heller J 2002 Polyanhydrides and poly(ortho esters) *Adv. Drug Deliv. Rev.* **54** 887–8
- [98] Westphal M, Ram Z, Riddle V, Hilt D and Bortey E 2006 Gliadel (R) wafer in initial surgery for malignant glioma: Long-term follow-up of a multicenter controlled trial *Acta Neurochir. (Wien)*. **148** 269–75
- [99] Shen E, Kipper M J, Dziadul B, Lim M K and Narasimhan B 2002 Mechanistic relationships between polymer microstructure and drug release kinetics in bioerodible polyanhydrides *J. Control. Release* **82** 115–25
- [100] Ulery B D, Phanse Y, Sinha A, Wannemuehler M J, Narasimhan B and Bellaire B H 2009 Polymer chemistry influences monocytic uptake of polyanhydride nanospheres *Pharm. Res.* **26** 683–90
- [101] Phanse Y, Lueth P, Ramer-Tait A E, Carrillo-Conde B R, Wannemuehler M J, Narasimhan B and Bellaire B H 2016 Cellular Internalization Mechanisms of Polyanhydride Particles: Implications for Rational Design of Drug Delivery Vehicles *J. Biomed. Nanotechnol.* **12** 1544–52
- [102] Meister S, Zlatev I, Stab J, Docter D, Baches S, Stauber R H, Deutsch M, Schmidt R, Ropele S, Windisch M, Langer K, Wagner S, von Briesen H, Weggen S and Pietrzik C U 2013 Nanoparticulate flurbiprofen reduces amyloid- β 42 generation in an in vitro blood-brain barrier model *Alzheimers. Res. Ther.* **5** 1–12

- [103] Kreuter J, Shamenkov D, Petrov V, Ränge P, Cychutek K, Koch-Brandt C and Alyautdin R 2002 Apolipoprotein-mediated transport of nanoparticle-bound drugs across the blood-brain barrier *J. Drug Target.* **10** 317–25
- [104] Sahni J K, Doggui S, Ali J, Baboota S, Dao L and Ramassamy C 2011 Neurotherapeutic applications of nanoparticles in Alzheimer's disease *J. Control. Release* **152** 208–31
- [105] Pan L, He Q, Liu J, Chen Y, Ma M, Zhang L and Shi J 2012 Nuclear-targeted drug delivery of TAT peptide-conjugated monodisperse mesoporous silica nanoparticles. *J. Am. Chem. Soc.* **134** 5722–5
- [106] Vela Ramirez J E, Boggiatto P M, Wannemuehler M J and Narasimhan B 2016 Polyanhydride Nanoparticle Interactions with Host Serum Proteins and Their Effects on Bone Marrow Derived Macrophage Activation *ACS Biomater. Sci. Eng.* **3** 160–8
- [107] Ross K A, Brenza T M, Binnebose A M, Phanse Y, Kanthasamy A G, Gendelman H E, Salem A K, Bartholomay L C, Bellaire B H and Narasimhan B 2015 Nano-Enabled Delivery of Diverse Payloads Across Complex Biological Barriers. *J. Control. Release* **10** 548–59
- [108] Enciu A M, Gherghiceanu M and Popescu B O 2013 Triggers and effectors of oxidative stress at blood-brain barrier level: Relevance for brain ageing and neurodegeneration *Oxid. Med. Cell. Longev.* **2013**
- [109] Oller-Salvia B, Sanchez-Navarro M, Giralt E and Teixido M 2016 Blood-brain barrier shuttle peptides: an emerging paradigm for brain delivery *Chem. Soc. Rev.* **45** 4690–707
- [110] Abbott N J, Patabendige A A K, Dolman D E M, Yusof S R and Begley D J 2010 Structure and function of the blood-brain barrier *Neurobiol. Dis.* **37** 13–25
- [111] Vela-Ramirez J E, Goodman J T, Boggiatto P M, Roychoudhury R, Pohl N L B, Hostetter J M, Wannemuehler M J and Narasimhan B 2015 Safety and Biocompatibility of Carbohydrate-Functionalized Polyanhydride Nanoparticles *AAPS J.* **17** 256–67
- [112] Patil Y B, Toti U S, Khdair A, Ma L and Panyam J 2009 Single-step surface functionalization of polymeric nanoparticles for targeted drug delivery *Biomaterials* **30** 859–66
- [113] Chen Y C, Chiang C F, Chen L F, Liang P C, Hsieh W Y and Lin W L 2014 Polymersomes conjugated with des-octanoyl ghrelin and folate as a BBB-penetrating cancer cell-targeting delivery system *Biomaterials* **35** 4066–81

- [114] Mallapragada S K, Brenza T M, McMillan J M, Narasimhan B, Sakaguchi D S, Sharma A D, Zbarska S and Gendelman H E 2015 Enabling nanomaterial, nanofabrication and cellular technologies for nanoneuromedicines *Nanomedicine Nanotechnology, Biol. Med.* **11** 715–29
- [115] Sharma H S, Castellani R J, Smith M A and Sharma A 2012 *The Blood-Brain Barrier in Alzheimer's Disease. Novel Therapeutic Targets and Nanodrug delivery.* vol 102(Elsevier Inc.)
- [116] Tian X, Nyberg S, S Sharp P, Madsen J, Daneshpour N, Armes S P, Berwick J, Azzouz M, Shaw P, Abbott N J and Battaglia G 2015 LRP-1-mediated intracellular antibody delivery to the Central Nervous System. *Sci. Rep.* **5** 11990
- [117] Gao H, Zhang S, Yang Z, Cao S, Jiang X and Pang Z 2014 In vitro and in vivo intracellular distribution and anti-glioblastoma effects of docetaxel-loaded nanoparticles functionalized with IL-13 peptide. *Int. J. Pharm.* **466** 8–17
- [118] Madhankumar A B, Slagle-Webb B, Wang X, Yang Q X, Antonetti D a, Miller P a, Sheehan J M and Connor J R 2009 Efficacy of interleukin-13 receptor-targeted liposomal doxorubicin in the intracranial brain tumor model. *Mol. Cancer Ther.* **8** 648–54
- [119] Karatas H, Aktas Y, Gursoy-Ozdemir Y, Bodur E, Yemisci M, Caban S, Vural A, Pinarbasli O, Capan Y, Fernandez-Megia E, Novoa-Carballal R, Riguera R, Andrieux K, Couvreur P and Dalkara T 2009 A nanomedicine transports a peptide caspase-3 inhibitor across the blood-brain barrier and provides neuroprotection. *J. Neurosci.* **29** 13761–9
- [120] Kabanov A V and Gendelman H E 2007 Nanomedicine in the diagnosis and therapy of neurodegenerative disorders *Prog. Polym. Sci.* **32** 1054–82
- [121] Hu K, Li J, Shen Y, Lu W, Gao X, Zhang Q and Jiang X 2009 Lactoferrin-conjugated PEG-PLA nanoparticles with improved brain delivery: In vitro and in vivo evaluations *J. Control. Release* **134** 55–61
- [122] Qiao R 2012 Receptor-Mediated Delivery of Magnetic Nanoparticles across the Blood Brain Barrier 3304–10
- [123] Loureiro J, Andrade S, Duarte A, Neves A, Queiroz J, Nunes C, Sevin E, Fenart L, Gosselet F, Coelho M and Pereira M 2017 Resveratrol and Grape Extract-loaded Solid Lipid Nanoparticles for the Treatment of Alzheimer's Disease *Molecules* **22** 277
- [124] Loureiro J A, Gomes B, Fricker G, Cardoso I, Ribeiro C A, Gaiteiro C, Coelho M A N, Pereira M do C and Rocha S 2015 Dual ligand immunoliposomes for drug delivery to the brain *Colloids Surfaces B Biointerfaces* **134** 213–9

- [125] Mourtas S, Canovi M, Zona C, Aurilia D, Niarakis A, La Ferla B, Salmona M, Nicotra F, Gobbi M and Antimisiaris S G 2011 Curcumin-decorated nanoliposomes with very high affinity for amyloid-beta1-42 peptide *Biomaterials* **32** 1635–45
- [126] Watts R J and Dennis M S 2013 Bispecific antibodies for delivery into the brain *Curr. Opin. Chem. Biol.* **17** 393–9
- [127] Yu Y J, Atwal J K, Zhang Y, Tong R K, Wildsmith K R, Tan C, Bien-Ly N, Hersom M, Maloney J A, Meilandt W J, Bumbaca D, Gadkar K, Hoyte K, Luk W, Lu Y, Ernst J A, Searce-Levie K, Couch J A, Dennis M S and Watts R J 2014 Therapeutic bispecific antibodies cross the blood-brain barrier in nonhuman primates *Sci Transl Med* **6**
- [128] Accardo A, Aloj L, Aurilio M, Morelli G and Tesauro D 2014 Receptor binding peptides for target-selective delivery of nanoparticles encapsulated drugs *Int. J. Nanomedicine* **9** 1537–57
- [129] Kraiss A, Wortmann L, Hermanns L, Feliu N, Vahter M, Stucky S, Mathur S and Fadeel B 2014 Targeted uptake of folic acid-functionalized iron oxide nanoparticles by ovarian cancer cells in the presence but not in the absence of serum *Nanomedicine Nanotechnology, Biol. Med.* **10** 1421–31
- [130] Lochhead J J and Thorne R G 2012 Intranasal delivery of biologics to the central nervous system *Adv. Drug Deliv. Rev.* **64** 614–28
- [131] Kim J-Y, Choi W Il, Kim Y H and Tae G 2013 Brain-targeted delivery of protein using chitosan- and RVG peptide-conjugated, pluronic-based nano-carrier *Biomaterials* **34** 1170–8
- [132] Chaturbedy P, Kumar M, Salikolimi K, Das S, Sinha S H, Chatterjee S, Suma B S, Kundu T K and Eswaramoorthy M 2015 Shape-directed compartmentalized delivery of a nanoparticle-conjugated small-molecule activator of an epigenetic enzyme in the brain *J. Control. Release* **217** 151–9
- [133] Dhar S, Baker E W, Marrache S and West F D 2016 Therapeutic Nanoparticles for Accumulation in the Brain. Patent WO/2016/022462, 2016.
- [134] Batrakova E V and Kabanov A V 2013 Cell-mediated drug delivery to the brain *J. Drug Deliv. Sci. Technol.* **23** 419–33

- [135] Kanmogne G, Singh S, Roy U, Liu X, McMillan J, Gorantla S, Balkundi S, Smith N, Zhou Y, Alnouti Y, Gautam N, Poluektova L, Kabanov A, Bronich T and Gendelman H 2012 Mononuclear phagocyte intercellular crosstalk facilitates transmission of cell-targeted nanoformulated antiretroviral drugs to human brain endothelial cells *Int. J. Nanomedicine* **7** 2373–88
- [136] Gautam N, Puligujja P, Balkundi S, Thakare R, Liu X, Fox H S and Mcmillan J 2014 Pharmacokinetics, Biodistribution, and Toxicity of Folic Acid-Coated Antiretroviral Nanoformulations *Antimicrob. Agents Chemother.* **58** 7510–9
- [137] Puligujja P, Balkundi S S, Kendrick L M, Baldrige H M, Hilaire J R, Bade A N, Dash P K, Zhang G, Poluektova L Y, Gorantla S, Liu X, Ying T, Feng Y, Wang Y, Dimitrov D S, Mcmillan J M and Gendelman H E 2015 Pharmacodynamics of long-acting folic acid-receptor targeted ritonavir-boosted atazanavir nanoformulations *Biomaterials* **41** 141–50
- [138] Puligujja P, McMillan J, Kendrick L, Li T, Balkundi S, Smith N, Veerubhotla R S, Edagwa B J, Kabanov A V, Bronich T, Gendelman H E and Liu X-M 2013 Macrophage folate receptor-targeted antiretroviral therapy facilitates drug entry, retention, antiretroviral activities and biodistribution for reduction of human immunodeficiency virus infections *Nanomedicine* **9** 1263–73
- [139] Puligujja P, Araínga M, Dash P, Palandri D, Mosley R L, Gorantla S, Poluektova L, McMillan J and Gendelman H E 2015 Pharmacodynamics of folic acid receptor targeted antiretroviral nanotherapy in HIV-1-infected humanized mice *Antiviral Res.* **120** 85–8
- [140] Shang D S, Yang Y M, Zhang H, Tian L, Jiang J S, Dong Y B, Zhang K, Li B, Zhao W D, Fang W G and Chen Y H 2016 Intracerebral GM-CSF contributes to transendothelial monocyte migration in APP/PS1 Alzheimer's disease mice *J. Cereb. Blood Flow Metab.* **36** 1978–91
- [141] Aryal M, Vykhodtseva N, Zhang Y-Z and McDannold N 2015 Multiple sessions of liposomal doxorubicin delivery via focused ultrasound mediated blood-brain barrier disruption: a safety study. *J. Control. Release* **204** 60–9
- [142] Taylor J P, Mata I F and Farrer M J 2006 LRRK2: A common pathway for parkinsonism, pathogenesis and prevention? *Trends Mol. Med.* **12** 76–82
- [143] Stanimirovic D, Kemmerich K, Haqqani A S and Farrington G K 2014 *Engineering and pharmacology of blood-brain barrier-permeable bispecific antibodies* vol 71(Elsevier Inc.)

- [144] Ruozi B, Belletti D, Bondioli L, De Vita A, Forni F, Vandelli M A and Tosi G 2012 Neurotrophic Factors and Neurodegenerative Diseases. A Delivery Issue. *Int. Rev. Neurobiol.* **102** 207–47
- [145] Vytla D, Combs-Bachmann R E, Hussey A M, McCarron S T, McCarthy D S and Chambers J J 2012 Prodrug approaches to reduce hyperexcitation in the CNS *Adv. Drug Deliv. Rev.* **64** 666–85
- [146] Stavrovskaya I G and Kristal B S 2005 The powerhouse takes control of the cell: Is the mitochondrial permeability transition a viable therapeutic target against neuronal dysfunction and death? *Free Radic. Biol. Med.* **38** 687–97
- [147] Yun X, Maximov V D, Yu J, Zhu H, Vertegel A a and Kindy M S 2013 Nanoparticles for targeted delivery of antioxidant enzymes to the brain after cerebral ischemia and reperfusion injury *J. Cereb. Blood Flow Metab.* **33** 583–92
- [148] Wiemerslage L and Lee D 2016 Quantification of mitochondrial morphology in neurites of dopaminergic neurons using multiple parameters. *J. Neurosci. Methods* **262** 56–65
- [149] Varkouhi A K, Scholte M, Storm G and Haisma H J 2011 Endosomal escape pathways for delivery of biologicals. *J. Control. Release* **151** 220–8
- [150] Torchilin V P 2006 Recent approaches to intracellular delivery of drugs and DNA and organelle targeting. *Annu. Rev. Biomed. Eng.* **8** 343–75
- [151] Wen R, Umeano A, Francis L, Sharma N, Tundup S and Dhar S 2016 Mitochondrion: A Promising Target for Nanoparticle-Based Vaccine Delivery Systems *Vaccines* **4** 18
- [152] Wongrakpanich A, Geary S M, Joiner M A, Anderson M E and Salem A K 2014 Mitochondria-targeting particles. *Nanomedicine (Lond).* **9** 2531–43
- [153] Denora N, Laquintana V, Lopalco A, Iacobazzi R M, Lopedota A, Cutrignelli A, Iacobellis G, Annese C, Cascione M, Leporatti S and Franco M 2013 In vitro targeting and imaging the translocator protein TSPO 18-kDa through G(4)-PAMAM-FITC labeled dendrimer. *J. Control. Release* **172** 1111–25
- [154] Kim D H and Rossi J J 2007 Strategies for silencing human disease using RNA interference. *Nat. Rev. Genet.* **8** 173–84
- [155] Kordower J H 2000 Neurodegeneration Prevented by Lentiviral Vector Delivery of GDNF in Primate Models of Parkinson's Disease *Science (80-.)*. **290** 767–73

- [156] Tu Z, Yang W, Yan S, Guo X and Li X-J 2015 CRISPR/Cas9: a powerful genetic engineering tool for establishing large animal models of neurodegenerative diseases. *Mol. Neurodegener.* **10** 35
- [157] Luo M L, Mullis A S, Leenay R T and Beisel C L 2015 Repurposing endogenous type I CRISPR-Cas systems for programmable gene repression *Nucleic Acids Res.* **43** 674–81
- [158] Pouton C W, Wagstaff K M, Roth D M, Moseley G W and Jans D A 2007 Targeted delivery to the nucleus. *Adv. Drug Deliv. Rev.* **59** 698–717
- [159] Van Der Aa M A E M, Mastrobattista E, Oosting R S, Hennink W E, Koning G A and Crommelin D J A 2006 The nuclear pore complex: The gateway to successful nonviral gene delivery *Pharm. Res.* **23** 447–59
- [160] Shi J, Chou B, Choi J L, Ta A L and Pun S H 2013 Investigation of Polyethylenimine/DNA Polyplex Transfection to Cultured Cells Using Radiolabeling and Subcellular Fractionation Methods. *Mol. Pharm.* **10** 2145–56
- [161] Lanford R E, Kanda P and Kennedy R C 1986 Induction of nuclear transport with a synthetic peptide homologous to the SV40 T antigen transport signal *Cell* **46** 575–82
- [162] Escriou V, Carrière M, Scherman D and Wils P 2003 NLS bioconjugates for targeting therapeutic genes to the nucleus *Adv. Drug Deliv. Rev.* **55** 295–306
- [163] Vives E, Brodin P and Lebleu B 1997 A Truncated HIV-1 Tat Protein Basic Domain Rapidly Translocates through the Plasma Membrane and Accumulates in the Cell Nucleus *J. Biol. Chem.* **272** 16010–7
- [164] Namvar A, Bolhassani A, Khairkhah N and Motevalli F 2015 Physicochemical properties of polymers: An important system to overcome the cell barriers in gene transfection *Biopolymers* **103** 363–75
- [165] Rass U, Ahel I and West S C 2007 Defective DNA repair and neurodegenerative disease. *Cell* **130** 991–1004
- [166] Zhao H, Li H, Ruberu K and Garner B 2015 Impaired lysosomal cobalamin transport in Alzheimer's disease. *J. Alzheimers. Dis.* **43** 1017–30
- [167] Maity A R and Stepensky D 2015 Delivery of drugs to intracellular organelles using drug delivery systems: Analysis of research trends and targeting efficiencies *Int. J. Pharm.* **496** 268–74

- [168] Vasa D M, O'Donnell L A and Wildfong P L D 2015 Influence of Dosage Form, Formulation, and Delivery Device on Olfactory Deposition and Clearance: Enhancement of Nose-to-CNS Uptake *J. Pharm. Innov.* **10** 200–10
- [169] Foo M Y, Cheng Y-S, Su W-C and Donovan M D 2007 The Influence of Spray Properties on Intranasal Deposition *J. Aerosol Med.* **20** 495–508
- [170] Jabbal-Gill I 2010 Nasal vaccine innovation. *J. Drug Target.* **18** 771–86
- [171] Biddlestone-Thorpe L, Marchi N, Guo K, Ghosh C, Janigro D, Valerie K and Yang H 2012 Nanomaterial-mediated CNS delivery of diagnostic and therapeutic agents *Adv. Drug Deliv. Rev.* **64** 605–13
- [172] Li Z, Dong K, Huang S, Ju E, Liu Z, Yin M, Ren J and Qu X 2014 A Smart Nanoassembly for Multistage Targeted Drug Delivery and Magnetic Resonance Imaging *Adv. Funct. Mater.* **24** 3612–20
- [173] Kamaly N, Xiao Z, Valencia P M, Radovic-Moreno A F and Farokhzad O C 2012 Targeted polymeric therapeutic nanoparticles: design, development and clinical translation *Chem. Soc. Rev.* **41** 2971
- [174] Meng Y, Sohar I, Sleat D E, Richardson J R, Reuhl K R, Jenkins R B, Sarkar G and Lobel P 2014 Effective intravenous therapy for neurodegenerative disease with a therapeutic enzyme and a Peptide that mediates delivery to the brain. *Mol. Ther.* **22** 547–53
- [175] Allen M H, Day K N, Hemp S T and Long T E 2013 Synthesis of folic acid-containing imidazolium copolymers for potential gene delivery applications *Macromol. Chem. Phys.* **214** 797–805
- [176] Wang Y, Cao X, Guo R, Shen M, Zhang M, Zhu M and Shi X 2011 Targeted delivery of doxorubicin into cancer cells using a folic acid–dendrimer conjugate *Polym. Chem.* **2** 1754

CHAPTER 3: BIODEGRADABLE POLYANHYDRIDE NANOPARTICLE-BASED DELIVERY SYSTEM FOR ENHANCED BLOOD-BRAIN BARRIER TRANSPORT

Manuscript in progress; to be submitted to *Acta Biomaterialia* in 2017

Timothy M. Brenza^a, Benjamin W. Schlichtmann^a, Julia E. Vela Ramirez^a, JoEllyn M. McMillan^b, Balaraman Kalyanaraman^c, Howard E. Gendelman^b, Surya Mallapragada^a, Balaji Narasimhan^{a,*} and Georgette D. Kanmogne^b

^a Department of Chemical and Biological Engineering, Iowa State University, Ames, IA USA

^b Department of Pharmacology and Experimental Neuroscience, University of Nebraska Medical Center, Omaha, NE USA

^c Department of Biophysics, Medical College of Wisconsin, Milwaukee, WI, USA

*To whom correspondence should be addressed

Key words: nanoparticles; blood-brain barrier; cell-mediated transcytosis; polyanhydrides; Mito-apocynin

3.1 Abstract

There is an urgent need to deliver anti-oxidant and anti-inflammatory therapeutics across the blood-brain barrier (BBB) to treat a variety of brain disorders, including neurodegenerative diseases ranging from Parkinson's Disease to traumatic brain injury and

chemical exposure. In this work, using an *in vitro* BBB model, we demonstrate that a biodegradable polyanhydride nanoparticle-based delivery system effectively traverses the BBB. Using a combination of confocal microscopy, flow cytometry, and liquid chromatography/tandem mass spectroscopy, our data demonstrate the internalization of both non-functionalized and folic acid functionalized polyanhydride nanoparticles by primary human monocytes and human brain microvascular endothelial cells (HBMEC) and efficient transfer of the nanoparticles from monocytes to primary HBMEC *in vitro*. These nanoparticle formulations contained Mito-apocynin, a promising anti-oxidant compound, and the efficient transport of this payload into the HBMEC was confirmed using chromatography. The versatility of the polyanhydride nanoparticle platform design was exemplified by the ability to incorporate targeting ligands *via* two different functionalization methods, bulk and surface functionalization, which can be used for cellular targeting downstream of the BBB. Collectively, these studies demonstrate that polyanhydride nanoparticle-based delivery systems show promise for enhancing the effectiveness of therapeutics that require transport across the BBB and efficient internalization by neuronal cells.

3.2 Introduction

Age-related neurodegenerative disorders including Alzheimer's and Parkinson's Disease (AD and PD, respectively), and stroke are becoming more prominent as the world population ages [1]. These diseases typically manifest mid- to late-life and progressively worsen with increased morbidity. The economic burden associated with increased medical management as well as decreased individual productivity is likely to increase in the following years, making it increasingly urgent to develop effective medications. Currently, a

number of drugs are available in the market that manage the symptoms of AD and PD. However these drugs treat only the symptoms and do not slow disease progression.

In neurodegenerative diseases, one of the major causes of neurodegeneration is mitochondrial dysfunction, which leads to a build-up of reactive oxygen and nitrogen species (ROS and RNS, respectively), and oxidative stress. While there has been some success in the development of anti-inflammatory and antioxidant drugs, the efficacy of those drugs can be affected by factors such as drug metabolism, which can reduce its bioavailability and appropriate localization, and therefore increase its cytotoxicity and potential side effects. An example of such an antioxidant drug that is targeted towards mitochondria is Mito-apocynin (mAPO), which was shown in previous studies to reduce oxidative stresses, preserve motor coordination, and retain olfactory function in mouse models [2].

For treatment of central nervous system (CNS) diseases, the major factor that reduces drug efficacy is the poor penetration of therapeutics across the blood-brain barrier (BBB) [3]. Some classes of polymeric nanoparticles (NPs) have been shown to enhance drug delivery across the BBB [4,5]. Polyanhydride particles can provide sustained delivery of a broad range of therapeutics [6–16]. Additionally, polyanhydride NPs are biocompatible and degrade by surface erosion, which is favorable for therapeutic delivery [17]. Our recent work has indicated that mAPO encapsulated in polyanhydride nanoparticles functionalized with folic acid were internalized effectively by neuronal cells and provided protection against H₂O₂-induced oxidative stress and 6-OHDA-induced neurodegeneration [18]. However, the ability of polyanhydride NPs (with or without folic acid functionalization) to efficiently cross the BBB has not yet been investigated.

In the present study, we investigated the effects of polyanhydride NP formulations of different chemistries on their uptake by primary human brain microvascular endothelial cells (HBMEC), the major BBB constituent, as well as by primary human monocytes. The effects of monocyte-endothelial cell interactions on NP uptake and cell-to-cell transfer were also studied.

3.3 Experimental Methods

3.3.1 Polyanhydride synthesis

Synthesis of sebacic anhydride (SA) and 1,6-bis(*p*-carboxyphenoxy)hexane (CPH) pre-polymers and copolymers was performed as previously described [19,20]. The resulting 20:80 CPH:SA copolymer was characterized using ^1H nuclear magnetic resonance spectroscopy (^1H NMR; VXR-300, Varian, Palo Alto, CA) to verify copolymer composition and molecular weight. Appropriate molecular weight of the synthesized copolymers was confirmed [19,20].

3.3.2 Folic acid bulk functionalization

Bulk functionalization of 20:80 CPH:SA copolymer with folic acid (FA) (bFA-poly) was performed using an anhydride interchange mechanism. First, a mass of FA equivalent to 10 times the molar concentration of copolymer to be reacted was added to a three-pronged round bottom flask with 5 mL acetic anhydride and acetylated by refluxing for 60 min at 150°C under N_2 . The remaining solution was immediately added to 20:80 CPH:SA copolymer, which was reacted at 180°C under 0.5 torr vacuum for 20 min, and dissolved in 15-20 mL methylene chloride overnight. Undissolved free FA was removed by centrifugation

at 10,000 rpm for 5 min. Functionalized, purified polymer was precipitated drop-wise into hexanes at a 1:20 methylene chloride:hexanes ratio. The resulting FA-functionalized copolymer was characterized using ^1H NMR (MR-400, Varian; CDCl_3) to estimate the percentage of end groups that were functionalized with FA. Additionally, gel permeation chromatography (GPC) was used to characterize polymer molecular weight before and after functionalization. Finally, Fourier transform infrared spectroscopy (FTIR; Nicolet iS50 FTIR, ThermoFisher, Waltham, MA) attenuated total reflectance (ATR; Nicolet Smart iTX accessory, ThermoFisher; FTIR-ATR) was used to analyze the presence of anhydride peaks associated with the polymer before and after functionalization.

3.3.3 Mito-apocynin synthesis

Mito-apocynin (mAPO) was kindly provided by the Kalyanaraman laboratory at the Medical College of Wisconsin. Product synthesis and characterization was performed as described previously [2,21,22].

3.3.4 NP synthesis

Rhodamine B (Sigma, St. Louis, MO) or mAPO were incorporated into the core of 20:80 CPH:SA NPs by an anti-solvent nano-encapsulation method [23]. The synthesized polymer (100 mg) and rhodamine B (5 mg) or mAPO (0.2 mg) were dispersed into 4-5 mL of methylene chloride (Fisher Scientific, Pittsburgh, PA) and sonicated for 30-60s with a probe sonicator (Sonics and Materials, Newtown, CT). The solution was poured into 1 L pentane (Fisher Scientific) for non-functionalized NP (NF-NP) or 2 L pentane for bulk-FA functionalized NPs (bFA-NP), stirring rapidly, and the particles were immediately recovered

by vacuum filtration. The particle morphology and size were evaluated with scanning electron microscopy (Quanta 250 FE-SEM, FEI, Hillsboro, OR). ImageJ software (National Institutes of Health, Bethesda, MD) was used to determine primary particle sizes.

3.3.5 NP surface functionalization

Surface functionalization of 20:80 CPH:SA NF-NPs with FA was performed using a two-step amine-carboxylic acid coupling reaction with 1-ethyl-3-(3-dimethylaminopropyl) carbodiimide (EDC) and N-hydroxysuccinimide (NHS) [24,25]. The morphology and size of the resulting NPs (sFA-NPs) were determined using scanning electron microscopy and ImageJ 1.43u software was utilized to determine primary particle sizes.

3.3.6 Human monocyte isolation

Monocytes were obtained from HIV-1, HIV-2 and hepatitis B seronegative donor leukopaks, and separated by countercurrent centrifugal elutriation and characterized as previously described [26,27]. Freshly elutriated monocytes were re-suspended in Dulbecco's Modified Eagles Media (DMEM) containing 2 mM L-glutamine (Invitrogen, Carlsbad, CA), 10% heat-inactivated human serum, 100 µg/mL gentamicin, and 10 µg/mL ciprofloxacin. All reagents were prescreened for endotoxin (<10 pg/mL, Associates of Cape Cod, Woods Hole, MA) and mycoplasma contamination (Gen-probe II, Gen-probe, San Diego, CA).

3.3.7 Brain endothelial cell culture

Primary HBMEC were isolated from brain tissue obtained during surgical removal of epileptogenic cerebral cortex in adult patients as we previously described [27–30]. Routine

evaluation by immunostaining for von-Willebrand factor, *Ulex europaeus* lectin and CD31 (all from Abcam, Cambridge, MA) demonstrated that cells were >99% pure. Freshly isolated cells were cultured on collagen-coated culture plates as we previously described [27–29] and cells at passage 2 to 4 were used in this study.

3.3.8 Cytotoxicity assays

Monocytes were cultured at a concentration of 6.25×10^5 cells/mL and HBMEC cultured to confluence. For all cell experiments, NPs were suspended in 1 mL of working media, and sonicated for 30s. If suspension quality was poor (i.e., if NPs displayed aggregation), 0.1% PVA was added as a surfactant. This step was repeated up to 0.4% PVA, if necessary. To determine any potential toxic effects of NPs on cells, monocytes and confluent HBMEC were treated with NPs at concentrations of 1 to 500 $\mu\text{g/mL}$ for 48 h at 37°C and 5% CO₂. Following loading of each NP formulation, cells were washed with serum-free culture media to remove excess drugs and cytotoxicity was assessed over 24 h using alamarBlue™ assay (Life Technologies) as we previously described [4,31], per manufacturer's instructions. All experiments were performed in triplicate for each experimental condition.

3.3.9 Endothelial cell-monocyte NP transfers

Primary HBMEC were cultured to confluence on glass coverslips as previously described [32]. For endothelial cell-monocyte communication, freshly elutriated human monocytes were loaded with either 100 or 250 $\mu\text{g/mL}$ rhodamine-encapsulated NF-NPs (NF-NP-rho), bFA-NPs (bFA-NP-rho), or sFA-NPs (sFA-NP-rho) for 48 h. Following NP

loading, monocytes were washed 3 times with PBS to remove any free NPs. Monocytes were then co-cultured with endothelial cells for 2 h and HBMEC monolayers were washed 3 to 5 times with PBS to remove monocytes.

3.3.10 Immunofluorescence and confocal microscopy

Confluent HBMEC cultured on glass coverslips were fluorescently labeled using the Vybrant 1,1'-dioctadecyl-3,3,3',3'-tetramethylindodicarbocyanine perchlorate (DiO) cell-labeling solution (excitation 484 nm; emission 501 nm) as we previously described [4]. DiO-labeled HBMEC were co-cultured for two hours with NF-NP-rho, bFA-NP-rho, or sFA-NP-rho. Following endothelial cell-monocyte co-culture, HBMEC monolayers were washed 3 to 5 times with PBS to remove monocytes, mounted in Prolong Gold antifade reagent containing DAPI (for nuclear staining) (Life Technologies, Grand Island, NY) and analyzed by fluorescence or confocal microscopy as we previously described [4]. To determine the localization of NPs in endothelial cells, the triple labeled cell samples were examined under a Zeiss LSM 710 confocal laser scanning microscope using Zeiss Zen software.

3.3.11 Fluorescence-activated cell sorting (FACS)

For FACS quantification of NP uptake by monocytes or HBMEC, the cells were exposed to either 100 or 250 $\mu\text{g}/\text{mL}$ NF-NP-rho, bFA-NP-rho, or sFA-NP-rho for 48 h, and washed 3 to 5 times with PBS to remove free NPs. Monocytes and HBMEC were then fixed by incubation in 1% paraformaldehyde for 20 min, washed, resuspended in PBS and analyzed by FACS, using a FACScan flow cytometer (BD Bioscience, San Jose, CA). The mean fluorescence channel – mean number of rhodamine positive cells was derived using

CellQuest software (BD Bioscience). To determine the levels of NPs in monocytes and HBMEC following monocyte-endothelial cell communication, monocytes loaded with either 100 or 250 $\mu\text{g}/\text{mL}$ NF-NP-rho, bFA-NP-rho or sFA-NP-rho were co-cultured for 2 to 4 h with HBMEC (unloaded), then washed 3 to 5 times to separate monocytes from endothelial cells. HBMEC and monocytes recovered from co-cultures were then fixed by incubation in 1% paraformaldehyde for 20 min, washed, resuspended in PBS and analyzed by FACS. Unloaded monocytes were used for gating when analyzing monocytes samples, while unloaded HBMEC were used for gating when analyzing HBMEC from direct loading or co-cultured experiments. The mean fluorescence channels – mean number of rhodamine positive cells was derived using CellQuest software (BD Bioscience). For all FACS analyses, each experimental condition was performed in duplicate.

3.3.12 Ultra Performance Liquid Chromatography tandem mass spectrometry (UPLC – MS/MS)

Freshly elutriated human monocytes and HBMEC were loaded with 250 $\mu\text{g}/\text{mL}$ of mAPO-encapsulated NF-NP (NF-NP-mAPO) or sFA-NP (sFA-NP-mAPO) for 48 h as described above, were washed 3 to 5 times with PBS to remove free NPs, and harvested and pelleted by centrifugation. For monocyte-endothelial cell co-cultures, freshly elutriated human monocytes were loaded with 250 $\mu\text{g}/\text{mL}$ of NF-NP-mAPO and sFA-NP-mAPO for 48 h, washed 3 to 5 times with PBS to remove free NPs, and co-cultured with HBMEC for 2 to 4 h. Following co-cultures, monocytes and HBMEC were harvested separately and pelleted by centrifugation. Controls consisted of unloaded cells, with and without co-cultures.

Controls included untreated HBMEC and HBMEC treated for 2 h with conditioned media from NP-free monocytes. HBMEC were then harvested and pelleted by centrifugation.

For UPLC-MS/MS, each cell pellet was sonicated in 20 μ L of 0.5 M NaOH, and incubated for 30 min at 23°C. Each sample was then mixed with 180 μ L of methanol, centrifuged at 16,000 rcf for 10 min at 4°C; and 70 μ L transferred to columns and analyzed by HPLC (mobile phase: 60% of 0.1% TFA in HPLC H₂O, 40% of 0.1% TFA in ACN; flow rate: 1.0 mL/min; wavelength for detection: 262 nm). A standard curve of 0 to 6 μ g/mL of mAPO was used for quantitation of NPs in samples.

3.4 Results

3.4.1 Synthesis and characterization of FA-functionalized polyanhydrides

A new functionalization method was used to conjugate FA to 20:80 CPH:SA copolymer, prior to NP synthesis. End-group functionalization by FA was estimated by ¹H NMR analysis of purified polymer, by comparing the percentage of non-functionalized methyl end-groups (3H, 2.22 ppm) to functionalized FA end-groups using a specific FA-based aliphatic carbon (2H, 2.05 ppm) (Sup. Fig. 3.3A). This analysis indicated that approximately 75% of the end groups were functionalized by FA. GPC analysis of functionalized vs. non-functionalized polymer revealed a negligible change in polymer molecular weight after bulk functionalization. FTIR-ATR spectroscopy showed a shift in anhydride peak composition, reflective of an increase in SA-FA anhydride bonds (Sup. Fig. 3.3B).

3.4.2 Polyanhydride NP synthesis and characterization

The polyanhydride NPs (with or without FA functionalization) were synthesized by flash nanoprecipitation for toxicity, imaging, and BBB transport studies. Different payloads (i.e., mAPO or rhodamine B) were successfully incorporated into the NPs, which were spherical in shape as anticipated. The characterization data for the NPs used in these studies are presented in Table 3.1. All the particle formulations synthesized were approximately 400 nm in diameter and their surface charge as indicated by zeta potential measurements were negative, in agreement with previous studies on NF-NPs and sFA-NPs [18]. No significant differences were observed in terms of particle size, morphology and surface charge between the NF-NPs, bFA-NPs and sFA-NPs (Table 3.1).

3.4.3 Limited cytotoxicity of polyanhydride NPs in human monocytes and HBMEC

The toxicity of NF-NPs was evaluated in human monocytes and HBMEC, with each experimental condition tested in triplicate. At concentrations of 1 to 100 $\mu\text{g/mL}$, the NF-NPs showed limited cytotoxicity in human monocytes, but higher NF-NP concentrations (250 and 500 $\mu\text{g/mL}$) resulted in increased cytotoxicity and reduced cell viability, compared to untreated controls (Fig. 3.1A). Similarly, at concentrations of 1 to 500 $\mu\text{g/mL}$, NF-NPs showed limited to no cytotoxicity in HBMEC, but treatment of HBMEC with 500 $\mu\text{g/mL}$ of NF-NPs resulted in limited cytotoxicity, compared to untreated controls (Fig. 3.1C). The toxicity of bFA-NPs and sFA-NPs was also evaluated and these formulations showed low to negligible cytotoxicity from 3 to 300 $\mu\text{g/mL}$ (Sup. Fig. 3.1). Based on these studies, NP concentrations of 100 or 250 $\mu\text{g/mL}$ were selected for subsequent studies.

3.4.4 Monocyte-endothelial cell co-cultures transfer NF-NPs to HBMEC

HBMEC, the major component of the BBB, is regularly in direct contact with circulating blood and separates the systemic circulation from brain tissues. We have previously shown uptake of polyanhydride NPs by primary human monocytes [23]. Our previous studies also indicated that antigen presenting cells such as dendritic cells and macrophages effectively internalize 20:80 CPH:SA nanoparticles, primarily through phagocytosis [33,34]. To determine whether circulating monocytes containing NF-NPs can transfer the NPs to cells of the brain endothelium, HBMEC were co-cultured with human monocytes containing 100 $\mu\text{g}/\text{mL}$ or 250 $\mu\text{g}/\text{mL}$ NF-NP-rho and the cells were investigated using three different methods: confocal microscopy, fluorescence microscopy, and flow cytometry.

Following 2 h of co-culture, transfer of NF-NPs from monocytes to HBMEC occurred, and NF-NPs were observed in and around the HBMEC, as shown by confocal microscopy (Fig. 3.2). Furthermore, analyses using XZ or YZ line scan mode of the Zeiss LSM 710 confocal imaging program demonstrated localization of NF-NPs at both 250 $\mu\text{g}/\text{mL}$ and 100 $\mu\text{g}/\text{mL}$ in the cytoplasm and nucleus of the cells (Fig. 3.2A and 3.2B, respectively). Independent validation of NF-NP transfer to HBMEC was performed using fluorescence microscopy. Following 2 h of co-culture of HBMEC with NF-NP-loaded monocytes, these experiments confirmed that the NPs entered the endothelial cells (Sup. Fig. 3.2A). Next, FACS was used to quantify the uptake of NF-NPs by monocytes and HBMEC and the transfer of NF-NPs through monocyte-endothelial cell communication. Data showed efficient uptake of NF-NPs by monocytes (Fig. 3.3A) at 250 $\mu\text{g}/\text{mL}$ and 100 $\mu\text{g}/\text{mL}$ (Fig. 3.3A). Co-culture of NF-NP-loaded monocytes with non-loaded HBMEC was associated

with transfer of NF-NPs from monocytes to HBMEC (Fig. 3.3B), and this transfer was associated with decreased levels of NF-NPs in the monocytes (Fig. 3.3A). Finally, when the particles were directly incubated with the endothelial cells, they were efficiently internalized by the endothelial cells (Fig. 3.3C).

3.4.5 UPLC-MS/MS quantification of mAPO in human monocytes and HBMEC

We used UPLC-MS/MS to quantify mAPO levels in monocytes loaded with 250 $\mu\text{g}/\text{mL}$ mAPO encapsulated in NF-NPs, before and after monocyte-endothelial cell co-cultures. Unloaded monocytes and monocytes loaded with 250 μM (or about 125 $\mu\text{g}/\text{mL}$) free mAPO were used as controls. The mAPO levels in NF-NP-loaded monocytes were approximately two-fold higher than mAPO levels in monocytes, with significantly less mAPO loaded in NF-NP-mAPO compared to the free mAPO group (Fig. 3.4A). Co-culture of HBMEC with monocytes loaded with mAPO-encapsulated NF-NPs or free mAPO decreased mAPO levels in monocytes by 66% and 92%, respectively (Fig. 3.4A).

Additionally, we used UPLC-MS/MS to quantify mAPO levels in HBMEC directly loaded with 250 $\mu\text{g}/\text{mL}$ of mAPO encapsulated in NF-NPs as well as mAPO levels in HBMEC co-cultured with NF-NP-loaded monocytes. Untreated HBMEC and HBMEC loaded with 250 μM (or about 125 $\mu\text{g}/\text{mL}$) of free mAPO were used as controls. Co-culture of HBMEC with monocytes loaded with mAPO encapsulated in NF-NPs resulted in mAPO transfer to HBMEC, and higher transfer occurred in co-cultures with NF-NP-loaded monocytes compared to co-cultures with monocytes loaded with free mAPO. While mAPO in HBMEC co-cultured with NF-NP-loaded monocytes was detected, no detectable levels of mAPO were observed in HBMEC co-cultured with monocytes loaded with free mAPO (Fig.

3.4A). The levels of mAPO in NF-NP-loaded HBMEC were more than seven-fold higher than mAPO levels in HBMEC loaded with significantly less mAPO loaded in NF-NP-mAPO compared to the free mAPO group (Fig. 3.4B).

3.4.6 Internalization of FA-functionalized NPs by HBMEC

Our previous work has demonstrated that FA-functionalized polyanhydride NPs were internalized more effectively by neurons compared to NF-NPs and protected the cells from H₂O₂-induced oxidative stress and 6-OHDA-induced neurodegeneration [18]. To evaluate the ability of the FA-functionalized NPs to cross the BBB, we synthesized two types of FA-functionalized NPs: in the first method, we conjugated FA to 20:80 CPH:SA copolymer and prepared NPs based on this conjugated polymer (referred to as bFA-NPs), as described in the Methods section. The second method was used to covalently attach FA to 20:80 CPH:SA NPs (referred to as sFA-NPs), as described previously [25]. To determine whether circulating monocytes containing bFA-NPs and sFA-NPs can also transfer the NPs to cells of the brain endothelium, we co-cultured HBMEC with human monocytes containing 100 µg/mL bFA-NP-rho or sFA-NP-rho. Following 2 h of co-culture, transfer of bFA-NP-rho and sFA-NP-rho from monocytes to HBMEC occurred, and bFA-NP-rho and sFA-NP-rho were observed in and around the HBMEC, as indicated by confocal microscopy (Fig. 3.5A). Next, FACS was used to quantify the uptake of bFA-NPs and sFA-NPs by monocytes and HBMEC as well as the transfer of these NPs through monocyte-endothelial cell communication. Data showed uptake of bFA-NP-rho and sFA-NP-rho by monocytes (Fig. 3.5B). To further verify whether the sFA-NP-rho transferred to HBMEC entered endothelial cells, we performed

fluorescence microscopy. Following 2 h of co-culture of HBMEC with sFA-NP-loaded monocytes, the NPs were observed to have entered endothelial cells (Sup. Fig. 3.2B).

Co-culture of bFA-NP-rho and sFA-NP-rho-loaded monocytes with non-loaded HBMEC was associated with transfer of bFA-NP-rho and sFA-NP-rho from monocytes to HBMEC (Fig. 3.5B), and this transfer was associated with decreased levels of bFA-NP-rho and sFA-NP-rho in the monocytes (Fig. 3.5B). Finally, the FACS analysis also demonstrated direct uptake of bFA-NPs and sFA-NPs by endothelial cells (Fig. 3.5C).

UPLC-MS/MS was used to quantify the amount of mAPO in monocytes incubated with 250 $\mu\text{g/mL}$ sFA-NP-mAPO. The levels of mAPO in monocytes loaded with sFA-NP-mAPO were 2.5-fold lower than mAPO levels in monocytes, however with less mAPO in sFA-NP-mAPO than in free mAPO (Fig. 3.5D). Co-culture of HBMEC with monocytes loaded with sFA-NP-mAPO or free mAPO, decreased mAPO levels in monocytes by 79% and 92% respectively (Fig. 3.5D). Additionally, co-culture of HBMEC with monocytes loaded with sFA-NP-mAPO resulted in mAPO transfer to HBMEC. While mAPO in HBMEC co-cultured with sFA-NP-mAPO-loaded monocytes was detected, no detectable levels of mAPO were observed in HBMEC co-cultured with monocytes loaded with free mAPO (Fig. 3.5E).

3.5 Discussion

There is an urgent need to synthesize delivery platforms that can cross the BBB and deliver payloads to neurons and other cells of the CNS to reduce the progression of neurodegeneration. Biodegradable polyanhydride nanoparticles represent an attractive platform in this regard, based on their high biocompatibility [35–37] and extensive use in

drug and vaccine delivery [6–12,14,18,38–43]. Furthermore, carriers based on polyanhydrides (i.e., the Gliadel[®] wafer) have been approved by the U.S. FDA for use in humans to treat glioblastoma [44]. However, the ability of polyanhydride NPs (functionalized or not) to cross the BBB has not been investigated. In our previous work we demonstrated that folate-modified polyanhydride nanoparticles were internalized more effectively by neurons compared to NF nanoparticles, which resulted in subsequent protection against oxidative stress and neurodegeneration [18]. Since polyanhydride particles undergo surface erosion, we developed a bulk functionalization technique in which the polyanhydride backbone was conjugated with folic acid to improve the likelihood folic acid is present on the surface of the polyanhydride nanoparticles once they arrive at their target (e.g., neurons). In this work, two methods of transport of both NF and folic acid-functionalized NPs across the BBB were investigated *in vitro*: direct particle interaction with the HBMEC and monocyte-mediated transport to the HBMEC.

Polyanhydride NPs have previously been shown to be non-toxic to multiple cell types [18,45,46]. In this work we established that polyanhydride NP concentrations at 250 $\mu\text{g/mL}$ resulted in limited toxicity to primary human monocytes, as shown in Figure 3.1A, and no toxicity to primary HBMEC, as shown in Figure 3.1B. We observed similar biocompatibility of the sFA and bFA NP, as indicated in Supplementary Figure 3.1. We have previously shown polyanhydride NP compatibility with primary mouse cortical cells up to concentrations of 100 $\mu\text{g/mL}$ [18]. The toxicity data obtained in this work provides a wide administration window for further studies with polyanhydride NPs for delivery of therapeutic cargo across the BBB. Based on these findings, we tested the transfer of 100 and 250 $\mu\text{g/mL}$ polyanhydride NPs of different chemistries (NF, sFA, bFA) from monocytes to HBMEC.

Previous work with 20:80 CPH:SA NPs demonstrated high levels of particle internalization by a human monocyte cell line [23]. This polyanhydride NP backbone formulation, 20:80 CPH:SA, has shown superior cellular internalization compared to other polyanhydride formulations and does so primarily *via* phagocytosis [33]. Studies have also shown increased macrophage uptake of polyester NPs with the functionalization of folic acid [5]. These observations led us to speculate that folic acid modified polyanhydride particles would be a prime candidate for use in cell-mediated delivery of encapsulated payloads to the brain. However, in these experiments we found that sFA-NP and bFA-NP resulted in similar, if not lower, levels of particle uptake by primary human monocytes, as shown in Figure 3.5. This suggests that the FA modification may alter the internalization mechanism of the NPs from non-specific internalization (i.e., phagocytosis) of the NF polyanhydride NPs to receptor-mediated endocytosis of the FA-modified NPs.

While we have shown non-specific polyanhydride NP internalization by APCs, we have also shown the need for ligands to enhance cellular internalization with other cell types [18]. When the polyanhydride NPs were incubated directly with HBMEC, we observed enhanced internalization of these particles resulting in dye positive and high drug concentrations, as shown in Figures 3.3C and 3.4B, respectively. This suggests that polyanhydride NPs are capable of achieving endothelial transcytosis [3]. In work with poly(butyl cyanoacrylate) (PCBA) nanoparticles, it was shown that polysorbate surfactant and apolipoproteins on the surface of these NPs enhanced BBB transport [47]. In previous work, we observed that apolipoproteins were among the serum proteins that adsorbed to the surface of polyanhydride NPs upon incubation with serum [48]. This would suggest that

polyanhydride NPs with adsorbed serum proteins will also have the potential to interact with the BBB and may be capable of crossing the BBB via receptor-mediated transcytosis.

In this work we have observed similar cellular interactions and transport for the sFA-NP and bFA-NP, as shown in Figure 3.5. This suggests that the amount of FA on the surface of the bFA-NP is maintained for longer periods of time during the degradation process. Although the sFA-NP were less effectively internalized by monocytes than the NF-NP, we still observed quantifiable drug transport from the monocyte-loaded cells to the HBMEC, as shown in Figure 3.5D,E. Based on this work, it is clear that bFA-functionalized, sFA-functionalized, and NF polyanhydride NPs can be transported across the BBB via cell-mediated methods.

In previous studies, mAPO treated transgenic mice showed less motor coordination loss [2]. The current studies show that encapsulation of mAPO in polyanhydride NPs can increase the availability of the mAPO at the BBB interface by both direct NP- and cell-mediated interactions with the HBMEC, as shown in Figure 3.4. Other recent work from our laboratories showed enhanced protection of primary mouse neuronal cells with folate modified mAPO-loaded polyanhydride NPs [18]. Therefore, the bFA-NP represents the most promising formulation for the delivery of mAPO to neuronal cells. Collectively, these studies demonstrate that polyanhydride NP-based delivery systems show promise for enhancing the effectiveness of therapeutics that require transport across the BBB and for their enhanced delivery to neurons.

3.6 Conclusions

This work expands the literature on the excellent biocompatibility of polyanhydride NPs with different types of cellular systems. We have shown the internalization of both NF and folic acid functionalized NPs by primary human monocytes and efficient transfer of the NPs by the monocytes to primary HBMEC *in vitro*. There is also evidence that the NF polyanhydride NPs could be internalized directly by primary HBMEC *in vitro*. Based on this work, polyanhydride NPs show promise as a drug delivery vehicle to enhance the effectiveness of therapeutics that require transport across the BBB.

3.7 Author Information

Corresponding Authors:

*G.D. Kanmogne, Department of Pharmacology and Experimental Neuroscience, University of Nebraska Medical Center, Omaha, NE USA. Tel: +1 402 559 4084; email:

gkanmogne@unmc.edu

B. Narasimhan, Department of Chemical and Biological Engineering, Iowa State University, 2035 Sweeney Hall, Ames, IA 50011, USA. Tel: +1 515 294 8019; e-mail:

nbalaji@iastate.edu.

3.8 Author Contributions

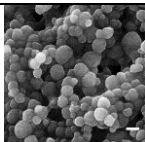
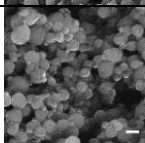
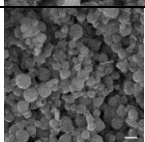
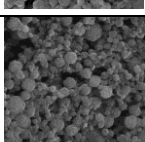
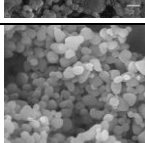
All authors have given approval to the current version of the manuscript.

3.9 Acknowledgments

The authors acknowledge financial support from the US Army Medical Research and Materiel Command (Grant No. W81XWH-11-1-0700) and the Iowa State University Nanovaccine Initiative. B.N. also acknowledges the Vlasta Klima Balloun Chair. The authors also acknowledge financial support from the National Institute of Health grants R01MH081780 and P01DA028555; and thank Ms. Sangya Singh for technical assistance.

3.10 Tables and Figures

Table 3.1. Particle Characteristics. Scale bar on images is 500 nm.

Surface	Loading	SEM photomicrographs	Geometric Diameter (nm)	Zeta Potential (mV)
Unmodified 20:80 CPH:SA (NP)	RhoB		410 ± 21	-21.5 ± 0.7
Unmodified 20:80 CPH:SA (NP)	mAPO		398	-19 ± 0.5
sFA-modified 20:80 CPH:SA (sFA-NP)	RhoB		457 ± 74	-12.0 ± 1.4
sFA-modified 20:80 CPH:SA (sFA-NP)	mAPO		425	N/A
bFA-modified 20:80 CPH:SA (bFA-NP)	RhoB		414 ± 39	-21.9 ± 0.6

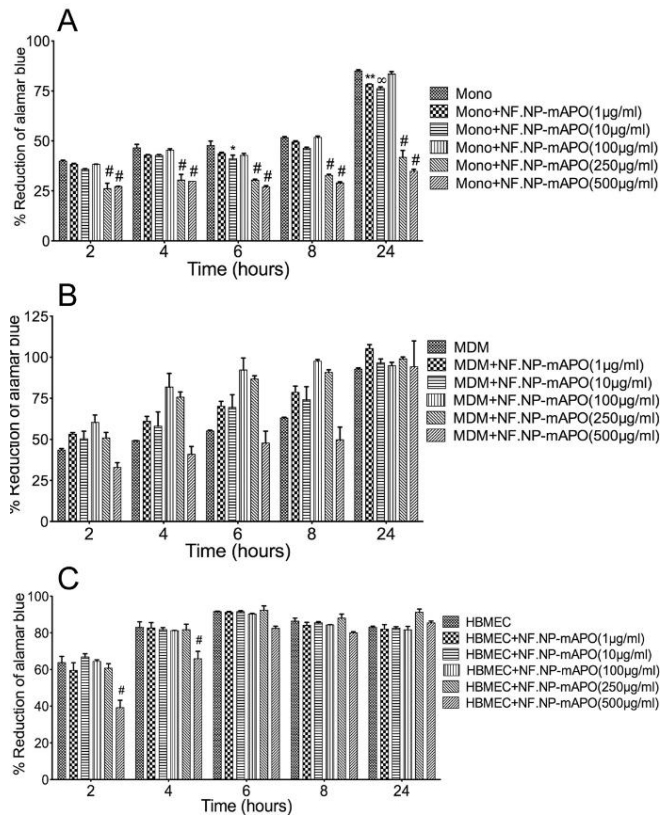


Figure 3.1: Effect of NF-NP concentration on the viability of human monocytes (A), human MDM (B), and HBMEC (C). Cells from human donors were isolated and cultured as described in the Methods, loaded with NPs at different concentrations (1 µg/mL, 10 µg/mL, 100 µg/mL, 250 µg/mL and 500 µg/mL) for 48 h and toxicity was assessed over 24 h using the alamarBlue™ assay. * $p < 0.05$, ** $p < 0.01$, ∞ $p < 0.001$, # $p < 0.0001$, compared to untreated controls.

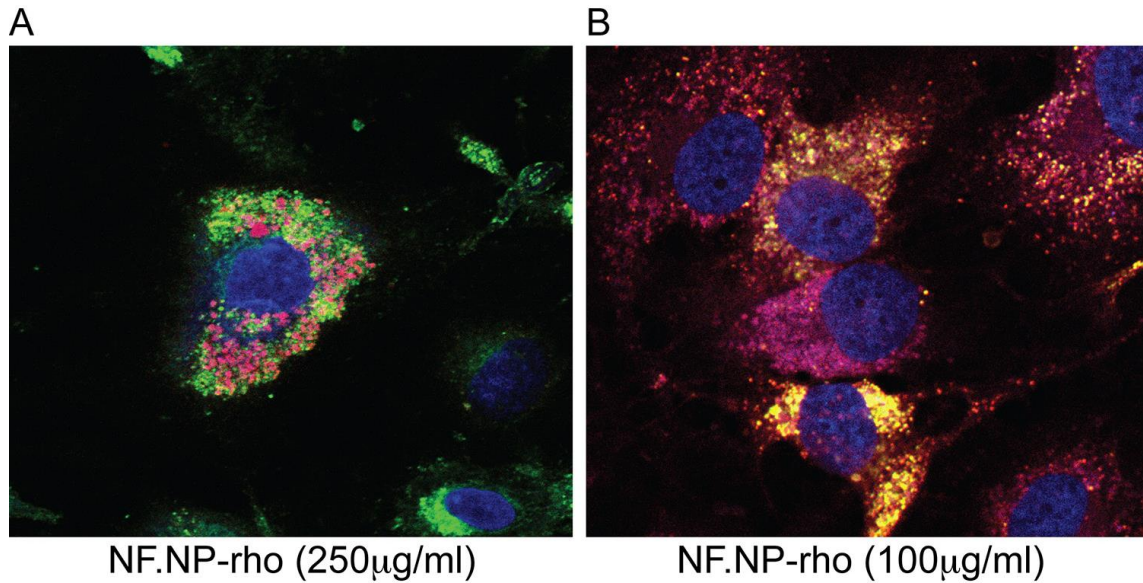


Figure 3.2. NF-NP-rho are efficiently internalized by HBMEC following co-culture with NF-NP-rho-loaded monocytes. Monocytes loaded with NF-NP-rho were co-cultured with HBMEC labeled with DiO (green), and NF-NP-rho uptake following endothelial-monocyte communication was visualized by confocal microscopy. Representative images showing uptake of NF-NP-rho at 250 µg/mL (A) and 100 µg/mL (B) by primary HBMEC.

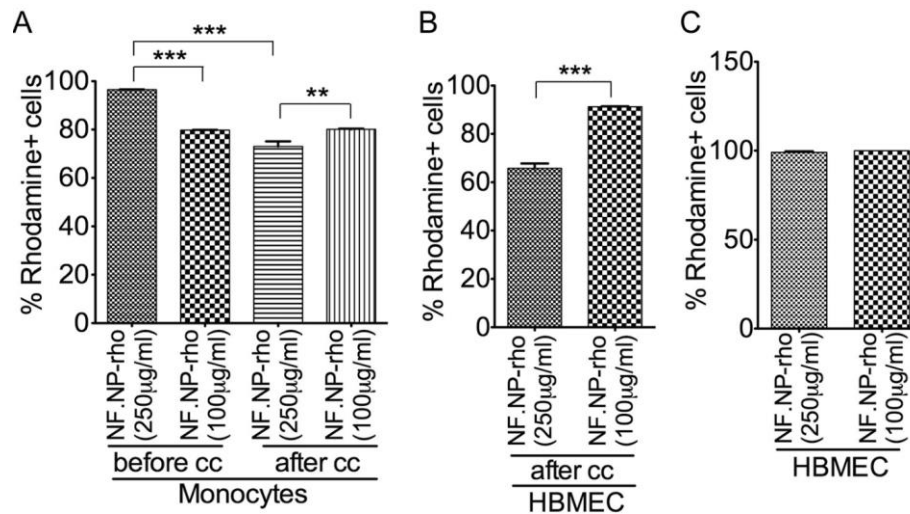


Figure 3.3: FACS quantification of direct uptake of NF-NP-rho by primary human monocytes (A), cell-to-cell transfer of NPs following co-culture of HBMEC with NF-NP-rho-loaded monocytes (B), and direct uptake by HBMEC. “Before cc”: NPs levels in cells before monocytes-endothelial co-culture. “After cc”: NPs levels in cells after monocytes-endothelial co-culture. Experiments were performed with both 250 µg/mL and 100 µg/mL NF-NP-rho. Data represents mean \pm SEM of three replicates (** $p < 0.01$, *** $p < 0.001$).

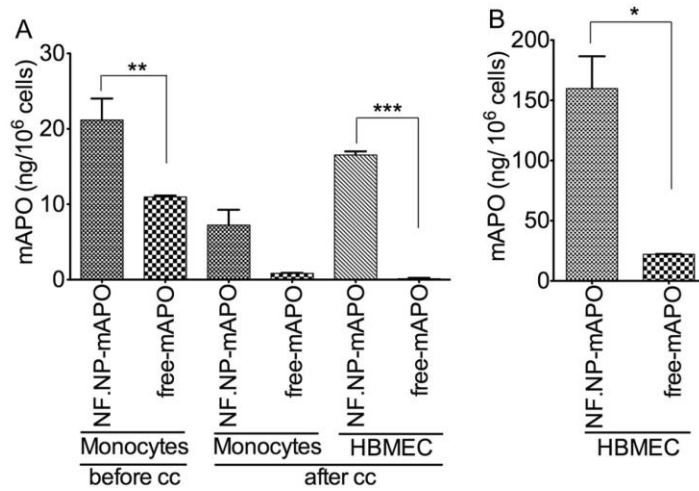


Figure 3.4: HPLC quantification of NF-NP-mAPO and free-mAPO direct uptake by primary human monocytes, cell-to-cell transfer of NPs following co-culture of HBMEC with NP-loaded monocytes (A), and direct uptake by HBMEC (B). “Before cc”: NPs levels in cells before monocytes-endothelial co-culture. “After cc”: NPs levels in cells after monocytes-endothelial co-culture. Experiments were performed with 250 μ g/mL NF-NP-mAPO, and with 250 μ M free mAPO. Data represents mean \pm SEM of three replicates (* p <0.05, ** p <0.01, *** p <0.001).

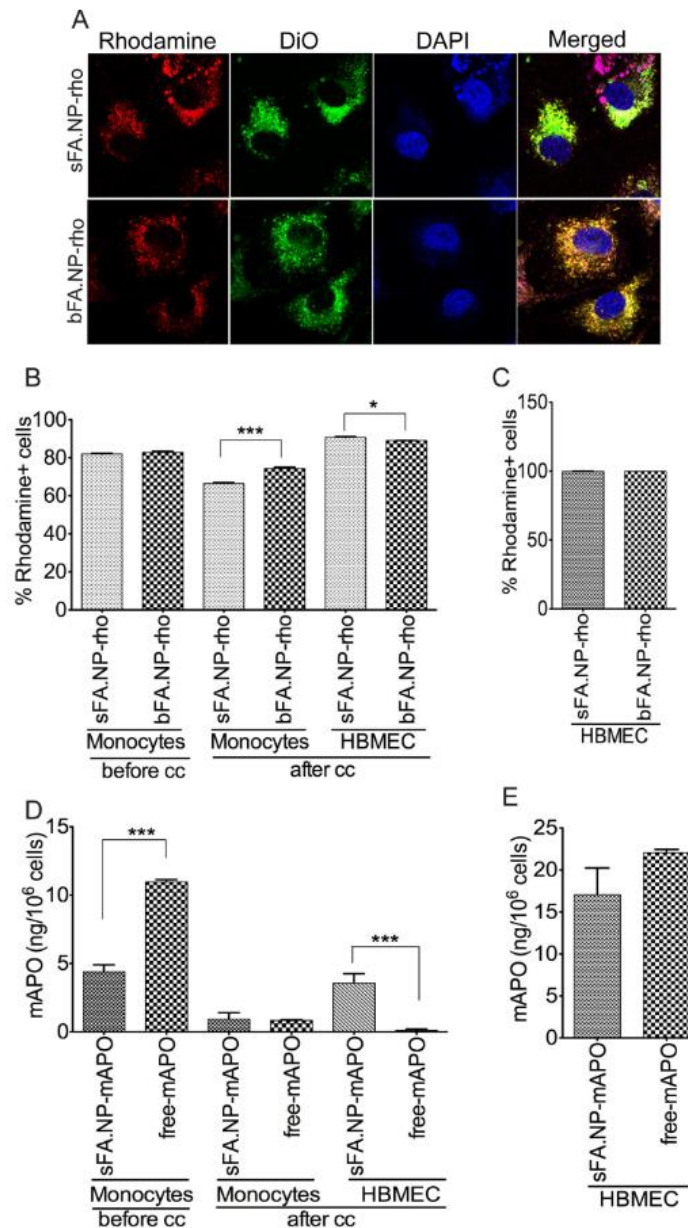
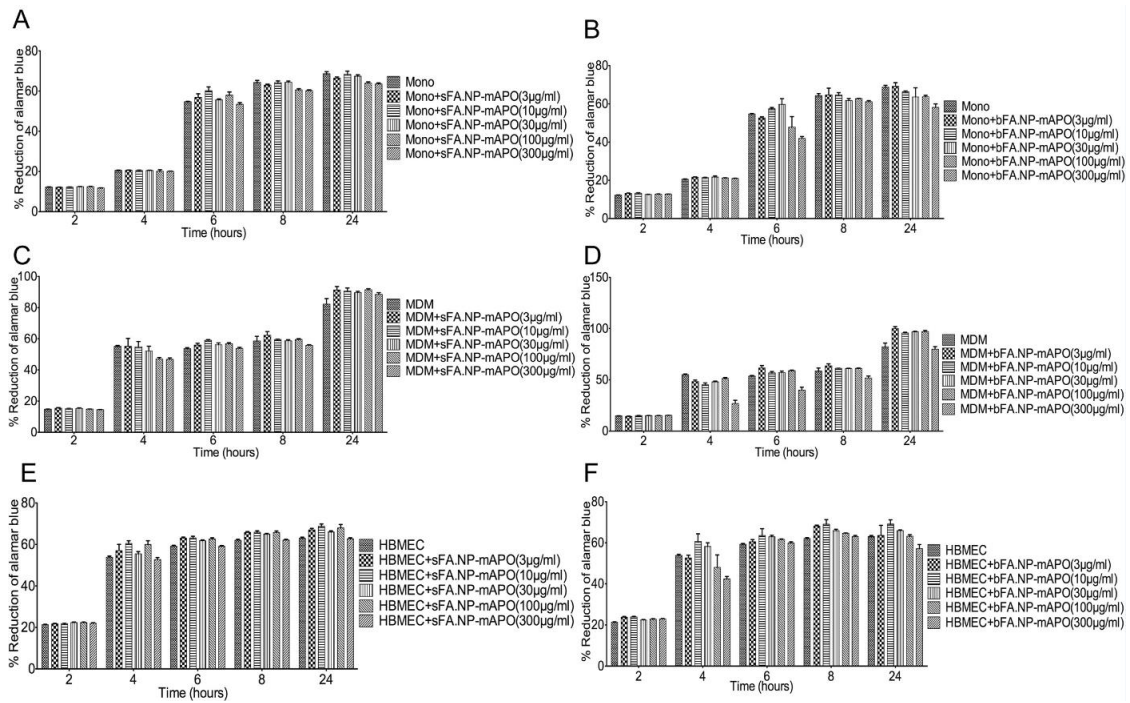
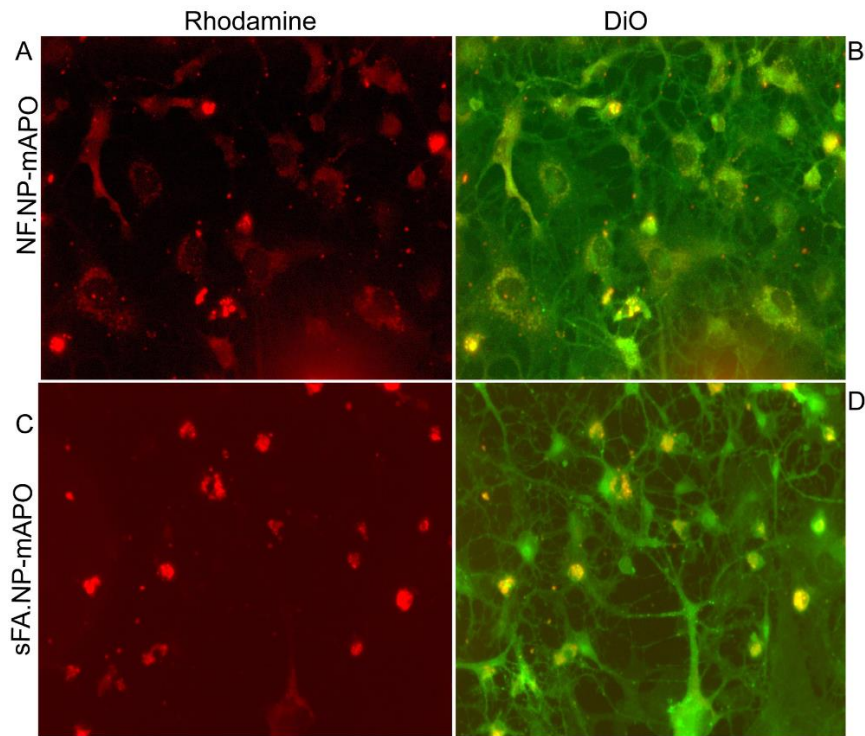


Figure 3.5: Quantification of sFA-NP and bFA-NP uptake in HBMEC and monocytes. **(A)** Representative confocal microscopy images showing sFA-NP-rho and bFA-NP-rho uptake by HBMEC after co-culture with monocytes. **(B)** Monocytes were loaded with 100 $\mu\text{g}/\text{mL}$ sFA-NP-rho or bFA-NP-rho, and co-cultured with HBMEC. FACS quantification of sFA-NP-rho and bFA-NP-rho in primary human monocytes before co-culture and monocytes and HBMEC after co-culture. **(C)** FACS quantification showing direct uptake of sFA-NP-rho and bFA-NP-rho NPs in HBMEC. **(D)** HBMEC were co-cultured with monocytes loaded with 250 $\mu\text{g}/\text{mL}$ sFA-NP-mAPO or 250 μM free mAPO. mAPO levels in monocytes before and after co-culture, and in HBMEC after co-culture were quantified by HPLC at 262 nm. **(E)** HPLC quantification of direct uptake of sFA-NP-mAPO and free mAPO in HBMEC. * $p < 0.05$, *** $p < 0.001$.

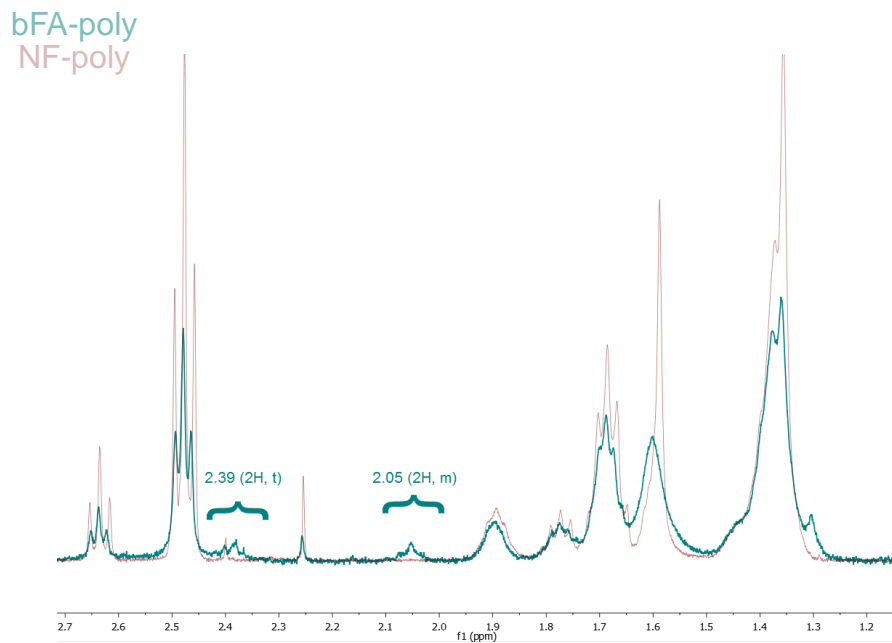


Supplementary Figure 3.1: Effects of sFA-NP and bFA-NP on the viability of human monocytes (**A & B**), human MDM (**C & D**), and HBMEC (**E & F**). Cells from human donors were isolated and cultured as described in the Methods, incubated with NPs of different concentrations (3 µg/mL, 10 µg/mL, 30 µg/mL, 100 µg/mL and 300 µg/mL) for 48 h and toxicity was assessed over 24 h by the alamarBlueTM assay.

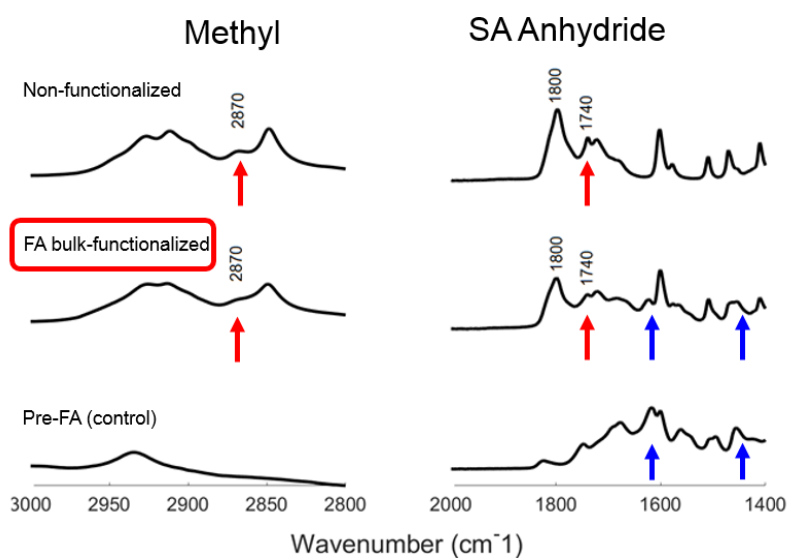


Supplementary Figure 3.2: Representative immunofluorescence images showing endothelial uptake of NF-NP-rho (A, B) and sFA-NP-rho (C, D) following co-culture with monocytes. Primary human monocytes loaded with NF-NP-rho or sFA-NP-rho were co-cultured with HBMEC labeled with DiO (Green), washed and NP uptake analyzed by immunofluorescence and confocal microscopy.

(A)



(B)



Supplementary Figure 3.3. Characterization of bFA- vs. non-functionalized 20:80 CPH:SA copolymer. (A) ¹H NMR of bFA- vs non-functionalized 20:80 CPH:SA copolymer. Appearance of an FA-based aliphatic carbons ($\delta=2.05$ (2H, m), 2.39 (2H, t)) in FA-polymer indicates functionalization. Percent functionalization was estimated by end-group analysis of purified polymer, by back-calculating the molar ratio of FA to 20:80 CPH:SA. (B) FTIR-ATR spectroscopy of FA- vs. non-functionalized 20:80 CPH:SA copolymer, after purification. Red arrows indicate the decrease in the relative peak height of methyl end-groups (2870 cm⁻¹) and SA-SA anhydride bonds (1740 cm⁻¹). Blue arrows at 1460 cm⁻¹ and 1610 cm⁻¹ indicate the appearance of new peaks representing FA in the copolymer.

3.11 References

- [1] G.K. Tofaris, A.H. V Schapira, Neurodegenerative diseases in the era of targeted therapeutics: How to handle a tangled issue, *Mol. Cell. Neurosci.* 66 (2015) 1–2. doi:10.1016/j.mcn.2015.03.002.
- [2] B.P. Dranka, A. Gifford, D. McAllister, J. Zielonka, J. Joseph, C.L. O’Hara, C.L. Stucky, A.G. Kanthasamy, B. Kalyanaraman, A novel mitochondrially-targeted apocynin derivative prevents hyposmia and loss of motor function in the leucine-rich repeat kinase 2 (LRRK2(R1441G)) transgenic mouse model of Parkinson’s disease, *Neurosci. Lett.* 583 (2014) 159–164. doi:10.1016/j.neulet.2014.09.042.
- [3] S.K. Mallapragada, T.M. Brenza, J.M. McMillan, B. Narasimhan, D.S. Sakaguchi, A.D. Sharma, S. Zbarska, H.E. Gendelman, Enabling nanomaterial, nanofabrication and cellular technologies for nanoneuromedicines, *Nanomedicine Nanotechnology, Biol. Med.* 11 (2015) 715–729. doi:10.1016/j.nano.2014.12.013.
- [4] G. Kanmogne, S. Singh, U. Roy, X. Liu, J. McMillan, S. Gorantla, S. Balkundi, N. Smith, Y. Zhou, Y. Alnouti, N. Gautam, L. Poluektova, A. Kabanov, T. Bronich, H. Gendelman, Mononuclear phagocyte intercellular crosstalk facilitates transmission of cell-targeted nanoformulated antiretroviral drugs to human brain endothelial cells, *Int. J. Nanomedicine.* 7 (2012) 2373–2388. doi:10.2147/IJN.S29454.
- [5] P. Puligujja, J. McMillan, L. Kendrick, T. Li, S. Balkundi, N. Smith, R.S. Veerubhotla, B.J. Edagwa, A. V Kabanov, T. Bronich, H.E. Gendelman, X.-M. Liu, Macrophage folate receptor-targeted antiretroviral therapy facilitates drug entry, retention, antiretroviral activities and biodistribution for reduction of human immunodeficiency virus infections, *Nanomedicine.* 9 (2013) 1263–73. doi:10.1016/j.nano.2013.05.003.
- [6] E.S. Park, M. Maniar, J.C. Shah, Biodegradable polyanhydride devices of cefazolin sodium, bupivacaine, and taxol for local drug delivery: Preparation, and kinetics and mechanism of in vitro release, *J. Control. Release.* 52 (1998) 179–189. doi:10.1016/S0168-3659(97)00223-X.
- [7] P.B. Storm, J.L. Moriarity, B. Tyler, P.C. Burger, H. Brem, J. Weingart, Polymer delivery of camptothecin against 9L gliosarcoma: Release, distribution, and efficacy, *J. Neurooncol.* 56 (2002) 209–217. doi:10.1023/A:1015003232713.
- [8] D.B. Masters, C.B. Berde, S. Dutta, T. Turek, R. Langer, Sustained Local Anesthetic Release from Bioerodible Polymer Matrices: A Potential Method for Prolonged Regional Anesthesia, *Pharm. Res. An Off. J. Am. Assoc. Pharm. Sci.* 10 (1993) 1527–1532. doi:10.1023/A:1018995913972.

- [9] G.P. Carino, J.S. Jacob, E. Mathiowitz, Nanosphere based oral insulin delivery, *J. Control. Release.* 65 (2000) 261–269. doi:10.1016/S0168-3659(99)00247-3.
- [10] A.A. Weiner, E.A. Bock, M.E. Gipson, V.P. Shastri, Photocrosslinked anhydride systems for long-term protein release, *Biomaterials.* 29 (2008) 2400–2407. doi:10.1016/j.biomaterials.2008.01.013.
- [11] A.S. Determan, B.G. Trewyn, V.S.Y. Lin, M. Nilsen-Hamilton, B. Narasimhan, Encapsulation, stabilization, and release of BSA-FITC from polyanhydride microspheres, *J. Control. Release.* 100 (2004) 97–109. doi:10.1016/j.jconrel.2004.08.006.
- [12] M.P. Torres, A.S. Determan, G.L. Anderson, S.K. Mallapragada, B. Narasimhan, Amphiphilic polyanhydrides for protein stabilization and release, *Biomaterials.* 28 (2007) 108–116. doi:10.1016/j.biomaterials.2006.08.047.
- [13] B. Carrillo-Conde, E. Schiltz, J. Yu, F.C. Minion, G.J. Phillips, M.J. Wannemuehler, B. Narasimhan, Encapsulation into amphiphilic polyanhydride microparticles stabilizes *Yersinia pestis* antigens, *Acta Biomater.* 6 (2010) 3110–3119. doi:10.1016/j.actbio.2010.01.040.
- [14] B.R. Carrillo-Conde, R.J. Darling, S.J. Seiler, A.E. Ramer-Tait, M.J. Wannemuehler, B. Narasimhan, Sustained release and stabilization of therapeutic antibodies using amphiphilic polyanhydride nanoparticles, *Chem. Eng. Sci.* 125 (2015) 98–107. doi:10.1016/j.ces.2014.08.015.
- [15] L. Erdmann, K.E. Uhrich, Synthesis and Degradation Characteristics of Salicylic Acid-derived Poly(anhydride-esters)., *Biomaterials.* 21 (2000) 1941–1946.
- [16] J.-S. Deng, M. Meisters, L. Li, J. Setesak, L. Claycomb, Y. Tian, D. Stephens, M. Widman, The Development of an Injection-Molding Process for a Polyanhydride Implant Containing Gentamicin Sulfate, *PDA J. Pharm. Sci. Technol.* 56 (2002) 65–77.
- [17] F. Von Burkersroda, L. Schedl, A. G??pferich, Why degradable polymers undergo surface erosion or bulk erosion, *Biomaterials.* 23 (2002) 4221–4231. doi:10.1016/S0142-9612(02)00170-9.
- [18] T.M. Brenza, S.G. Ms, J.E.V. Ramirez, D. Harischandra, V. Anantharam, B. Kalyanaraman, A.G. Kanthasamy, B. Narasimhan, Neuronal Protection against Oxidative Insult by Polyanhydride Nanoparticle-based Mitochondria-targeted Antioxidant Therapy, *Nanomedicine Nanotechnology, Biol. Med.* 13 (2017) 809–820. doi:10.1016/j.nano.2016.10.004.

- [19] M.J. Kipper, E. Shen, A. Determan, B. Narasimhan, Design of an injectable system based on bioerodible polyanhydride microspheres for sustained drug delivery, *Biomaterials*. 23 (2002) 4405–4412. doi:10.1016/S0142-9612(02)00181-3.
- [20] E. Shen, M.J. Kipper, B. Dziadul, M.K. Lim, B. Narasimhan, Mechanistic relationships between polymer microstructure and drug release kinetics in bioerodible polyanhydrides, *J. Control. Release*. 82 (2002) 115–125. doi:10.1016/S0168-3659(02)00125-6.
- [21] G.F. Kelso, C.M. Porteous, G. Hughes, E.C. Ledgerwood, A.M. Gane, R.A.J. Smith, M.P. Murphy, Prevention of Mitochondrial Oxidative Damage Using Targeted Antioxidants, *New York Academy Sci.* 959 (2002) 263–274.
- [22] A. Ghosh, K. Chandran, S. V. Kalivendi, J. Joseph, W.E. Antholine, C.J. Hillard, A. Kanthasamy, A. Kanthasamy, B. Kalyanaraman, Neuroprotection by a mitochondria-targeted drug in a Parkinson’s disease model, *Free Radic. Biol. Med.* 49 (2010) 1674–1684. doi:10.1016/j.freeradbiomed.2010.08.028.
- [23] B.D. Ulery, Y. Phanse, A. Sinha, M.J. Wannemuehler, B. Narasimhan, B.H. Bellaire, Polymer chemistry influences monocytic uptake of polyanhydride nanospheres, *Pharm. Res.* 26 (2009) 683–690. doi:10.1007/s11095-008-9760-7.
- [24] A. V. Chavez-Santoscoy, R. Roychoudhury, N.L.B. Pohl, M.J. Wannemuehler, B. Narasimhan, A.E. Ramer-Tait, Tailoring the immune response by targeting C-type lectin receptors on alveolar macrophages using “pathogen-like” amphiphilic polyanhydride nanoparticles, *Biomaterials*. 33 (2012) 4762–4772. doi:10.1016/j.biomaterials.2012.03.027.
- [25] B. Carrillo-Conde, E.H. Song, A. Chavez-Santoscoy, Y. Phanse, A.E. Ramer-Tait, N.L.B. Pohl, M.J. Wannemuehler, B.H. Bellaire, B. Narasimhan, Mannose-functionalized “pathogen-like” polyanhydride nanoparticles target C-type lectin receptors on dendritic cells, *Mol. Pharm.* 8 (2011) 1877–1886. doi:10.1021/mp200213r.
- [26] H.E. Gendelman, J.M. Orenstein, M.A. Martin, C. Ferrua, R. Mitra, T. Phipps, L.A. Wahl, H.C. Lane, A.S. Fauci, D.S. Burke, Efficient isolation and propagation of human immunodeficiency virus on recombinant colony-stimulating factor 1-treated monocytes, *J. Exp. Med.* 167 (1988) 1428–41.
- [27] G.D. Kanmogne, K. Schall, J. Leibhart, B. Knipe, H.E. Gendelman, Y. Persidsky, HIV-1 gp120 compromises blood-brain barrier integrity and enhances monocyte migration across blood-brain barrier: implication for viral neuropathogenesis, *J. Cereb. Blood Flow Metab.* 27 (2007) 123–34.

- [28] A. Chaudhuri, F. Duan, B. Morsey, Y. Persidsky, G.D. Kanmogne, HIV-1 activates proinflammatory and interferon-inducible genes in human brain microvascular endothelial cells: putative mechanisms of blood-brain barrier dysfunction., *J. Cereb. Blood Flow Metab.* 28 (2008) 697–711.
- [29] A. Chaudhuri, B. Yang, H.E. Gendelman, Y. Persidsky, G.D. Kanmogne, STAT1 signaling modulates HIV-1-induced inflammatory responses and leukocyte transmigration across the blood-brain barrier., *Blood.* 111 (2008) 2062–72.
- [30] M.J. Bernas, F.L. Cardoso, S.K. Daley, M.E. Weinand, A.R. Campos, A.J. Ferreira, J.B. Hoying, M.H. Witte, D. Brites, Y. Persidsky, S.H. Ramirez, M.A. Brito, Establishment of primary cultures of human brain microvascular endothelial cells to provide an in vitro cellular model of the blood-brain barrier., *Nat. Protoc.* 5 (2010) 1265–72.
- [31] R.F. Bressani, A.S. Nowacek, S. Singh, S. Balkundi, B. Rabinow, J. McMillan, H.E. Gendelman, G.D. Kanmogne, Pharmacotoxicology of monocyte-macrophage nanoformulated antiretroviral drug uptake and carriage., *Nanotoxicology.* 5 (2011) 592–605. doi:10.3109/17435390.2010.541292.
- [32] B. Yang, S. Akhter, A. Chaudhuri, G.D. Kanmogne, HIV-1 gp120 induces cytokine expression, leukocyte adhesion, and transmigration across the blood-brain barrier: modulatory effects of STAT1 signaling., *Microvasc. Res.* 77 (2009) 212–9.
- [33] Y. Phanse, P. Lueth, A.E. Ramer-Tait, B.R. Carrillo-Conde, M.J. Wannemuehler, B. Narasimhan, B.H. Bellaire, Cellular Internalization Mechanisms of Polyanhydride Particles: Implications for Rational Design of Drug Delivery Vehicles, *J. Biomed. Nanotechnol.* 12 (2016) 1544–1552. doi:10.1166/jbn.2016.2259.
- [34] L.K. Petersen, L. Xue, M.J. Wannemuehler, K. Rajan, B. Narasimhan, The simultaneous effect of polymer chemistry and device geometry on the in vitro activation of murine dendritic cells, *Biomaterials.* 30 (2009) 5131–5142. doi:10.1016/j.biomaterials.2009.05.069.
- [35] D.S. Katti, S. Lakshmi, R. Langer, C.T. Laurencin, Toxicity, biodegradation and elimination of polyanhydrides, *Adv. Drug Deliv. Rev.* 54 (2002) 933–961. doi:10.1016/S0169-409X(02)00052-2.
- [36] N. Kumar, R.S. Langer, A.J. Domb, Polyanhydrides: An overview, *Adv. Drug Deliv. Rev.* 54 (2002) 889–910. doi:10.1016/S0169-409X(02)00050-9.
- [37] J. Heller, Polyanhydrides and poly(ortho esters), *Adv. Drug Deliv. Rev.* 54 (2002) 887–888.

- [38] A.M. Binnebose, S.L. Haughney, R. Martin, P.M. Imerman, B. Narasimhan, B.H. Bellaire, Polyanhydride Nanoparticle Delivery Platform Dramatically Enhances Killing of Filarial Worms, *PLoS Negl. Trop. Dis.* 9 (2015) 1–18. doi:10.1371/journal.pntd.0004173.
- [39] T.M. Brenza, L.K. Petersen, Y. Zhang, L.M. Huntimer, A.E. Ramer-Tait, J.M. Hostetter, M.J. Wannemuehler, B. Narasimhan, Pulmonary biodistribution and cellular uptake of intranasally administered monodisperse particles, *Pharm. Res.* 32 (2015) 1368–1382. doi:10.1007/s11095-014-1540-y.
- [40] A.S. Determan, J.H. Wilson, M.J. Kipper, M.J. Wannemuehler, B. Narasimhan, Protein stability in the presence of polymer degradation products: Consequences for controlled release formulations, *Biomaterials.* 27 (2006) 3312–3320. doi:10.1016/j.biomaterials.2006.01.054.
- [41] S.L. Haughney, L.K. Petersen, A.D. Schoofs, A.E. Ramer-Tait, J.D. King, D.E. Briles, M.J. Wannemuehler, B. Narasimhan, Retention of structure, antigenicity, and biological function of pneumococcal surface protein A (PspA) released from polyanhydride nanoparticles, *Acta Biomater.* 9 (2013) 8262–8271. doi:10.1016/j.actbio.2013.06.006.
- [42] J.E. Vela Ramirez, R. Roychoudhury, H.H. Habte, M.W. Cho, N.L.B. Pohl, B. Narasimhan, Carbohydrate-functionalized nanovaccines preserve HIV-1 antigen stability and activate antigen presenting cells, *J. Biomater. Sci. Polym. Ed.* 25 (2014) 1387–1406. doi:10.1080/09205063.2014.940243.
- [43] K.A. Ross, Synthetic nanoparticle-based vaccines against respiratory pathogens, *Grad. Theses Diss. Paper 1357* (2013).
- [44] M. Westphal, Z. Ram, V. Riddle, D. Hilt, E. Bortey, Gliadel (R) wafer in initial surgery for malignant glioma: Long-term follow-up of a multicenter controlled trial, *Acta Neurochir. (Wien).* 148 (2006) 269–275. doi:10.1007/s00701-005-0707-z.
- [45] L. Huntimer, A.E. Ramer-Tait, L.K. Petersen, K.A. Ross, K.A. Walz, C. Wang, J. Hostetter, B. Narasimhan, M.J. Wannemuehler, Evaluation of Biocompatibility and Administration Site Reactogenicity of Polyanhydride-Particle-Based Platform for Vaccine Delivery, *Adv. Healthc. Mater.* 2 (2013) 369–378. doi:10.1002/adhm.201200181.
- [46] J.E. Vela-Ramirez, J.T. Goodman, P.M. Boggiatto, R. Roychoudhury, N.L.B. Pohl, J.M. Hostetter, M.J. Wannemuehler, B. Narasimhan, Safety and Biocompatibility of Carbohydrate-Functionalized Polyanhydride Nanoparticles, *AAPS J.* 17 (2015) 256–267. doi:10.1208/s12248-014-9699-z.

- [47] J. Kreuter, D. Shamenkov, V. Petrov, P. Ränge, K. Cychutek, C. Koch-Brandt, R. Alyautdin, Apolipoprotein-mediated transport of nanoparticle-bound drugs across the blood-brain barrier, *J. Drug Target.* 10 (2002) 317–325.
doi:10.1080/10611860290031877|10.1080/10611860290031877.
- [48] J. Vela-Ramirez, P.M. Boggiatto, M.J. Wannemuehler, B. Narasimhan, Polyanhydride nanoparticle interactions with host serum proteins and their effects on bone marrow derived macrophage activation Polyanhydride nanoparticle interactions with host serum proteins and their effects on bone marrow derived macrophage activation, 2016, submitted.

CHAPTER 4: NEURONAL TARGETING OF TRIPHENYLPHOSPHONIUM-FUNCTIONALIZED POLYANHYDRIDE NANOPARTICLES TO COMBAT OXIDATIVE STRESS

Manuscript in progress; to be submitted to *Acta Biomaterialia* in 2017

Ben Schlichtmann¹, Shivani Ghaisas², Rainie Nelson¹, Matthew Panthani¹, Vellareddy Anantharam², Anumantha Kanthasamy², Surya Mallapragada¹, Balaji Narasimhan^{1,*}

¹Department of Chemical and Biological Engineering, Iowa State University, Ames, IA 50011

²Department of Biomedical Sciences, Iowa State University, Ames, IA 50011

*To whom correspondence should be addressed

Key words: Oxidative stress; Polyanhydride nanoparticles; Mito-apocynin; Drug delivery; Triphenylphosphonium

4.1 Abstract

Neurodegeneration due to chemical exposure and/or conditions such as Parkinson's disease and traumatic brain injury leads to significant deleterious events that affect the performance of neurons. Even with survival after acute exposure, affected neurons experience oxidative stress. Treatment of oxidative stress using antioxidants is essential for preventing irreversible damage to the central nervous system. Targeting specific ligands to nano-carriers that encapsulate anti-oxidant drugs is a valuable approach to overcome the complex hurdles associated with central nervous system delivery that block efficient drug bioavailability and lead to protection of cells by lowering the oxidative stress. In this context,

polyanhydride nanoparticles containing anti-oxidants have shown the ability to improve drug delivery to neurons. This work expands upon the design of the polyanhydride nanoparticle platform by using a novel functionalization method to conjugate polyanhydrides with a blood-brain barrier and mitochondrial targeting ligand, triphenylphosphonium (TPP), prior to nanoparticle synthesis. Enhanced internalization of the TPP functionalized nanoparticles by neurons was demonstrated using flow cytometry and supported by confocal microscopy. Finally, improvements in the efficacy of a mitochondrially-targeted antioxidant, Mito-apocynin, for protection against oxidative stress were observed when treating the cells with Mito-Apo containing functionalized nano-carriers, while also providing dose-sparing effects. These studies lay the platform for therapeutic delivery to the brain and set the stage for in vivo studies in the appropriate disease models.

4.2 Introduction

Exposure to toxic organophosphates affects as many as three million individuals each year, with as many as 10% of these exposures resulting in death [1]. In order to prevent the development of chronic symptoms and progression of neurodegeneration, rapid treatment in the hours to days after exposure is essential. Antioxidants are a class of drugs used to treat mitochondrial oxidative stress that often follows chemical exposure in this timescale and is also present in many chronic neurodegenerative conditions [2].

Apocynin is an antioxidant that has been used in several studies for treatment of oxidative stress in pre-clinical Parkinson's disease models [3–5]. The dimer diapocynin has also shown protection against oxidative stress in mouse models [6,7]. In order to improve drug targeting to mitochondria, a lipophilic cation, triphenylphosphonium (TPP), has been

conjugated to apocynin (Mito-Apo) [6,8,9]. An eleven carbon chain derivative of Mito-Apo (Mito-Apo C11) has shown protection in MitoPark and LRRK2R1441G transgenic mouse models [6,8], while a two carbon chain derivative (Mito-Apo C2) has shown protection in a (1-methyl-4-phenyl-1,2,3,6-tetrahydropyridine) (MPTP) model [9]. To further improve drug efficacy of Mito-Apo, nano-carriers can be used to encapsulate and provide sustained release of the drug.

Nano-carriers can improve drug bioavailability and efficacy for central nervous system (CNS) delivery by achieving passage across complex physiological hurdles while protecting the drug from degradation [10]. Furthermore, targeting ligands can be conjugated to antioxidant-encapsulated biodegradable nanomaterials to improve the ability to cross the blood-brain barrier (BBB), be internalized by diseased neurons, and co-localize with the mitochondria [10,11]. In this regard, biodegradable polyanhydride nanoparticles (NPs) represent an attractive nanoscale drug delivery platform technology, and have demonstrated sustained release of therapeutics to counter a broad range of diseases [11–25]. The Gliadel[®] wafer, an FDA-approved polyanhydride-based drug delivery product for delivery of the drug carmustine to treat cancer, is an excellent example of CNS drug delivery [26].

The clinical applicability of polyanhydrides is attributed to their high biocompatibility [27]. In addition, polyanhydrides are relatively hydrophobic polymers, and therefore tend to degrade by surface erosion [28,29]. This feature is particularly advantageous compared to bulk eroding drug release platforms, because it allows for predictable drug release rate that can be altered by simply changing the copolymer composition [27,30,31]. By enabling sustained and local release of drug to diseased neurons and protecting it from systemic degradation, polyanhydride NPs have shown superior dose-sparing effects [17,32].

Neuronal delivery of antioxidants encapsulated within NPs based on 1,6-bis-(*p*-carboxyphenoxy)hexane and sebacic acid (i.e., 20:80 CPH:SA) significantly improved protection against oxidative stress [11]. In addition to the improved efficacy and targeting to neurons, 20:80 CPH:SA NPs are internalized effectively by phagocytic cells [33], can rapidly deliver payloads for combating oxidative stress [34,35], and efficiently encapsulate the therapeutic Mito-Apo [36]. This makes 20:80 CPH:SA NPs an excellent candidate for CNS drug delivery.

Efficacy and localization of nanoscale delivery platforms can be further improved through functionalization with targeting ligands [37–39]. For example, folic acid (FA) has improved neuronal targeting of 20:80 CPH:SA NPs [11]. However, this functionalization did not improve transport across the BBB compared to the non-functionalized counterpart, as demonstrated in Chapter 3. It is necessary to design a delivery platform that can effectively surmount multiple complex hurdles associated with CNS drug delivery, including crossing the BBB and enhancing neuronal targeting and uptake. The targeting ligand, triphenylphosphonium (TPP), has shown the ability to improve BBB transport and enable mitochondrial targeting of delivery platforms [40–43], and additionally improve drug efficacy by direct conjugation [6,8,9], making it an excellent choice of targeting ligand to further optimize the 20:80 CPH:SA NP-based nanomedicine platform.

Many targeting ligands used for drug delivery are conjugated on the surface of the nanoscale delivery platform [11]; this may cause a loss of the ligand by degradation before achieving its targeting goal when administered *in vivo*. To enable prolonged persistence of a ligand such as TPP to more effectively improve CNS delivery, this work investigated the use of a novel functionalization method that conjugates the targeting ligand to the polymer prior

to NP synthesis. The molecule (3-carboxypropyl)triphenylphosphonium (CPTP, a derivative of TPP) was used to synthesize functionalized 20:80 CPH:SA NPs (CPTP-NPs), which contained quantum dots (QDs; QD:(CPTP-NP)s) and the internalization of these NPs by N27 cells, a rat mesencephalic neuronal cell line, was compared to that of non-functionalized 20:80 CPH:SA NPs containing QDs (or QD:NPs). The efficacy of CPTP-NPs against hydrogen peroxide (H₂O₂)-induced oxidative stress was tested after encapsulating Mito-Apo C2 (or simply Mito-Apo) into both NPs and CPTP-NPs (represented by M:NPs and M:(CPTP-NP)s, respectively).

4.3 Experimental Methods

4.3.1 Materials

20:80 CPH:SA copolymer synthesis was performed as described previously [34,44]. ¹H nuclear magnetic resonance (NMR; MR-400, Varian) was used to measure the polymer molecular weight and purity. MTS cell viability dye (Catalog # G3580) was purchased from Promega. Caspase-3 substrate (Catalog # 556449) was purchased from BD Biosciences. MitoTracker® Red and Hoechst 34580 were purchased from ThermoFisher Scientific. HEPES, 3-[(3-Cholamidopropyl)-dimethylammonio]-1-propanesulfonate (CHAPS), 2,2',2'',2'''-(Ethane-1,2-diyl)dinitrilo)tetraacetic acid (EDTA), dithiothreitol (DTT) and sucrose were purchased from Sigma (St. Louis, MO). Dulbecco's modified Eagle's medium (DMEM), Roswell Park Memorial Institute medium (RPMI) 1640, fetal bovine serum (FBS), trypsin/EDTA (TE), L-glutamine, penicillin, and streptomycin were purchased from Invitrogen (Carlsbad, CA). Mito-Apo was kindly provided by the Kalyanaraman laboratory

at the Medical College of Wisconsin. Synthesis and characterization of the final product were performed as described previously [11].

4.3.2 Synthesis of CdSe-ZnS core-shell nanoparticles

Cadmium selenide NPs were synthesized following a standard air-free hot-injection reaction procedure modified from Pu et al. [45] and ZnS shell growth was achieved using a procedure modified from Talapin et al. [46]. Cadmium oxide (0.25 mmol, 32 mg) was dissolved in 2 mL of 1-octadecene (ODE) and 218 μ L oleic acid (OA) in a 4 mL glass vial. A 0.4 M stock solution of selenium in ODE was prepared by sonicating 384 mg of selenium in 12.190 mL ODE using bath sonication. A Zn:S precursor solution was prepared by dissolving zinc chloride (0.19 mmol, 26 mg) and 51.43 μ L of bis(trimethylsilyl) sulfide in 1.436 mL of trioctylphosphine (TOP). To synthesize CdSe NPs, the solution of CdO in ODE and OA was heated to 240°C on an aluminum reaction block under nitrogen atmosphere. 310 μ L of Se in ODE was injected into the reaction vial and the vial was removed from heat. To synthesize CdSe-ZnS core-shell NPs, the crude solution of CdSe as prepared above was cooled slightly to 220°C and the aforementioned Zn:S precursor solution was added dropwise to the CdSe solution under vigorous stirring. The resultant nanoparticles were washed once with methanol and twice with ethanol before being dispersed in methylene chloride.

4.3.3 Poly(arylene ether sulfone) bulk functionalization

An excess of CPTP was acetylated under N₂ in approximately 5 mL acetic anhydride for 60 min at 150 °C. Excess acetic anhydride was removed using a rotary evaporator. The

remaining solution was immediately pipetted into 20:80 CPH:SA copolymer. Conjugation of CPTP to copolymer by an anhydride interchange mechanism was performed by reacting under vacuum at 0.5 torr for 20 min at 180 °C. The conjugated copolymer was dissolved in methylene chloride (Fisher Scientific, Pittsburgh, PA) overnight. Functionalized copolymer was precipitated into hexanes at a methylene chloride:hexanes volume ratio of 1:25 and filtered.

After polymer precipitation, excess free CPTP was purified from the copolymer by sonicating in nanopure water for 30 s, centrifuging at 10,000 rpm for 5 min, and removing the supernatant. Percentage end-group functionalization of copolymer was characterized using ^1H NMR (MR-400 MHz, Varian, Palo Alto, CA; $\text{CHCl}_3\text{-d}_1$) end-group analysis. Specifically, percent functionalization was estimated by back-calculating the molar ratio of CPTP to 20:80 CPH:SA using the area under characteristic peaks from each material. Fourier transform infrared (FTIR; Nicolet iS50 FTIR, ThermoFisher, Waltham, MA) attenuated total reflectance (ATR; Nicolet Smart iTX accessory, ThermoFisher; FTIR-ATR) spectroscopy was also used to characterize structural changes after functionalization. Confirmation of polymer molecular weight after functionalization was evaluated using gel permeation chromatography (GPC; Optilab[®] T-rEX, Wyatt, Santa Barbara, CA). The same functionalization procedure was used for FA-functionalized polymer, except purification was with methylene chloride, retaining the polymer in the solution and disposing un-dissolved free FA.

4.3.4 Nanoparticle synthesis and characterization

Either QD or Mito-Apo was encapsulated into 20:80 CPH:SA NPs by a modified anti-solvent nano-encapsulation method [47]. Briefly, the synthesized polymer (100 mg) and QD (5 mg) or Mito-Apo (0.2 mg) were dispersed into 5 mL of methylene chloride and sonicated for 60 s with a probe sonicator (Sonics and Materials, Newtown, CT). The solution was poured into 1 L of pentane (Fisher Scientific) and the particles were recovered by vacuum filtration. The particle morphology and size were determined using scanning electron microscopy (SEM; Quanta 250 FE-SEM, FEI, Hillsboro, OR). ImageJ software (National Institutes of Health, Bethesda, MD) was used to quantify particle size distribution. Solvents and glassware used to prepare NPs were sterile.

To evaluate drug release kinetics, NPs with or without Mito-Apo were suspended at 10 mg/mL in 1x phosphate-buffered saline (PBS), and sonicated for 30 s. Samples were then incubated in a 37 °C rotator. At respective time points, supernatant from samples was collected *via* centrifugation. Samples were replaced with fresh PBS to maintain perfect sink conditions. The supernatant was analyzed for drug concentration using high-performance liquid chromatography (HPLC, Agilent Technologies 1200, Santa Clara, CA).

To evaluate surface charge, NPs and CPTP-NPs were weighed at approximately 1 mg and brought to 1 mg/mL in nanopure water. The suspension was sonicated for 30 s and diluted to 0.1 mg/mL in nanopure water, and sonicated for 30 s. The zeta potential measurement was recorded immediately using a ZetaSizer (Zetasizer Nano, Malvern Instruments Ltd., Malvern, UK).

4.3.5 N27 cell culture and cytotoxicity testing

A rat mesencephalic neuronal cell line (N27) was used for cytotoxicity, efficacy and localization experiments. Cells were thawed from liquid nitrogen, and immediately added to RPMI media (RPMI 1640, B27 supplement, 10% fetal bovine serum (FBS), L-glutamine, penicillin, and streptomycin). Cells were centrifuged for 5 min at 1,000 rpm, aspirating supernatant. 15 mL RPMI was added to suspend cells, which were plated onto a T75 flask, replacing media the next day. Upon reaching 70% confluence, N27 cells were passaged by trypsinization using trypsin/EDTA. Cells were mixed and counted using a Vi-Cell XR instrument (Beckman Coulter, Brea, CA). For seeding a T75 flask, one million cells were added. To plate into 96, 24, or 6-well plates, cells were plated at approximately 5,000 cells/well, 20,000 cells/well, or 200,000 cells/well, respectively. After 24 h, media was aspirated and the appropriate treatment was added to cells in 2% FBS-containing RPMI (2% RPMI).

To test NP and CPTP-NP cytotoxicity, cells were grown to 70% confluence in 96-well plates in 10% RPMI. NP stock suspensions were sonicated in 2% RPMI for 60 s using a bath sonicator. Old media on cells was aspirated and replaced by 2% RPMI containing NPs or CPTP-NPs. At 24 h, 10 μ L MTS dye was added to each well. 96 well plates were read 1 h after adding the dye using a spectrophotometer (SpectraMax 190, Molecular Devices, Sunnyvale, California; 490nm). The experiments were performed in triplicate.

4.3.6 Fluorescence-activated cell sorting

Cells were grown to 70% confluence in 6 well plates with 10% RPMI. Stock suspensions of 5% QD:NPs and QD:(CPTP-NP)s were sonicated in 2% RPMI for ~60s using

a bath sonicator. Old media was aspirated from 6-well plates and cells were treated with 30 $\mu\text{g}/\text{mL}$ of either QD:NPs or QD:(CPTP-NP)s. After 20 h, media was aspirated and wells were washed with PBS. Cells were collected using a cell scraper, transferred to individual 1.5 mL microcentrifuge tubes and centrifuged at 1,000 rpm for 7 min. PBS was aspirated and replaced with 4% paraformaldehyde (PFA). Each tube was mixed thoroughly by pipetting to ensure fixation. Cells were stored in 4 °C in the dark. Immediately before analysis, the cells were centrifuged and PFA was replaced with 1% bovine serum albumin (BSA) in PBS, and processed *via* flow cytometry using a 488 nm laser (FACSCanto, BD Biosciences, San Jose, CA). The experiments were performed in triplicate.

4.3.7 Confocal microscopy

Cells were grown to 70% confluence in 24-well plates on Poly D-Lysine-coated glass coverslips in 10% RPMI. NP stock suspensions were sonicated in 2% RPMI for ~60 s using a bath sonicator. Cells were treated with 30 $\mu\text{g}/\text{mL}$ QD:NPs or QD:(CPTP-NP)s in 2% RPMI for 24 h. Then, media was aspirated and cells were washed in pre-warmed (37 °C) HEPES buffered saline solution (HBSS). Next, HBSS was aspirated and the cells were incubated with HBSS containing 1/7,000 MitoTracker[®] Red, and 1/5,000 Hoechst dyes for 8 min. HBSS was aspirated and the cells were then washed two times with room temperature PBS and fixed with room temperature 4% PFA. The coverslips were mounted onto SuperFrost[®] Slides (Sigma) for confocal microscopy (Leica SP5 X MP confocal/multiphoton microscope). The experiments were performed in triplicate.

4.3.8 Cell viability by MTS assay

Cells were grown to 70% confluence in 96-well plates in 10% RPMI. NP stock suspensions were sonicated in 2% RPMI for ~60 s using a bath sonicator. Old media on the cells was aspirated and replaced by 2% RPMI containing 30 $\mu\text{g}/\text{mL}$ NPs or 10 μM soluble Mito-Apo C2. At 18 h, cells were challenged with 100 μM H_2O_2 (+/- challenge control). After a 6 h H_2O_2 challenge, 10 μL MTS dye was added to each well. 96-well plates were read 1.5 h after adding the dye using a 96-well plate reader. The experiments were performed in triplicate.

4.3.9 Cleaved caspase-3 quantification

Cells were grown to 70% confluence in 6-well plates in 10% RPMI. NP stock suspensions were sonicated in 2% RPMI for ~60 s using a bath sonicator. Old media was aspirated and cells were treated with either soluble 10 μM Mito-Apo C2 or 30 $\mu\text{g}/\text{mL}$ Mito-Apo C2-encapsulated NPs. At 18 h, cells were challenged with 100 μM H_2O_2 (+/- challenge control). After 6 h H_2O_2 challenge, supernatant from each well was centrifuged in individual microcentrifuge tubes at 1,000 rpm for 5 min to collect floating cells. Adherent cells were detached by aspirating media and adding 0.5 mL TE for 2 min. TE was neutralized by adding 1.0 mL 2% RPMI, and cells were centrifuged at 1,000 rpm for 5 min in corresponding tubes. Supernatant was aspirated and cells were rinsed with ice-cold PBS, followed by centrifugation at 1,000 rpm for 5 min. Supernatant was aspirated and 250 μL caspase buffer (50 mM HEPES, 10% sucrose, 0.1% CHAPS, 1 mM EDTA, 10 mM DTT) was added to each sample, vortexing to lyse cells. Samples were incubated at 37 $^\circ\text{C}$ for 20 min on a shaker. Samples were centrifuged at 13,200 rpm for 5 min before transferring 190 μL

supernatant from each sample to a 96 well plate. To each sample, 10 μL caspase-3 substrate was added. After incubating at 37 $^{\circ}\text{C}$ for one hour on a shaker, the fluorescence was quantified using a 96-well plate reader (ex: 380 nm, em: 460 nm). A NP only control was used for both NP and CPTP-NP remove fluorescent signal associated with NPs. The experiments were performed in triplicate.

4.3.10 Statistical analysis

Graphical data were statistically analyzed using a one or two-way ANOVA for multiple comparisons, or a student's t-test for individual comparisons, on GraphPad Prism[®] software. Comparisons were marked for significance at *p*-values less than 0.05, 0.01 or 0.001.

4.4 Results

4.4.1 Characterization of functionalized polymer

Previous studies demonstrate that 20:80 CPH:SA molecular weights between 10-15 kDa were suitable for synthesizing NPs [47]. Molecular weights for the polymer used in this study were confirmed to be in this range by ^1H NMR. After bulk functionalization with CPTP, a small change in copolymer molecular weight was observed using GPC.

Functionalization of CPTP was indicated by ^1H NMR analysis, which showed the existence of phenyl group peaks representing CPTP after purification (δ 7.73-7.83 (15H, m), Figure 4.1 A). Simultaneously, a decrease in the non-functionalized methyl end-group (δ 2.22 (3H, s)) was observed. The percent conjugation was determined by calculating the peak area ratio of CPTP to 20:80 CPH:SA copolymer peaks in a purified solution, and then back-

calculating the molar ratio (with two moles of possible end-groups available for functionalization on each copolymer chain), leading to an estimated 45% functionalization of the polymer used in this study.

Previous analysis of 20:80 CPH:SA copolymer by FTIR-ATR showed peaks from 1700-1800 cm^{-1} indicative of SA-SA anhydride bonds [48]; further, peaks were present at 2900 cm^{-1} indicative of methyl end-groups from the non-functionalized polymer. After functionalization with CPTP followed by polymer purification, a shift in the composition of anhydride bonds was observed in the 1700-1800 cm^{-1} range indicating a change in the proportion of anhydride bonds. Additionally, a decrease in the intensity of methyl group peaks was observed, indicating a change in the proportion of functional end-groups of the polymer (Fig. 4.1 B). Furthermore, new peaks were observed in the spectrum of the functionalized polymer at 1440 cm^{-1} and 1720 cm^{-1} representative of the targeting ligand, CPTP. Taken together, all of these methods demonstrated CPTP functionalization of the 20:80 CPH:SA copolymer.

4.4.2 Characterization of nanoparticles and drug release kinetics

Table 4.1 lists the morphology, size, and zeta potential of the formulations synthesized for this study. All NP formulations were spherical and the sizes were within range of previously reported values, which demonstrated optimal cellular internalization [47]. Additionally, a release study with 5 wt% M:NPs showed a drug encapsulation efficiency of 20%, with about one third of the drug being released from the NPs within the first day of incubation in PBS (Fig. 4.2). Studies with 0.2 wt% M:NPs and 0.2 wt% M:(CPTP-NP)s are currently underway to characterize release kinetics of the NP formulations used in this study.

4.4.3 Cytotoxicity and internalization in N27 cells

NPs and CPTP-NPs were evaluated for potential cytotoxicity in the N27 cells. Up to a concentration of 30 µg/mL, neither formulation showed any detrimental effects on cell viability (Fig. 4.3). Next, differences in internalization capability of QD:NPs and QD:(CPTP-NP)s in N27 neurons were evaluated using flow cytometry and confocal microscopy. The flow cytometric data indicated that QD:(CPTP-NP)s were internalized more efficiently than QD:NPs, with 37% of cells internalizing QD:(CPTP-NP)s and only 19% of cells internalizing QD:NPs (Fig. 4.4). Additionally, confocal microscopy of cells incubated with QD:NPs and QD:(CPTP-NP)s for 24 h confirmed neuronal internalization of both formulations (Fig. 4.5).

4.4.4 Protection against H₂O₂ challenge in N27 cells

The viability of N27 cells incubated with M:NPs or M:(CPTP-NP)s after H₂O₂ challenge was evaluated to observe whether there were improvements in drug efficacy elicited by M:(CPTP-NP)s. It was found that after a 6 h H₂O₂ challenge, 0.2 wt% M:(CPTP-NP)s improved protection against oxidative stress over 0.2 wt% M:NPs by an MTS assay (Fig. 4.6). Additionally, a caspase-3 assay was performed on cells treated with 0.2 wt% M:NPs and 0.2 wt% M:(CPTP-NP)s 18 h prior to a 6 h H₂O₂ challenge to further evaluate enhancement of protection elicited by M:(CPTP-NP)s. It was found that both M:NPs and M:(CPTP-NP)s sufficiently protected against H₂O₂ – induced toxicity after a 6 hour challenge (Fig. 4.7). This further emphasizes the dose-sparing properties of the M:(CPTP-NP)s as observed in the MTS assay.

4.5 Discussion

There is an urgent need to develop more effective therapeutic options for treatment of chemical exposure. Mito-Apo has demonstrated efficacy in protecting against oxidative stress both *in vitro* and *in vivo* [6,8,9,11]. However, some potential improvements that can be attained include sustained drug release to increase the bioavailability, and lowering the therapeutic dose to avoid systemic toxicity. In this work, we used a rat mesencephalic neuronal cell line to demonstrate that nano-carriers based on CPTP-functionalized polyanhydrides were internalized more effectively by the cells and protected the cells from H₂O₂ challenge in comparison with their non-functionalized nano-carrier counterparts.

An important characteristic of CNS delivery platforms is the ability to target the complex hurdles impeding efficient drug protection. The development of a bulk functionalization method enables the conjugation of the targeting ligand to the polymer prior NP synthesis; after NP synthesis, CPTP will exist throughout the bulk of the NP, rather than just on the surface as is the case when NPs are functionalized with ligands [11]. Therefore, as the NP degrades, the CPTP will persist as part of the NPs, enabling prolonged targeting capability. This is particularly advantageous over surface functionalization methods of NPs, in which the targeting ligand is released immediately upon onset of degradation.

The structural characteristics of the NPs were relatively unchanged after functionalization and no detrimental effects of the targeting ligand were observed during NP synthesis. Size and morphology of CPTP-NPs, with or without Mito-Apo or QDs, was unchanged after functionalization (Table 4.1). Additionally, studies comparing the release profiles of 5 wt% M:NPs and FA-functionalized 5 wt% M:NPs (M:(FA-NP)s) showed no change in drug EE of M:(FA-NP)s compared to M:NPs (Fig. 4.2), indicating that the bulk

functionalization method does not negatively impact the EE of Mito-Apo within 20:80 CPH:SA NPs. It is expected that the 0.2 wt% M:NPs and 0.2 wt% M:(CPTP-NP)s used in this study will have a larger EE due to a smaller diffusion gradient forcing the drug out of the polymer matrix during NP synthesis, compared to 5 wt% M:NPs. Additionally, it is expected that 0.2 wt% M:(CPTP-NP)s will have a similar EE to 0.2 wt% M:NPs. Studies are currently underway to assess these hypotheses.

The mitochondrial-targeting properties of TPP make it an excellent choice for improving delivery of antioxidants [6,41,49–62]. Incorporation of this cationic targeting ligand into NPs did not affect the biocompatibility of the NPs in N27 cells (Fig. 4.3), and a non-toxic concentration of 30 $\mu\text{g}/\text{mL}$ NPs was therefore used in all the subsequent localization and efficacy studies. By incorporating TPP within this NP formulation, it was expected that cellular internalization *via* adsorptive-mediated endocytosis would be further enhanced. Flow cytometry was performed to evaluate this hypothesis. The CPTP-functionalized formulation demonstrated enhanced cellular internalization compared to the NPs (Fig. 4.4). This enhanced targeting may be due to a higher affinity of the more positively charged CPTP-NPs for the negative neuronal membrane and therefore enhance adsorptive-mediated endocytosis by non-specific electrostatic interaction [58,63]. It is also known that 20:80 CPH:SA NPs may be internalized by non-specific, non-adsorptive mechanisms as well [33] (Chapter 3).

Confocal microscopy was used to corroborate the internalization behavior observed with the flow cytometric analysis. After 24 h, both NPs and CPTP-NPs were localized around the cells (Fig. 4.5 A and B, respectively). This suggests that both NPs and CPTP-NPs are able to achieve rapid cellular entry in order to quickly deliver drug for immediate

protection against oxidative stress, as shown in the efficacy studies (Figs. 4.6 and 4.7) and supported by the burst release profile observed in the first few hours after incubation (Fig. 4.2). This suggests that incorporating a cationic ligand with the negatively charged 20:80 CPH:SA NPs may improve the affinity of the CPTP-NPs for the negatively charged mitochondrial membrane [64,65].

In addition to testing for enhanced neuronal internalization and mitochondrial co-localization, the ability to enhance drug efficacy is important for therapeutic delivery platforms. The toxin H_2O_2 is widely used to test the efficacy of antioxidants, because it leads to the formation of dangerous superoxide radicals in the cell [11]. Therefore, H_2O_2 was used in this study to evaluate the ability of the NP formulations to enhance the protective capability of Mito-Apo in N27 cells. An added benefit of NPs is the ability to provide sustained release to protect the cells for a longer period of time than would administration of a large bolus of drug. After encapsulating Mito-Apo in both NPs and FA-NPs, functionalized in the same way as CPTP-NPs, the rate of drug release was observed to be zero-order over the first few days of release (Fig 4.2). This constant release rate may lead to increased local bioavailability around the site of the diseased neurons. The enhanced protection over soluble drug after the 6 h challenge by an MTS cell viability assay (Fig. 4.6) indicates that the sustained release properties enabled by these NP formulations increased the local bioavailability of the drug and helped lower oxidative stress over several hours. These *in vitro* results are promising initial steps towards translating these studies into animal models.

To further evaluate the ability of CPTP-NPs to improve protection, a caspase-3 assay was performed to evaluate the amount of cell death [11,66–68]. After quantifying the amount of caspase-3 signal following H_2O_2 challenge, both NP formulations protected against

oxidative stress (Fig. 4.7). The EE of these 0.2% Mito-Apo-loaded NP formulations is expected to be of the order of 50-60% (studies are underway to measure the EE), indicating significantly less drug used compared to the soluble dose group. This observation demonstrates the dose-sparing properties of the bulk-functionalized polyanhydride NPs, in agreement with previous observations with surface-functionalized formulations [11].

4.6 Conclusions

Using a NP platform based on biodegradable polyanhydrides for cellular internalization and sustained release of therapeutics, a novel bulk functionalization method was used to conjugate a derivative of TPP to 20:80 CPH:SA copolymer before NP synthesis. CPTP-NPs showed enhanced cellular internalization over NPs in a rat mesencephalic neuronal cell line. Additionally, Mito-Apo containing functionalized NP formulations showed enhanced efficacy in protecting the cells against H₂O₂, with a significantly lower therapeutic drug concentration than administering the drug solubly. Furthermore, bulk-functionalizing TPP to 20:80 CPH:SA NPs may enhance neuronal membrane targeting and improve co-localization with the mitochondria *in vivo*. Therefore, it is a promising candidate for treatment of oxidative stress buildup in the brain.

4.7 Acknowledgments

The authors would like to acknowledge funding support from the US Army Medical Research and Materiel Command under contract W81XWH-11-1-0700. The authors also acknowledge financial support from the Nanovaccine Initiative at Iowa State University.

4.8 Author Information

Corresponding Author:

B. Narasimhan, Department of Chemical and Biological Engineering, Iowa State University,
2035 Sweeney Hall, Ames, IA 50011, USA. Tel: +1 515 294 8019; e-mail:

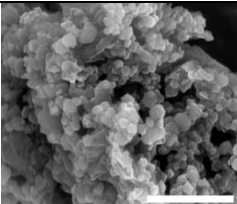
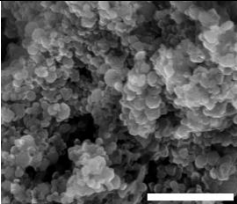
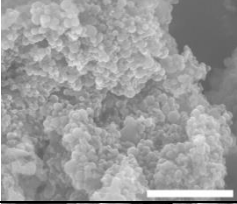
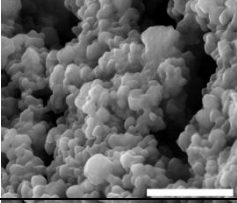
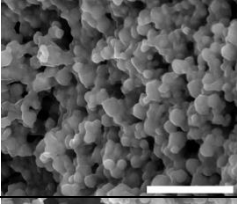
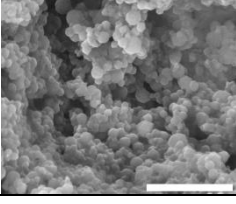
nbalaji@iastate.edu.

4.9 Author Contributions

All authors have given approval to the current version of the manuscript.

4.10 Tables and Figures

Table 4.1. Particle Characteristics. n=3 for size quantification and zeta potential measurements. Scale bar on images is 3 μm .

NP Formulation	Loading	SEM photomicrographs	Geometric Diameter (nm)	Zeta Potential (mV)
NP	None		295 ± 99	-18.3
	0.2% Mito-Apo		306 ± 99	-15.9
	5% QD		232 ± 68	-19.5
CPTP-NP	None		368 ± 109	-7.6
	0.2% Mito-Apo		371 ± 105	-3.8
	5% QD		314 ± 96	5.1

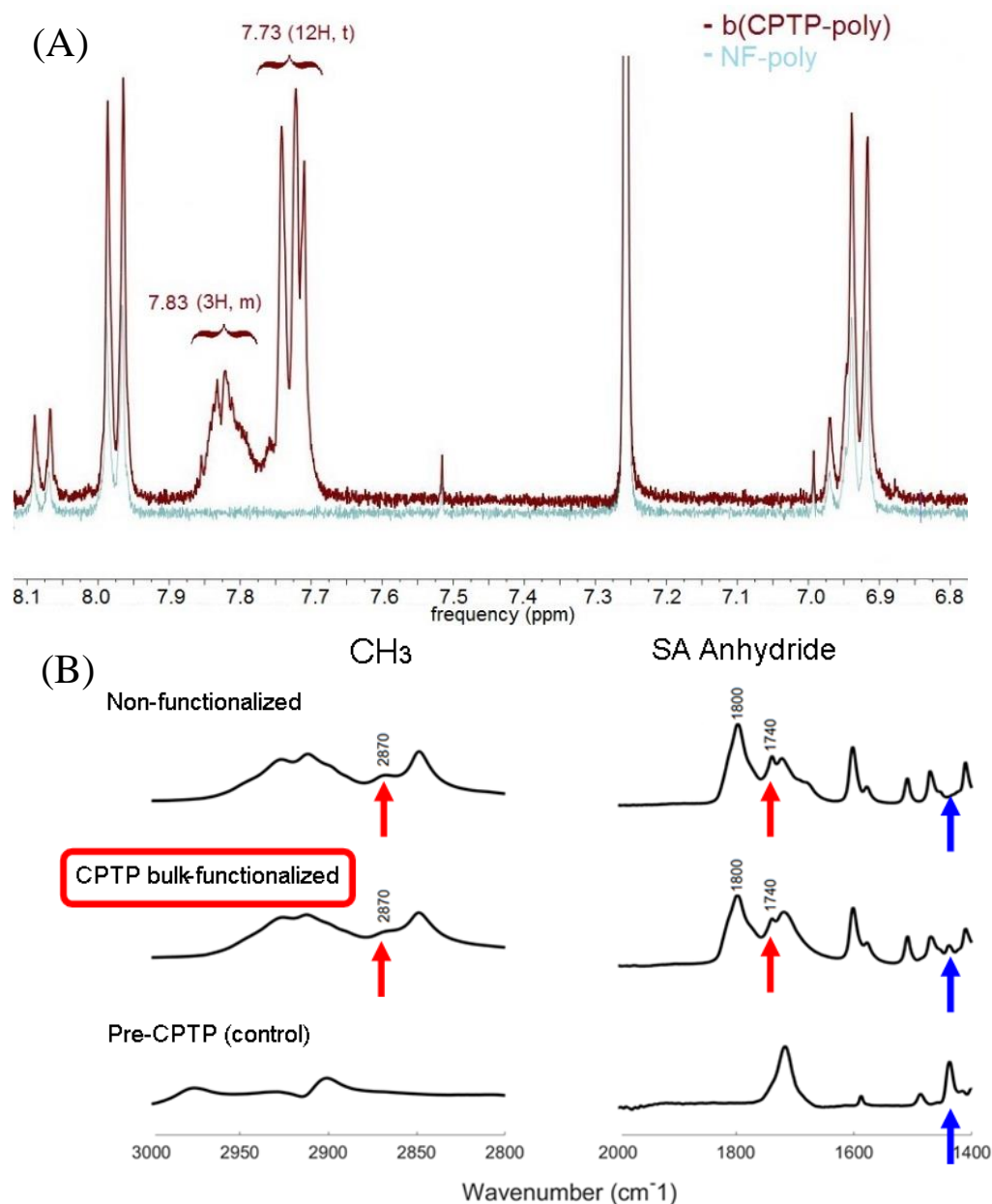


Figure 4.1. Characterization of CPTP- vs. non-functionalized 20:80 CPH:SA copolymer. (A) ¹H NMR of CPTP- vs non-functionalized 20:80 CPH:SA copolymer. Appearance of the phenyl group ($\delta=7.73-7.83$ (15H, m)) and decrease in the methyl functional group ($\delta=2.22$ (3H, s)) in CPTP-polymer indicates functionalization. Percent functionalization was estimated by end-group analysis of purified polymer, by back-calculating the molar ratio of CPTP to 20:80 CPH:SA. (B) FTIR-ATR spectroscopy of CPTP- vs non-functionalized 20:80 CPH:SA copolymer, after purification. Red arrows indicate the decrease in the relative peak height of methyl end-groups (2870 cm⁻¹) and SA-SA anhydride bonds (1740 cm⁻¹). Blue arrows at 1440 cm⁻¹ and 1720 cm⁻¹ indicate the appearance of new peaks representing CPTP in the copolymer.

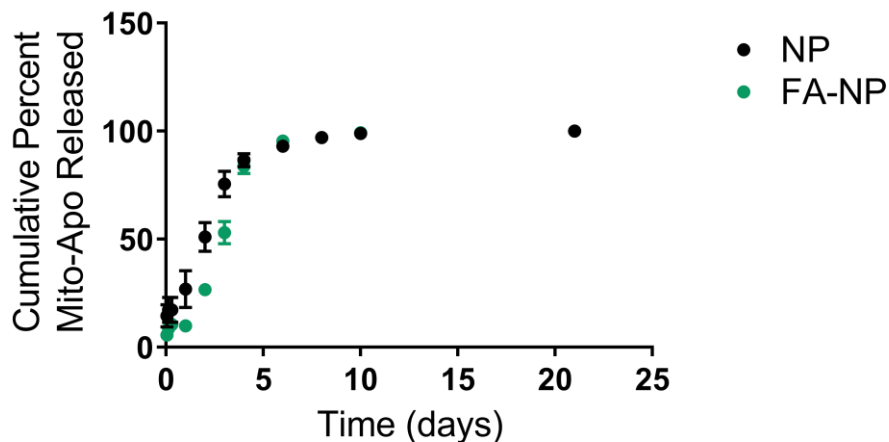
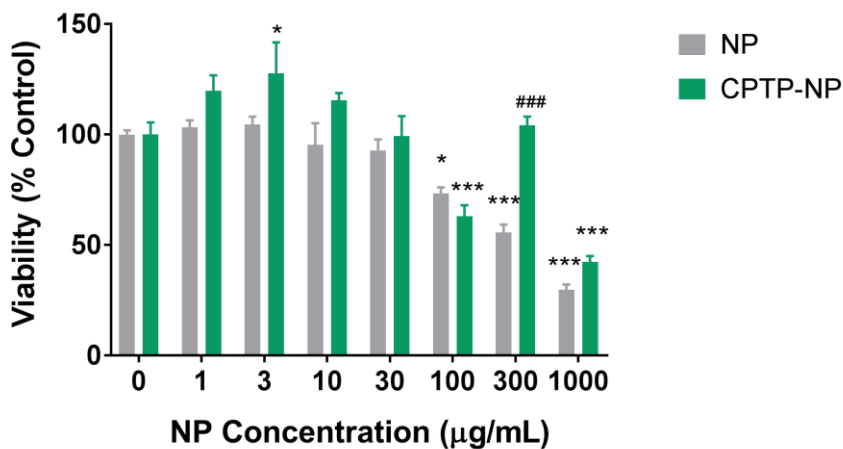


Figure 4.2. Mito-Apo release kinetics of 5%-loaded NPs. The concentration of Mito-Apo released over time in M:NPs and M:(FA-NP)s was measured using HPLC (Agilent Technologies 1200) and the amount of Mito-Apo released at each time point was normalized by the total amount of Mito-Apo released (20% drug EE for both NP formulations). Error bars represent standard error of the mean (n=3).



p<0.001 w.r.t. NP

* p<0.05 compared to respective 0 µg/mL control

*** p<0.001 compared to respective 0 µg/mL control

Figure 4.3. Biocompatibility of NPs and CPTP-NPs in N27 cells. NPs and CPTP-NPs at different concentrations as indicated were incubated with N27 cells in 2% RPMI for 24 h before adding 10 µL MTS dye to each well. Absorbance was measured after 1 h in MTS dye using a 96-well plate reader. Error bars represent the standard error of the mean (n=8).

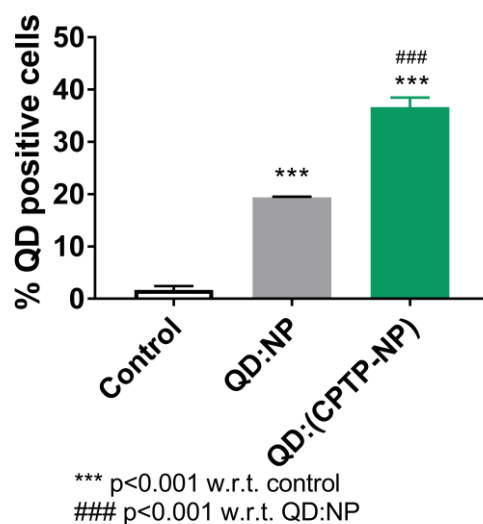
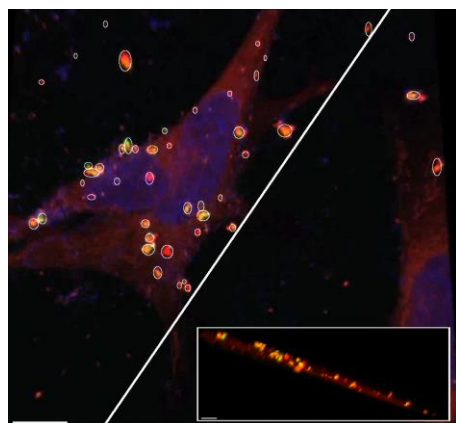


Figure 4.4. Cellular internalization of QD:NPs and QD:(CPTP-NP)s by flow cytometric analysis. N27 cells were incubated with QD:NPs) or CPTP-NPs for 20 h in 2% RPMI. The 6-well plates were then washed with PBS and cells were collected using a cell scraper. After centrifuging 1,000 rpm for 7 minutes, cells were fixed with PFA. Prior to analysis, cells were re-suspended in a 1% BSA buffer in glass test tubes. Fluorescence was measured using a 488 nm laser, and cells were separated from debris based on morphology. Error bars represent the standard error of the mean (n=3).

(A)



(B)

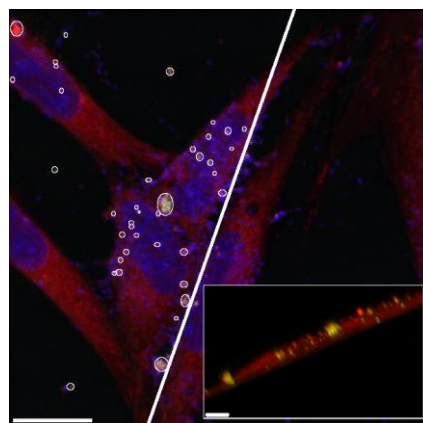


Figure 4.5. Cellular internalization of QD:NPs and QD:(CPTP-NP)s. Confocal microscopy of QD:NPs (A) and QD:(CPTP-NP)s (B) (green) incubated with cells for 24 h before staining for mitochondria (red) and nucleus (blue) and fixing. Internalization is confirmed by the existence of nanoparticles in plane with the cells both from a top-down view and in the cross section. Mitochondrial co-localization is represented by a yellow signal. Scale bar on images is 10 μm . Inset scale bar: 5 μm .

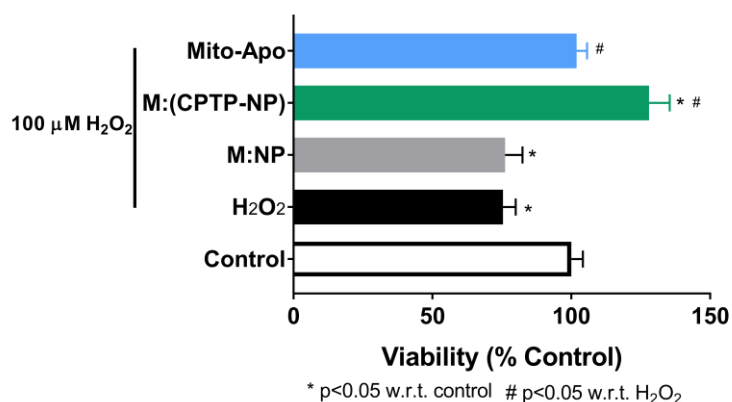


Figure 4.6. Protection against H₂O₂ – induced cell death in N27 neurons. After incubating cells for 18 h with either 30 μg/mL M:NPs, M:(CPTP-NP)s or soluble Mito-Apo (including +/- toxin challenge control), media was replaced with 2% RPMI containing 100 μM H₂O₂ as well as the same concentration of M:NPs, M:(CPTP-NP)s or soluble Mito-Apo and cells were challenged for 6 h. After 6 h challenge, 10 μL MTS dye was added and absorbance was measured after 1.5 h of incubation with MTS dye at 490 nm using a 96 well plate reader. Error bars represent standard error of the mean (n=3).

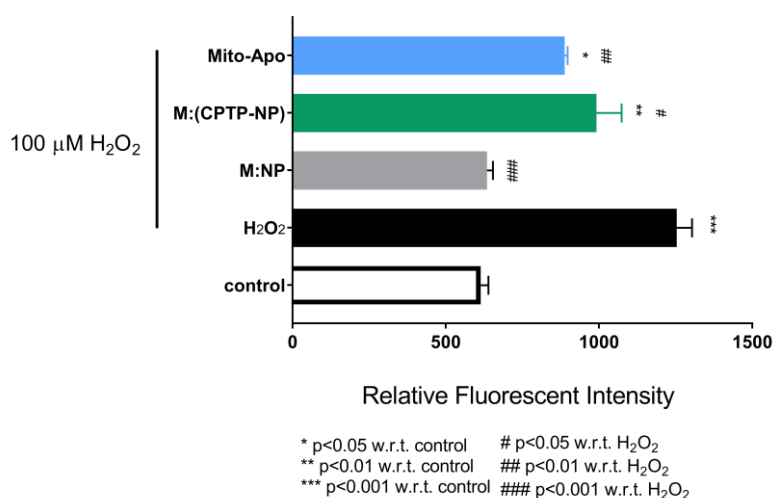


Figure 4.7. Protection against H₂O₂ – induced cell death in N27 neurons by cleaved caspase-3 quantification. After incubating cells for 18 h with either 30 μg/mL M:NPs, M:(CPTP-NP)s or 10 μM Mito-Apo (including +/- toxin challenge control), media was replaced with 2% RPMI containing 100 μM H₂O₂ as well as the same concentration of M:NPs, M:(CPTP-NP)s or soluble Mito-Apo for 6 h. After 6 h challenge, cells were collected using TE. Cells were lysed using a Caspase-3 buffer, and then supernatant from lysate was incubated with Caspase-3 substrate for 1 h before measuring fluorescence (em: 380, ex: 460 nm) using a 96 well plate reader. Error bars represent standard error of the mean (n=3).

4.11 References

- [1] S. Bird, S.J. Traub, J. Grayzel, Organophosphate and carbamate poisoning, *UpToDate*. 14 (2014) 339.
- [2] Y. Chen, Organophosphate-induced brain damage: Mechanisms, neuropsychiatric and neurological consequences, and potential therapeutic strategies, *Neurotoxicology*. 33 (2012) 391–400. doi:10.1016/j.neuro.2012.03.011.
- [3] H. Gao, B. Liu, W. Zhang, J. Hong, Critical role of microglial NADPH oxidase-derived free radicals in the in vitro MPTP model of Parkinson's disease, *FASEB J*. 17 (2003) 1954–6. doi:10.1096/fj.03-0109fje.
- [4] A.C. Cristovao, D.-H. Choi, G. Baltazar, M.F. Beal, Y.-S. Kim, The Role of NADPH Oxidase 1-Derived Reactive Oxygen Species in Paraquat-Mediated Dopaminergic Cell Death, *Antioxid. Redox Signal*. 11 (2009) 2105–18.
- [5] V. Anantharam, S. Kaul, C. Song, A. Kanthasamy, A.G. Kanthasamy, Pharmacological inhibition of neuronal NADPH oxidase protects against 1-methyl-4-phenylpyridinium (MPP⁺)-induced oxidative stress and apoptosis in mesencephalic dopaminergic neuronal cells, *Neurotoxicology*. 28 (2007) 988–997. doi:10.1016/j.neuro.2007.08.008.
- [6] B.P. Dranka, A. Gifford, D. McAllister, J. Zielonka, J. Joseph, C.L. O'Hara, C.L. Stucky, A.G. Kanthasamy, B. Kalyanaraman, A novel mitochondrially-targeted apocynin derivative prevents hyposmia and loss of motor function in the leucine-rich repeat kinase 2 (LRRK2(R1441G)) transgenic mouse model of Parkinson's disease, *Neurosci. Lett*. 583 (2014) 159–164. doi:10.1016/j.neulet.2014.09.042.
- [7] A. Ghosh, A. Kanthasamy, J. Joseph, V. Anantharam, P. Srivastava, B.P. Dranka, B. Kalyanaraman, A.G. Kanthasamy, Anti-inflammatory and neuroprotective effects of an orally active apocynin derivative in pre-clinical models of Parkinson's disease., *J. Neuroinflammation*. 9 (2012) 241. doi:10.1186/1742-2094-9-241.
- [8] M. Langley, A. Ghosh, A. Charli, S. Sarkar, M. Ay, J. Luo, J. Zielonka, T. Brenza, B. Bennett, H. Jin, S. Ghaisas, B. Schlichtmann, D. Kim, V. Anantharam, A. Kanthasamy, B. Narasimhan, B. Kalyanaraman, A. Kanthasamy, Mito-apocynin Prevents Mitochondrial Dysfunction, Microglial Activation, Oxidative Damage and Progressive Neurodegeneration in MitoPark Transgenic Mice, *Antioxid. Redox Signal*. 7 (2017). doi:10.1089/ars.2016.6905.
- [9] A. Ghosh, M.R. Langley, D.S. Harischandra, M.L. Neal, H. Jin, V. Anantharam, J. Joseph, T. Brenza, B. Narasimhan, A. Kanthasamy, B. Kalyanaraman, A.G. Kanthasamy, Mitoapocynin Treatment Protects Against Neuroinflammation and Dopaminergic Neurodegeneration in a Preclinical Animal Model of Parkinson's

- Disease, *J. Neuroimmune Pharmacol.* 11 (2016) 259–278. doi:10.1007/s11481-016-9650-4.
- [10] K.A. Ross, T.M. Brenza, A.M. Binnebose, Y. Phanse, A.G. Kanthasamy, H.E. Gendelman, A.K. Salem, L.C. Bartholomay, B.H. Bellaire, B. Narasimhan, Nano-Enabled Delivery of Diverse Payloads Across Complex Biological Barriers., *J. Control. Release.* 10 (2015) 548–59. doi:10.1016/j.jconrel.2015.08.039.
- [11] T.M. Brenza, S.G. Ms, J.E.V. Ramirez, D. Harischandra, V. Anantharam, B. Kalyanaraman, A.G. Kanthasamy, B. Narasimhan, Neuronal Protection against Oxidative Insult by Polyanhydride Nanoparticle-based Mitochondria-targeted Antioxidant Therapy, *Nanomedicine Nanotechnology, Biol. Med.* 13 (2017) 809–820. doi:10.1016/j.nano.2016.10.004.
- [12] E.S. Park, M. Maniar, J.C. Shah, Biodegradable polyanhydride devices of cefazolin sodium, bupivacaine, and taxol for local drug delivery: Preparation, and kinetics and mechanism of in vitro release, *J. Control. Release.* 52 (1998) 179–189. doi:10.1016/S0168-3659(97)00223-X.
- [13] P.B. Storm, J.L. Moriarity, B. Tyler, P.C. Burger, H. Brem, J. Weingart, Polymer delivery of camptothecin against 9L gliosarcoma: Release, distribution, and efficacy, *J. Neurooncol.* 56 (2002) 209–217. doi:10.1023/A:1015003232713.
- [14] D.B. Masters, C.B. Berde, S. Dutta, T. Turek, R. Langer, Sustained Local Anesthetic Release from Bioerodible Polymer Matrices: A Potential Method for Prolonged Regional Anesthesia, *Pharm. Res. An Off. J. Am. Assoc. Pharm. Sci.* 10 (1993) 1527–1532. doi:10.1023/A:1018995913972.
- [15] G.P. Carino, J.S. Jacob, E. Mathiowitz, Nanosphere based oral insulin delivery, *J. Control. Release.* 65 (2000) 261–269. doi:10.1016/S0168-3659(99)00247-3.
- [16] A.A. Weiner, E.A. Bock, M.E. Gipson, V.P. Shastri, Photocrosslinked anhydride systems for long-term protein release, *Biomaterials.* 29 (2008) 2400–2407. doi:10.1016/j.biomaterials.2008.01.013.
- [17] A.M. Binnebose, S.L. Haughney, R. Martin, P.M. Imerman, B. Narasimhan, B.H. Bellaire, Polyanhydride Nanoparticle Delivery Platform Dramatically Enhances Killing of Filarial Worms, *PLoS Negl. Trop. Dis.* 9 (2015) 1–18. doi:10.1371/journal.pntd.0004173.
- [18] B.R. Carrillo-Conde, R.J. Darling, S.J. Seiler, A.E. Ramer-Tait, M.J. Wannemuehler, B. Narasimhan, Sustained release and stabilization of therapeutic antibodies using amphiphilic polyanhydride nanoparticles, *Chem. Eng. Sci.* 125 (2015) 98–107. doi:10.1016/j.ces.2014.08.015.

- [19] T.M. Brenza, L.K. Petersen, Y. Zhang, L.M. Huntimer, A.E. Ramer-Tait, J.M. Hostetter, M.J. Wannemuehler, B. Narasimhan, Pulmonary biodistribution and cellular uptake of intranasally administered monodisperse particles, *Pharm. Res.* 32 (2015) 1368–1382. doi:10.1007/s11095-014-1540-y.
- [20] M.P. Torres, A.S. Determan, G.L. Anderson, S.K. Mallapragada, B. Narasimhan, Amphiphilic polyanhydrides for protein stabilization and release, *Biomaterials.* 28 (2007) 108–116. doi:10.1016/j.biomaterials.2006.08.047.
- [21] A.S. Determan, B.G. Trewyn, V.S.Y. Lin, M. Nilsen-Hamilton, B. Narasimhan, Encapsulation, stabilization, and release of BSA-FITC from polyanhydride microspheres, *J. Control. Release.* 100 (2004) 97–109. doi:10.1016/j.jconrel.2004.08.006.
- [22] A.S. Determan, J.H. Wilson, M.J. Kipper, M.J. Wannemuehler, B. Narasimhan, Protein stability in the presence of polymer degradation products: Consequences for controlled release formulations, *Biomaterials.* 27 (2006) 3312–3320. doi:10.1016/j.biomaterials.2006.01.054.
- [23] S.L. Haughney, L.K. Petersen, A.D. Schoofs, A.E. Ramer-Tait, J.D. King, D.E. Briles, M.J. Wannemuehler, B. Narasimhan, Retention of structure, antigenicity, and biological function of pneumococcal surface protein A (PspA) released from polyanhydride nanoparticles, *Acta Biomater.* 9 (2013) 8262–8271. doi:10.1016/j.actbio.2013.06.006.
- [24] J.E. Vela Ramirez, R. Roychoudhury, H.H. Habte, M.W. Cho, N.L.B. Pohl, B. Narasimhan, Carbohydrate-functionalized nanovaccines preserve HIV-1 antigen stability and activate antigen presenting cells, *J. Biomater. Sci. Polym. Ed.* 25 (2014) 1387–1406. doi:10.1080/09205063.2014.940243.
- [25] K.A. Ross, Synthetic nanoparticle-based vaccines against respiratory pathogens, *Grad. Theses Diss. Paper 1357* (2013).
- [26] M. Westphal, Z. Ram, V. Riddle, D. Hilt, E. Bortey, Gliadel (R) wafer in initial surgery for malignant glioma: Long-term follow-up of a multicenter controlled trial, *Acta Neurochir. (Wien).* 148 (2006) 269–275. doi:10.1007/s00701-005-0707-z.
- [27] J.P. Jain, S. Modi, N. Kumar, Hydroxy fatty acid based polyanhydride as drug delivery system : Synthesis , characterization , in vitro degradation , drug release , and biocompatibility, *Wiley Intersci.* (2007). doi:10.1002/jbm.a.
- [28] N. Kumar, R.S. Langer, A.J. Domb, Polyanhydrides: An overview, *Adv. Drug Deliv. Rev.* 54 (2002) 889–910. doi:10.1016/S0169-409X(02)00050-9.

- [29] A. Göpferich, J. Tessmar, Polyanhydride degradation and erosion, *Adv. Drug Deliv. Rev.* 54 (2002) 911–931. doi:10.1016/S0169-409X(02)00051-0.
- [30] Y. Tabata, R. Langer, Polyanhydride Microspheres that Display Near-Constant Release of Water-Soluble Model Drug Compounds, *Pharm. Res. An Off. J. Am. Assoc. Pharm. Sci.* 10 (1993) 391–399. doi:10.1023/A:1018988222324.
- [31] L. Shieh, J. Tamada, I. Chen, J. Pang, A. Domb, R. Langer, Erosion of a new family of biodegradable polyanhydrides, *Biomed. Mater. Res.* 28 (1994) 1465–1475.
- [32] L. Huntimer, J.H. Wilson Welder, K. Ross, B. Carrillo-Conde, L. Pruisner, C. Wang, B. Narasimhan, M.J. Wannemuehler, A.E. Ramer-Tait, Single immunization with a suboptimal antigen dose encapsulated into polyanhydride microparticles promotes high titer and avid antibody responses, *J. Biomed. Mater. Res. - Part B Appl. Biomater.* 101 B (2013) 91–98. doi:10.1002/jbm.b.32820.
- [33] Y. Phanse, P. Lueth, A.E. Ramer-Tait, B.R. Carrillo-Conde, M.J. Wannemuehler, B. Narasimhan, B.H. Bellaire, Cellular Internalization Mechanisms of Polyanhydride Particles: Implications for Rational Design of Drug Delivery Vehicles, *J. Biomed. Nanotechnol.* 12 (2016) 1544–1552. doi:10.1166/jbn.2016.2259.
- [34] M.J. Kipper, E. Shen, A. Determan, B. Narasimhan, Design of an injectable system based on bioerodible polyanhydride microspheres for sustained drug delivery, *Biomaterials.* 23 (2002) 4405–4412. doi:10.1016/S0142-9612(02)00181-3.
- [35] L.K. Petersen, C.K. Sackett, B. Narasimhan, Novel, high throughput method to study in vitro protein release from polymer nanospheres, *J. Comb. Chem.* 12 (2010) 51–56. doi:10.1021/cc900116c.
- [36] L.K. Petersen, L. Xue, M.J. Wannemuehler, K. Rajan, B. Narasimhan, The simultaneous effect of polymer chemistry and device geometry on the in vitro activation of murine dendritic cells, *Biomaterials.* 30 (2009) 5131–5142. doi:10.1016/j.biomaterials.2009.05.069.
- [37] Y. Phanse, B.R. Carrillo-Conde, A.E. Ramer-Tait, S. Broderick, C.S. Kong, K. Rajan, R. Flick, R.B. Mandell, B. Narasimhan, M.J. Wannemuehler, A systems approach to designing next generation vaccines: combining α -galactose modified antigens with nanoparticle platforms., *Sci. Rep.* 4 (2014) 3775. doi:10.1038/srep03775.
- [38] A. V. Chavez-Santoscoy, R. Roychoudhury, N.L.B. Pohl, M.J. Wannemuehler, B. Narasimhan, A.E. Ramer-Tait, Tailoring the immune response by targeting C-type lectin receptors on alveolar macrophages using “pathogen-like” amphiphilic polyanhydride nanoparticles, *Biomaterials.* 33 (2012) 4762–4772. doi:10.1016/j.biomaterials.2012.03.027.

- [39] B. Narasimhan, J.T. Goodman, J.E. Vela Ramirez, Rational Design of Targeted Next-Generation Carriers for Drug and Vaccine Delivery., *Annu. Rev. Biomed. Eng.* 18 (2016) 25–49. doi:10.1146/annurev-bioeng-082615-030519.
- [40] S. Dhar, E.W. Baker, S. Marrache, F.D. West, Therapeutic Nanoparticles for Accumulation in the Brain, WO/2016/022462, 2016.
- [41] T.A. Theodossiou, Z. Sideratou, D. Tsiourvas, C.M. Paleos, A novel mitotropic oligolysine nanocarrier: Targeted delivery of covalently bound D-Luciferin to cell mitochondria, *Mitochondrion*. 11 (2011) 982–986. doi:10.1016/j.mito.2011.08.004.
- [42] A. Wongrakpanich, S.M. Geary, M.A. Joiner, M.E. Anderson, A.K. Salem, Mitochondria-targeting particles., *Nanomedicine (Lond)*. 9 (2014) 2531–43. doi:10.2217/nmm.14.161.
- [43] S. Biswas, V.P. Torchilin, Nanopreparations for organelle-specific delivery in cancer, *Adv. Drug Deliv. Rev.* 66 (2014) 26–41. doi:10.1016/j.addr.2013.11.004.
- [44] E. Shen, M.J. Kipper, B. Dziadul, M.K. Lim, B. Narasimhan, Mechanistic relationships between polymer microstructure and drug release kinetics in bioerodible polyanhydrides, *J. Control. Release*. 82 (2002) 115–125. doi:10.1016/S0168-3659(02)00125-6.
- [45] C. Pu, J. Zhou, R. Lai, Y. Niu, W. Nan, X. Peng, Highly reactive, flexible yet green Se precursor for metal selenide nanocrystals: Se-octadecene suspension (Se-SUS), *Nano Res.* 6 (2013) 652–670.
- [46] D. V. Talapin, A.L. Rogach, A. Kornowski, M. Haase, H. Weller, Highly Luminescent Monodisperse CdSe and CdSe/ZnS Nanocrystals Synthesized in a Hexadecylamine-Trioctylphosphine Oxide-Trioctylphosphine Mixture, *Nano Lett.* 1 (2001) 207–211.
- [47] B.D. Ulery, Y. Phanse, A. Sinha, M.J. Wannemuehler, B. Narasimhan, B.H. Bellaire, Polymer chemistry influences monocytic uptake of polyanhydride nanospheres, *Pharm. Res.* 26 (2009) 683–690. doi:10.1007/s11095-008-9760-7.
- [48] B.M. Vogel, J.T. Cabral, N. Eidelman, B. Narasimhan, S.K. Mallapragada, Parallel synthesis and high throughput dissolution testing of biodegradable polyanhydride copolymers, *J. Comb. Chem.* 7 (2005) 921–928. doi:10.1021/cc050077p.
- [49] S. Biswas, N.S. Dodwadkar, A. Piroyan, V.P. Torchilin, Surface conjugation of triphenylphosphonium to target poly(amidoamine) dendrimers to mitochondria, *Biomaterials*. 33 (2012) 4773–4782. doi:10.1016/j.biomaterials.2012.03.032.
- [50] M.J. McManus, M.P. Murphy, J.L. Franklin, The Mitochondria-Targeted Antioxidant MitoQ Prevents Loss of Spatial Memory Retention and Early Neuropathology in a

- Transgenic Mouse Model of Alzheimer's Disease, *J. Neurosci.* 31 (2011) 15703–15715. doi:10.1523/JNEUROSCI.0552-11.2011.
- [51] M. Hardy, F. Poulh??s, E. Rizzato, A. Rockenbauer, K. Banaszak, H. Karoui, M. Lopez, J. Zielonka, J. Vasquez-Vivar, S. Sethumadhavan, B. Kalyanaraman, P. Tordo, O. Ouari, Mitochondria-targeted spin traps: Synthesis, superoxide spin trapping, and mitochondrial uptake, *Chem. Res. Toxicol.* 27 (2014) 1155–1165. doi:10.1021/tx500032e.
- [52] W. Lei, J. Xie, Y. Hou, G. Jiang, H. Zhang, P. Wang, X. Wang, B. Zhang, Mitochondria-targeting properties and photodynamic activities of porphyrin derivatives bearing cationic pendant, *J. Photochem. Photobiol. B Biol.* 98 (2010) 167–171. doi:10.1016/j.jphotobiol.2009.12.003.
- [53] E. Miquel, A. Cassina, L. Martínez-Palma, J.M. Souza, C. Bolatto, S. Rodríguez-Bottero, A. Logan, R.A.J. Smith, M.P. Murphy, L. Barbeito, R. Radi, P. Cassina, Neuroprotective effects of the mitochondria-targeted antioxidant MitoQ in a model of inherited amyotrophic lateral sclerosis, *Free Radic. Biol. Med.* 70 (2014) 204–213. doi:10.1016/j.freeradbiomed.2014.02.019.
- [54] M.P. Murphy, R.A.J. Smith, Targeting antioxidants to mitochondria by conjugation to lipophilic cations, *Annu. Rev. Pharmacol. Toxicol.* 47 (2007) 629–656. doi:10.1146/annurev.pharmtox.47.120505.105110.
- [55] V.J. Adlam, J.C. Harrison, C.M. Porteous, A.M. James, R. a J. Smith, M.P. Murphy, I. a Sammut, 1 Victoria J. Adlam, Joanne C. Harrison, Carolyn M. Porteous, Andrew M. James, Robin A. J. Smith, Michael P. Murphy, I.A. Sammut, Targeting an antioxidant to mitochondria decreases cardiac ischemia-reperfusion injury, *Faseb J.* 19 (2005) 1088–95. doi:10.1096/fj.04-3718com.
- [56] A. Ghosh, K. Chandran, S. V. Kalivendi, J. Joseph, W.E. Antholine, C.J. Hillard, A. Kanthasamy, A. Kanthasamy, B. Kalyanaraman, Neuroprotection by a mitochondria-targeted drug in a Parkinson's disease model, *Free Radic. Biol. Med.* 49 (2010) 1674–1684. doi:10.1016/j.freeradbiomed.2010.08.028.
- [57] S. Marrache, S. Dhar, Engineering of blended nanoparticle platform for delivery of mitochondria-acting therapeutics, *Proc. Natl. Acad. Sci. U. S. A.* 109 (2012) 16288–16293. doi:10.1073/pnas.1210096109.
- [58] X.-H. Wang, H.-S. Peng, L. Yang, F.-T. You, F. Teng, A.-W. Tang, F.-J. Zhang, X.-H. Li, Poly-l-lysine assisted synthesis of core-shell nanoparticles and conjugation with triphenylphosphonium to target mitochondria, *J. Mater. Chem. B.* 1 (2013) 5143–5152. doi:10.1039/c3tb20884b.

- [59] A.T. Hoye, J.E. Davoren, P. Wipf, M.P. Fink, V.E. Kagan, Targeting mitochondria, *Acc. Chem. Res.* 41 (2008) 87–97. doi:10.1021/ar700135m.
- [60] T.A. Theodossiou, Z. Sideratou, M.E. Katsarou, D. Tsiourvas, Mitochondrial delivery of doxorubicin by triphenylphosphonium- functionalized hyperbranched nanocarriers results in rapid and severe cytotoxicity, *Pharm. Res.* 30 (2013) 2832–2842. doi:10.1007/s11095-013-1111-7.
- [61] H.M. Cochemé, G.F. Kelso, A.M. James, M.F. Ross, J. Trnka, T. Mahendiran, J. Asin-Cayuela, F.H. Blaikie, A.R.B. Manas, C.M. Porteous, V.J. Adlam, R.A.J. Smith, M.P. Murphy, Mitochondrial targeting of quinones: Therapeutic implications, *Mitochondrion.* 7 (2007) 94–102. doi:10.1016/j.mito.2007.02.007.
- [62] J.T. Madak, N. Neamati, Membrane Permeable Lipophilic Cations as Mitochondrial Directing Groups, *Curr. Top. Med. Chem.* 15 (2015) 745–766.
- [63] C.L. Wladyka, D.L. Kunze, KCNQ/M-currents contribute to the resting membrane potential in rat visceral sensory neurons, *J. Physiol.* 575 (2006) 175–189.
- [64] M.F. Ross, A. Filipovska, R.A.J. Smith, M.J. Gait, M.P. Murphy, Cell-penetrating peptides do not cross mitochondrial membranes even when conjugated to a lipophilic cation: evidence against direct passage through phospholipid bilayers., *Biochem. J.* 383 (2004) 457–68. doi:10.1042/BJ20041095.
- [65] P.G. Finichiu, A.M. James, L. Larsen, R.A.J. Smith, M.P. Murphy, Mitochondrial accumulation of a lipophilic cation conjugated to an ionisable group depends on membrane potential, pH gradient and pK_a: Implications for the design of mitochondrial probes and therapies, *J. Bioenerg. Biomembr.* 45 (2013) 165–173. doi:10.1007/s10863-012-9493-5.
- [66] S. Kaul, A. Kanthasamy, M. Kitazawa, V. Anantharam, A.G. Kanthasamy, Caspase-3 dependent proteolytic activation of protein kinase C β mediates and regulates 1-methyl-4-phenylpyridinium (MPP⁺)-induced apoptotic cell death in dopaminergic cells: Relevance to oxidative stress in dopaminergic degeneration, *Eur. J. Neurosci.* 18 (2003) 1387–1401. doi:10.1046/j.1460-9568.2003.02864.x.
- [67] a G. Porter, R.U. Jänicke, Emerging roles of caspase-3 in apoptosis., *Cell Death Differ.* 6 (1999) 99–104. doi:10.1038/sj.cdd.4400476.
- [68] D. Tadokoro, S. Takahama, K. Shimizu, S. Hayashi, Y. Endo, T. Sawasaki, Characterization of a caspase-3-substrate kinome using an N- and C-terminally tagged protein kinase library produced by a cell-free system., *Cell Death Dis.* 1 (2010) e89. doi:10.1038/cddis.2010.65.

CHAPTER 5: CONCLUSIONS AND ONGOING/FUTURE WORK

5.1 Conclusions

Rapid treatment of oxidative stress using antioxidants is necessary to combat neurodegeneration due to chemical exposure and other causes. Drug-encapsulating nanoscale delivery platforms with conjugated targeting moieties can significantly improve drug efficacy for treatment of oxidative stress. The 20 mol% 1,6-bis(*p*-carboxyphenoxy)hexane (CPH), 80 mol% sebacic acid (SA; 20:80 CPH:SA) polyanhydride nanoparticle (NP) platform has demonstrated sustained release, dose-sparing and cellular internalization properties that make it promising for central nervous system (CNS) drug delivery [1–3].

To effectively treat oxidative stress, a delivery platform should be able to effectively cross the blood-brain barrier (BBB), enable delivery to diseased neuron, and co-localize to the mitochondria (Chapter 2). To understand the BBB crossing capability of these NPs, internalization in both BBB endothelial cells and monocytes was evaluated using non-, surface-, and bulk-functionalized formulations using the targeting ligand, folic acid. The 20:80 CPH:SA NPs showed internalization by both the endothelial cells and the monocytes in this model; however, the targeting ligands did not improve internalization (Chapter 3). Then, to further test this platform, (3-carboxypropyl)triphenylphosphonium (CPTP) bulk-functionalized 20:80 CPH:SA NPs (CPTP-NPs) were synthesized and evaluated for the ability to be internalized by neurons, co-localize to the mitochondria, and overall improve the protection against oxidative stress after encapsulating the antioxidant Mito-apocynin. These CPTP-NPs were proven to be effective on all of these measures (Chapter 4). Further optimization of this platform is necessary to fully take advantage of the capability of this promising platform.

5.2 Ongoing and Future Work

To further optimize 20:80 CPH:SA NPs, they can be functionalized on the surface and in bulk simultaneously, with two different targeting ligands [2] (Chapters 3 and 4). A cascading, multiscale NP platform with bulk-conjugated moieties for targeting the neuron and mitochondria, and surface-conjugated moieties for targeting the BBB could significantly improve CNS delivery of therapeutics. This optimized platform would be tested using BBB and neuronal models, as described below. *In vivo* studies are then necessary to evaluate whether the developed NP platform can show this multiscale, cascading property and improve drug pharmacokinetics and pharmacodynamics for treatment of neurodegenerative disease.

5.2.1 *In vitro* polyanhydride NP formulation optimization

To optimize this polyanhydride NP platform, an optimal BBB-targeting ligand is needed. One strategy could involve conjugating chemokines to the surface of the NPs. These proteins can stimulate a pathway in the brain that ultimately enhances the immune response, which in doing so leads to more immune cell recruitment into the brain [4]. As discussed, 20:80 CPH:SA NPs additionally show superior uptake, and subsequent release, by immune cells [3] (Chapter 3). Therefore, surface functionalizing these NPs with a chemokine could lead to enhanced local NP concentration near the site of inflammation in the brain. Alternatively, surfactants have demonstrated the ability to inhibit efflux pumps on BBB endothelial cells, and additionally increase cell membrane fluidity, and therefore could also be incorporated into the NP platform to improve brain localization [5]. After enhanced brain localization provided by the surface-conjugated moiety, bulk-functionalization of NPs with a proven neuronal and mitochondrial targeting moiety such as CPTP could further enhance drug efficacy. Ultimately, platform

optimization using BBB and neuronal *in vitro* models would reveal a lead candidate for *in vivo* testing.

5.2.2 *In vivo* biodistribution studies

Internalization of NPs by BBB endothelial cells *in vivo* would prove significantly more challenging than for an *in vitro* BBB model. This necessitates an *in vivo* biodistribution study for the lead NP candidate. Brain bioavailability could be assessed at several different time points to generate a pharmacokinetic profile. Additionally, as mentioned in Chapter 2, the route of delivery plays an important role *in vivo*. Therefore, the choice between intranasal and intravenous delivery routes must be made for this study. Finally, as pathogenesis can play a role in BBB permeability, the study should test localization in both diseased and healthy mice.

5.2.3 *In vivo* protection studies

An *in vivo* protection study would evaluate whether the lead candidate can significantly improve drug pharmacodynamics. Parkinson's disease-based neurodegenerative models such as the MitoPark model and the 1-methyl-4-phenyl-1,2,3,6-tetrahydropyridine (MPTP) model could be considered for this study [6,7]. Alternatively, protection against irreversible neuronal damage after chemical exposure could also be evaluated with this platform *in vivo* by challenging mice with a toxic agent and evaluating protection afterwards using several behavioral characterization measures [8]. Overall, the optimization of this cascading, multiscale platform could significantly improve drug efficacy for neurodegenerative disease treatment, and would be evaluated by this study.

5.3 References

- [1] A.M. Binnebose, S.L. Haughney, R. Martin, P.M. Imerman, B. Narasimhan, B.H. Bellaire, Polyhydride Nanoparticle Delivery Platform Dramatically Enhances Killing of Filarial Worms, *PLoS Negl. Trop. Dis.* 9 (2015) 1–18. doi:10.1371/journal.pntd.0004173.
- [2] T.M. Brenza, S.G. Ms, J.E.V. Ramirez, D. Harischandra, V. Anantharam, B. Kalyanaraman, A.G. Kanthasamy, B. Narasimhan, Neuronal Protection against Oxidative Insult by Polyhydride Nanoparticle-based Mitochondria-targeted Antioxidant Therapy, *Nanomedicine Nanotechnology, Biol. Med.* 13 (2017) 809–820. doi:10.1016/j.nano.2016.10.004.
- [3] Y. Phanse, P. Lueth, A.E. Ramer-Tait, B.R. Carrillo-Conde, M.J. Wannemuehler, B. Narasimhan, B.H. Bellaire, Cellular Internalization Mechanisms of Polyhydride Particles: Implications for Rational Design of Drug Delivery Vehicles, *J. Biomed. Nanotechnol.* 12 (2016) 1544–1552. doi:10.1166/jbn.2016.2259.
- [4] C. Saraiva, C. Praca, R. Ferreira, T. Santos, L. Ferreira, L. Bernardino, Nanoparticle-mediated brain drug delivery: Overcoming blood-brain barrier to treat neurodegenerative diseases, *J. Control. Release.* 235 (2016) 34–47. doi:10.1016/j.jconrel.2016.05.044.
- [5] J. Kreuter, Drug delivery to the central nervous system by polymeric nanoparticles: What do we know?, *Adv. Drug Deliv. Rev.* 71 (2014) 2–14. doi:10.1016/j.addr.2013.08.008.
- [6] A. Ghosh, M.R. Langley, D.S. Harischandra, M.L. Neal, H. Jin, V. Anantharam, J. Joseph, T. Brenza, B. Narasimhan, A. Kanthasamy, B. Kalyanaraman, A.G. Kanthasamy, Mitoapocynin Treatment Protects Against Neuroinflammation and Dopaminergic Neurodegeneration in a Preclinical Animal Model of Parkinson’s Disease, *J. Neuroimmune Pharmacol.* 11 (2016) 259–278. doi:10.1007/s11481-016-9650-4.
- [7] M. Langley, A. Ghosh, A. Charli, S. Sarkar, M. Ay, J. Luo, J. Zielonka, T. Brenza, B. Bennett, H. Jin, S. Ghaisas, B. Schlichtmann, D. Kim, V. Anantharam, A. Kanthasamy, B. Narasimhan, B. Kalyanaraman, A. Kanthasamy, Mito-apocynin Prevents Mitochondrial Dysfunction, Microglial Activation, Oxidative Damage and Progressive Neurodegeneration in MitoPark Transgenic Mice, *Antioxid. Redox Signal.* 7 (2017). doi:10.1089/ars.2016.6905, accepted.
- [8] K.L. Brewer, M.M. Troendle, L. Pekman, W.J. Meggs, Naltrexone prevents delayed encephalopathy in rats poisoned with the sarin analogue diisopropylfluorophosphate, *Am. J. Emerg. Med.* 31 (2013) 676–679. doi:10.1016/j.ajem.2012.12.003.